PLASMA TREATMENT OF NATURAL FIBERS TO IMPROVE FIBER-MATRIX COMPATIBILITY

Rafael Cavalcante Cordeiro

Tese de Doutorado apresentada ao Programa de Pós-graduação em Engenharia Metalúrgica e de Materiais, COPPE, da Universidade Federal do Rio de Janeiro, como parte dos requisitos necessários à obtenção do título de Doutor em Engenharia Metalúrgica e de Materiais.

Orientador: Renata Antoun Simão

Rio de Janeiro

Fevereiro de 2016

PLASMA TREATMENT OF NATURAL FIBERS TO IMPROVE FIBER-MATRIX COMPATIBILITY

Rafael Cavalcante Cordeiro

TESE SUBMETIDA AO CORPO DOCENTE DO INSTITUTO ALBERTO LUIZ COIMBRA DE PÓS-GRADUAÇÃO E PESQUISA DE ENGENHARIA (COPPE) DA UNIVERSIDADE FEDERAL DO RIO DE JANEIRO COMO PARTE DOS REQUISITOS NECESSÁRIOS PARA A OBTENÇÃO DO GRAU DE DOUTOR EM CIÊNCIAS EM ENGENHARIA METALÚRGICA E DE MATERIAIS.

Examinada por:

_____
Prof. Renata Antoun Simão, D.Sc.

_____
Prof. Marysilvia Ferreira da Costa, D.Sc.

_____
Prof. José Roberto Moraes D'Almeida, D.Sc.

_____
Prof. Verônica Maria de Araújo Calado, D.Sc.

_____
Dr. Marcia Gomes de Oliveira, D.Sc.

RIO DE JANEIRO, RJ - BRASIL
FEVEREIRO DE 2016

Cordeiro, Rafael Cavalcante

Plasma treatment of natural fibers to improve fiber-matrix compatibility/ Rafael Cavalcante Cordeiro. – Rio de Janeiro: UFRJ/COPPE, 2016.

XII, 109 p.: il.; 29,7 cm.

Orientador: Renata Antoun Simão

Tese (doutorado) – UFRJ/ COPPE/ Programa de Engenharia Metalúrgica e de Materiais, 2016.

Referências Bibliográficas: p. 103-109.

1. Plasma treatment. 2. Surface modification. 3. Natural fiber composite. I. Simão, Renata Antoun. II. Universidade Federal do Rio de Janeiro, COPPE, Programa de Engenharia Metalúrgica e de Materiais. III. Título.

DEDICATORY

I dedicate this work to all scientists, researchers, enthusiasts or anyone who strives daily to make our planet a better place for all, who seek to enlighten our species and look for the balance between human development and environmental preservation.

ACKNOWLEDGMENTS

Before all else, I wish to thank my family: my father Marco, my mother Catarina and my sister Patricia, not only for all their support in these last years, but for a whole life of teaching, learning, exchanged experiences and encouragement. You have allowed me to follow my passions, find my own way in life and ultimately reach the title of doctor in science. Thank you.

I wish also to thank all my friends, who have played a major role in shaping my life, both in and out of academia. The friends from Brazil and also the friends I've made during my time researching in Germany, which include not only Germans but also Polish, Czech, Italians, Iranians, Ukrainians, Malaysians, French, Georgians, Russians, Finnish, Japanese, Pakistani, Bangladeshi and many people from all over. You served as role models, as inspiration and support in hard times, as the best company to have on leisure and fun times. Our conversations, discussions and laughs are part of who I am, of my opinion about the world and of how this thesis was done, from start to finish. You are too many to list here, but know that I think about you all constantly.

A special thanks to my advisor Dr. Renata Simão for allowing me to do this research, for all her help, guidance, advices, honest conversations and for your patience with my delays. Thank you for letting me do all sorts of experiments in your lab, including constructing and (sometimes) deconstructing reactors and other equipment. And to give me the opportunity to do part of my research abroad. Thank you also to all my colleges at UFRJ, both inside the lab I worked and on the department, who helped me with advices, suggestions, by hearing me complain when things didn't went as planed, for helping me procrastinate sometimes and for making this whole journey much more fun.

Thank you to Dr.-Ing. Prof. Lothar Kroll and the Technische Universität Chemnitz for receiving me for one and a half year and allowing me to conduct my research in your facilities and learn so much on my time in Germany. A special thanks to my colleges and friends who made me feel like I was home in Chemnitz: Marco Müller, Michael Heinrich, Ricardo Decker, Melanie Ploner, Erik Päßler, Tobias Hartmann, Patryk Nossol und vielen mehr, die zu vielen sind, um hier aufzuzahlen.

I would also like to thank CAPES for financing my time abroad through the PDSE program, TU Chemniz/SLK for the opportunity to work as a research assistant (HiWi or Hilfswissenschaftler), when I had to extend my stay and had to finance myself for the last months in Germany. For the time I've developed this thesis research in Brazil I want to thank the financial support of the PRH35 program from ANP.

Resumo da Tese apresentada à COPPE/UFRJ como parte dos requisitos necessários para a obtenção do grau de Doutor em Ciências (D.Sc.)

TRATAMENTO POR PLASMA DE FIBRAS NATURAIS PARA MELHORIA DA ADESÃO FIBRA-MATRIZ

Rafael Cavalcante Cordeiro

Fevereiro/2016

Orientador: Renata Antoun Simão

Programa: Engenharia Metalúrgica e de Materiais

Este trabalho analisa as alterações provocadas por tratamentos a plasma de baixa pressão em superfícies de fibras naturais vegetais, e avalia as mudanças no comportamento mecânico de compósitos preparados com estas fibras e matrizes poliméricas termoplásticas. É dada ênfase na análise dos mecanismos que causam alterações morfológicas e químicas na superfície das diferentes fibras, assim como os mecanismos que melhoram a interface fibra-matriz e, consequentemente, as propriedades mecânicas dos compósitos. Resultados significativos foram obtidos para compósitos de polipropileno reforçado tanto com fibras de linho quanto com fibras de madeira, quando estas foram submetidas a tratamento por plasma com o gás hexafluoreto de enxofre (SF_6), modificando o caráter químico superficial. Compósitos com matriz de amido termoplástico reforçado com fibras de coco também tiveram aumento significativo nas propriedades mecânicas após tratamento das fibras por plasma de ar e oxigênio.

Abstract of Thesis presented to COPPE/UFRJ as a partial fulfillment of the requirements for the degree of Doctor of Science (D.Sc.)

PLASMA TREATMENT OF NATURAL FIBERS TO IMPROVE FIBER-MATRIX COMPATIBILITY

Rafael Cavalcante Cordeiro

Fevereiro/2016

Advisor: Renata Antoun Simão

Department: Metallurgical and Materials Engineering

This work analyzes the modification on the surface of vegetable natural fibers caused by low pressure plasma treatment and evaluates the changes in mechanical properties of composites made of these fibers with thermoplastic polymeric matrices. Emphasis is given in analyzing the mechanisms that cause the morphological and chemical changes observed in the different fibers, as well as in understanding the mechanisms which improve fiber-matrix interface and, consequently, the mechanical properties of the composites. Significant results were found for polypropylene matrix composites reinforced with both flax and wood fibers, when these were treated by plasma of sulfur hexafluoride (SF_6) gas, which modified the surface chemical characteristic. Thermoplastic starch matrix composites reinforced with coconut fibers also displayed significant improvement in mechanical properties after the fibers have been plasma treated with air and oxygen.

SUMARY

FIGURES

1. Introduction

The development of renewable and biodegradable materials is a growing trend, given the increase in environmental awareness from the population, companies and governments. The impacts of humans on the planet is clear in many areas and with growing population and consumption, many issues must be addressed, including the final destination of our waste, the ever increasing amount of plastic particles in the oceans and land, as well as the energy consumption and renewability of the materials we produce. In this context, polymers reinforced with natural plant fibers are an interesting alternative, and research in this field has been growing continuously in the last two decades. These materials can be partially or fully renewable and biodegradable, while also consuming less energy during production and having adequate mechanical properties for many applications.

The use of composites reinforced with natural fibers is growing, but is still a small market due to many factors, including the poor adhesion between fibers and matrices. The solution for this issue is still an open scientific debate, with many different kinds of treatments being tested by different research groups. This situation is similar to what happened when glass fibers appeared as a reinforcement phase for polymers, until the silanization compatibilization treatment was developed and became the industrial standard. Natural plant fibers, however, come from many different species, with varying chemical composition, morphological characteristics and sizes, making the development of a single compatibilization treatment challenging. Between the different possibilities being studied, plasma modification of the fibers surfaces is considered very promising and the most environmental friendly, which is a desired characteristic, given the context of the development of these materials.

In this thesis, low-pressure low-temperature plasma treatments of different short natural plant fibers were studied. Surface analysis of the fibers and compounding of these with polymeric matrices were also performed, followed by mechanical and other analysis of the composites. The different aspects of surface modification and interaction are explored and discussed in an attempt to shed light on the mechanisms behind fiber-matrix compatibility.

As part of the thesis, the author has designed and build an inductively coupled RF plasma reactor, specifically made for the purpose of plasma treatment of multiple short fibers. The effective treatment time was modeled and the results show that the reactor is effective in modifying natural fibers surfaces. A commercial glow discharge plasma reactor was also used during the exchange research program (PDSE/Capes) period in which the author worked at the Technische Universität Chemnitz, in Germany.

A process gas not yet reported in the literature for this application was used in this work, sulfur hexafluoride (SF_6). This gas is highly stable and inert at normal conditions, but in a plasma environment it can be broken and the freed fluorine atoms react readily with the exposed surface. This is known to make many materials hydrophobic, but it has never been attempted as a modification for natural fibers to be incorporated in polymeric matrices. The use of SF_6 plasma has led to improvements in mechanical properties of composites made with different natural fibers in a polypropylene matrix due to improved fiber-matrix adhesion, which is attributed to the similar hydrophobic character of the matrix and the treated fibers.

While SF_6 plasma causes chemical modification of the surface with little or no effect in morphology, oxygen plasma leads to surface etching, increasing the surface roughness. This is another strategy to improve the fiber-matrix adhesion, by increased mechanical interlocking. In this work this kind of plasma treatment was successful in greatly increasing the mechanical properties of coir fiber/thermoplastic starch composites.

The work presented here is an evidence for the versatility and potential of plasma surface treatments to improve the adhesion of natural fibers with different kinds of polymers. This is a potentially effective and viable technique that, if further developed, can help improving the overall properties of composites reinforced with natural fibers, making them more attractive and expanding their use over traditional composites and polymers.

2. Literature Review

2.1. Natural Fibers (Lignocellulosic fibers)

The term “natural fibers” represent a broad group of materials that include mineral (e.g. asbestos), animal (e.g. wool, silk) and plant based fibers (e.g. hemp, flax, sisal, bamboo), as noted by GURUNATHAN *et al*. (2015). Most common in the study of composites are animal fibers, which are composed of proteins, and plant fibers, which have cellulose as their basic constituent. This last group has many sub-divisions, based on the plant structure from where the fibers are extracted, as shown schematically in figure 2.1 (GURUNATHAN *et al*., 2015).

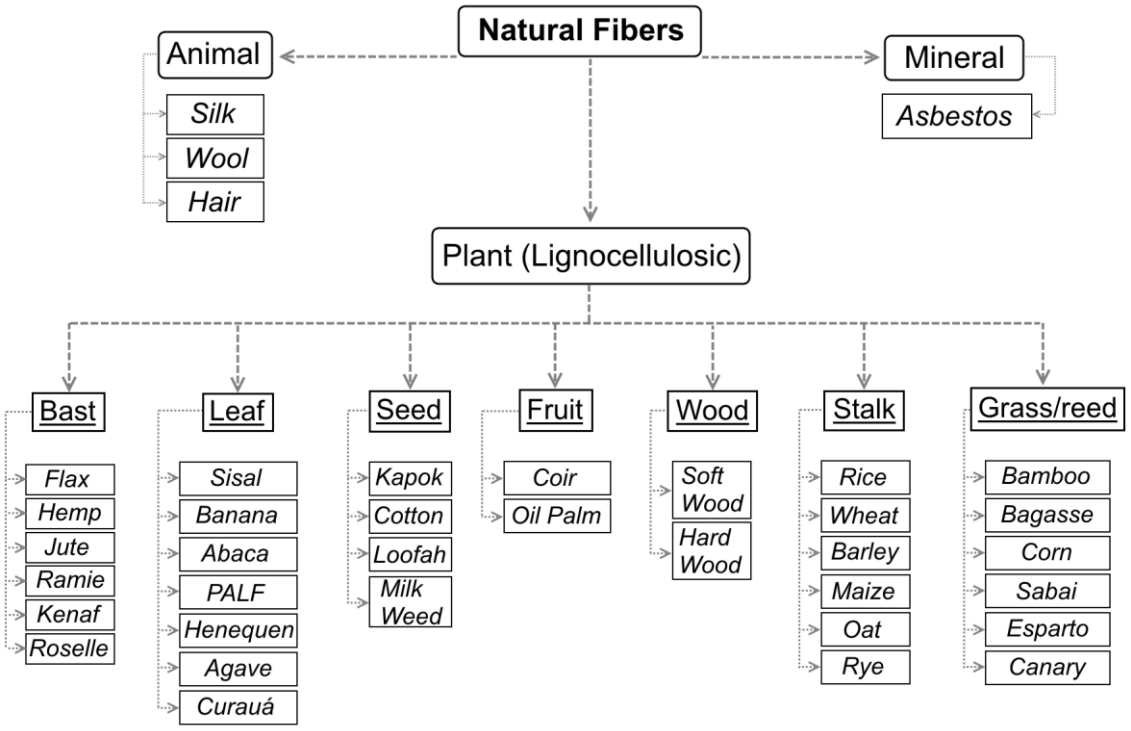

Figure 2.1 – Classification of some of the most common natural fibers. Adapted from GURUNATHAN *et al*. (2015).

Although in the literature (AZWA *et al*., 2013, FARUK *et al*. 2012, GURUNATHAN *et al*., 2015) it is common to use simply “natural fibers” and this term will be used frequently here as well, it is important to state that for the purpose of this work, the meaning intended is natural lignocellulosic plant fibers. These are composed mainly of three constituents: Cellulose, hemicellulose and lignin. Other components often found, but in much lower concentrations, are waxes, pectin, oils, starches and

water soluble substances, among others (BLEDZKI & GASSAN, 1999). Due to their complex internal structure and many components, natural fibers are considered a composite by themselves, and each plant species has different arrangements and concentrations of these constituents (DITTENBER & GANGARAO, 2012).

Cellulose is a linear polysaccharide macromolecule composed of ß-D-glucose units, which are linked together by ß-1,4-glycosidic linkages, always at the C_1 and C_4 positions of the cyclic structure, as shows schematically in figure 2.2. The repeating units contain hydroxyl groups which form hydrogen bonds with the macromolecule itself and with neighboring celluloses. For this reason, cellulose tends to form tightly packed, mostly crystalline, elongated structures called microfibrils, with approximately 3 nm to 5 nm in thickness. These have high tensile strength and are the reason why cellulose is considered the main structural component in plants and natural fibers. Due to the great concentration of hydroxyls, cellulose is also hydrophilic by nature, although it is insoluble in water, due to its compact and difficult to access structure (AZWA *et al*., 2013, GURUNATHAN *et al*., 2015, SUMMERSCALES *et al*, 2010).

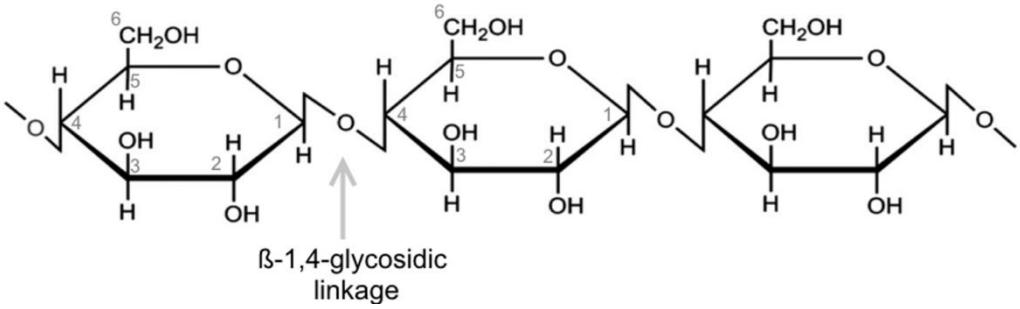

Figure 2.2 – Cellulose structure, adapted from GURUNATHAN *et al.* (2015).

Hemicellulose is also a polysaccharide, i.e. formed by bonded sugar monomers. However, unlike cellulose, hemicellulose is a heteropolymer, meaning its macromolecules can have a variety of different sugar monomers besides glucose (figure 2.3) arranged in different ways as the backbone and side chains. The macromolecule is also ramified, instead of linear, and has lower molecular weight than cellulose. In the plant structure, hemicellulose is present bonded to cellulose microfibrils, lignin and sometimes pectin. Together with lignin, hemicellulose acts as a kind of matrix for the cellulose microfibrils (AZWA *et al*., 2013, GURUNATHAN *et al*., 2015).

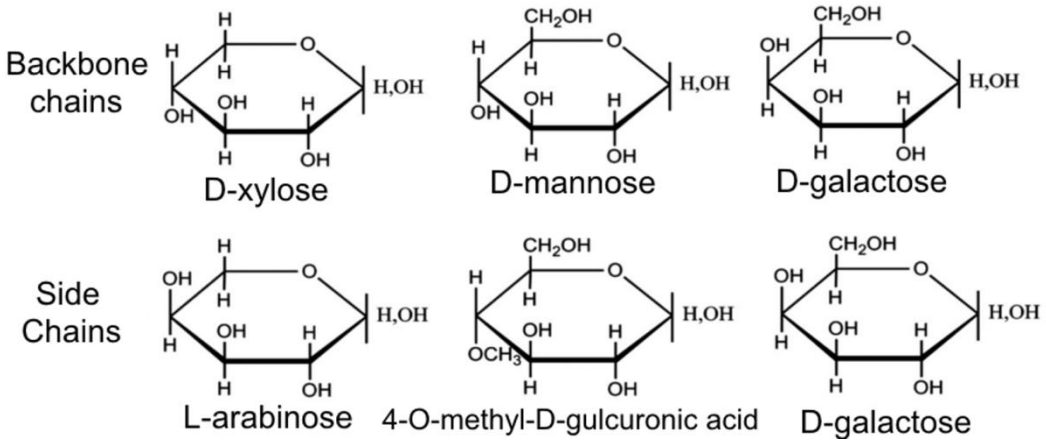

Figure 2.3 – Different sugars present in hemicellulose macromolecules. Adapted from GURUNATHAN *et al.* (2015).

Lignin is a highly ramified hydrocarbon heteropolymer formed mainly by three precursors: trans-coniferyl, trans-sinapyl, and trans- p-coumaryl (figure 2.4). These can be combined in many different configurations in a three dimensional complex structure. Lignin is partially covalently bound to hemicellulose and is a fundamental part of the cell wall structure, assuming the role of a coupling agent and matrix material, increasing the stiffness of the cellulose/hemicellulose network.

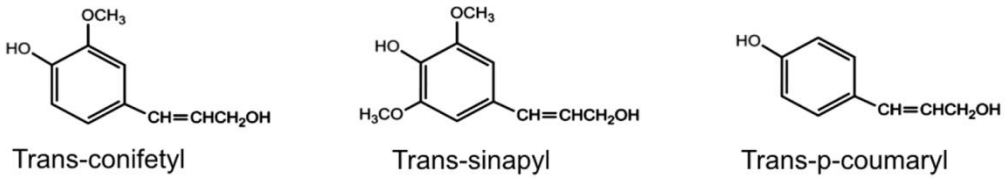

Figure 2.4 – Three main phenols which constitute lignin macromolecules

The arrangement of these components in an elementary fiber, or plant cell wall, is complex and layered, as shown schematically in figure 2.5a. The primary (outer) wall is composed of a network of randomly arranged cellulose microfibrils connected to an amorphous phase of hemicellulose and lignin, which act as a matrix for the cellulose bundles. On the inner secondary wall, three layers are usually present and in each one the cellulose microfibrils are helically arranged in relation to the long axis of the elementary fiber. The angle between each layer is different, and the microfibrillar angle (indicated in figure 2.5a) in relation to the long axis is an important factor that determines the mechanical properties of the fiber (AZWA *et al*., 2013, JOHN

& THOMAS, 2008). In many applications, the reduction of natural fibers to their elementary fibers is not economically viable or possible. Thus, natural fibers used in most applications and research are actually fiber bundles, also called technical fibers. As the name implies, these are formed of bundles of elementary fibers, as shown schematically in figure 2.5b (BOS *et al*., 2006).

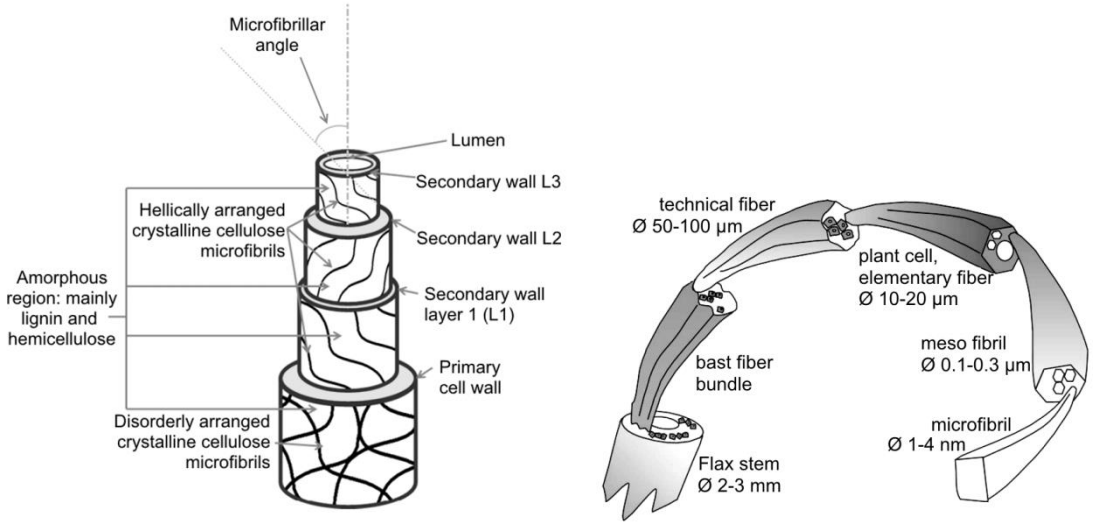

Figure 2.5 – (a) internal structure of an elementary natural fiber (adapted from AZWA *et al., 2013*). (b) Hierarchy of organization of natural fibers (adapted from BOS *et al.* 2006).

The micro fibrillar angles in the layers of secondary walls, the length and thickness of the vegetable cells, the relative amount of cellulose, hemicellulose, lignin and other minor constituents, among other factors vary from one plant species to the other. Not only that, but each individual plant shows variations in these variables according to growing conditions (FARUK *et al.*, 2012, AZWA *et al.* 2013, NECHWATAL *et al.*, 2003, HO *et al*., 2012). This explains both the broad range of values for mechanical properties in natural fibers, compared to glass fibers, and why different plant species can have such different mechanical behavior. These differences can be seen in table 2.1, which lists the currently most used and studied fibers.

The properties of glass fibers used for composite materials are also shown in table 2.1. It can be seen that the elastic modulus of some of the lignocellulosic natural fibers are comparable to glass fibers, while tensile strength of the later is clearly superior. However, when considering specific properties, that is, elastic modulus and tensile strength divided by the density of the material, some natural fibers have

comparable specific tensile strength and superior specific elastic modulus compared to glass fibers, thanks to their low density (GURUNATHAN *et al*., 2015, HO *et al.*, 2012). This makes natural fibers an interesting material for replacement of glass fibers in composites. Their use is growing in the industry and research areas for other factors as well. Natural fibers are renewable and abundantly available, being sometimes a waste product, with low prices compared to synthetic fibers like E-glass (aluminum-borosilicate glass, the most common type of glass fiber). Lignocellulosic fibers reinforced composites can be processed with the same machinery already used for polymer and traditional composite processing. Thanks to their flexibility and low abrasion, natural fibers also have reduced wear and thus reduced maintenance cost for these machines, when compared to glass fibers, for example. Being plant based, these fibers are also biodegradable, reducing the problem of massive waste production, whether this material is discarded in nature or in landfills (FARUK *et al.*, 2012, GURUNATHAN *et al*., 2015, Ho *et al.*, 2012). Another potential benefit of the wider use of these materials is thatthe growing, harvesting and processing of lignocellulosic fibers can also have a positive impact on local communities, creating new jobs and opportunities for farmers and other people on the vicinities of a manufacturing plant (RAMÍREZ *et al*., 2011, SATYANARAYANA *et al*., 2009).This is relevant for developing countries, many of which have adequate climate for the growth of many different specimens of plants.

Many studies concluded that the total energy consumption for production of lignocellulosic fibers is much lower than for glass fibers. MOHANTY *et al*. (2001) reported that natural fibers need only 20% to 25% of the energy used for synthetic fibers, by weight. MUELLER & KROBJILOWSKI (2003) concluded that the energy demand to produce nonwoven fabric of natural fibers is only 30% to 40% of the total consumed for a glass fibers mat. Life cycle energy assessment performed by MUTNURI *et* al. (2010) found that natural fibers reinforced polymers consumed 40% to 60% less energy compared to glass fibers reinforced polymers. This study considered the extraction, processing and transportation of raw material, as well as manufacturing of the composite. A more comprehensive study presented by PATEL & NARAYAN (2005) shows that energy usage of natural fibers, compared to glass fibers, could be from 14% up to 50% better, depending on many factors of the plants growth and fiber processing.

Table 2.1 – composition and properties of available natural fibers, adapted from GURUNATHAN *et al*., 2015.

Fiber	Tensile Strength (Mpa)	Young's Modulus (GPa)	Specific Strength (MPa)	Specific modulus (GPa)	Cellulose (wt%)	Hemi-cellulose (wt%)	Lignin (wt%)	Micro-fibrilar angle (deg)
Cotton	287-597	6-10	194-452	4-6.5	85-90	5.7	0.7-1.6	20-30
Jute	187-773	20-55	140-320	14-39	61-71.5	13.6-20	12-13	8
Flax	343-1035	50-70	345-620	34-48	71-78	18.6-21	2.2	5-10
Sisal	507-855	9-22	55-580	6-15	67-78	10-14	8-11	10-22
Ramie	400-938	61.4-128	590	29	68.6-76.2	13-16.7	0.7	7.5
Hemp	580-1110	30-60	210-510	20-41	70.2-74.4	18-22.4	3-5.7	2-6.2
Coir	175	6	92-152	5.2	36-43	0.15-0.25	41-45	30-49
Kenaf	295-930	22-60	246-993	18-50	45-57	21.5	8-13	n/a
Banana	529-914	27-32	392-677	20-24	63-64	10	5	11
Pinapple	170-1627	60-82	287-1130	42-57	80-83	15-20	8-12	10-22
Abaca	430-813	31.1-33.36	n/a	n/a	56-63	21.7	12-13	8-15
Bamboo	140-441	11-36	383	18	n/a	n/a	n/a	n/a
Nettle	650	38	n/a	n/a	86	4	5.4	n/a
Hardwood	51-120.7	5.2-15.6	n/a	n/a	43-47	25-35	16-24	n/a
Softwood	45.5-111.7	3.6-14.3	n/a	n/a	40-44	25-29	25-31	n/a
E-Glass	2000-3500	70-73	800-1400	29	-	-	-	-

2.2. Composites reinforced with natural fibers

Natural fibers as reinforcements in polymeric matrices have seen a considerable and constant growth in the industry recently, and research on this topic has also been growing in the last decades (FARUK *et al.*, 2012, GURUNATHAN *et al*., 2015). A growing trend in energy efficiency, environmental awareness and reduction of carbon footprint has stimulated the use of natural fibers of different kinds to improve the resistance of thermoplastics. As noted in section 2.1, these fibers have comparable or even better mechanical properties than commonly used E-glass fibers, once the weight is taken into account. They bring also a series of other advantages including low cost, lower wear to processing machinery, lower environmental impact considering all production stages, overall lower energy consumption and biodegradability after the end-of-life (HERRERA-FRANCO & VALADEZ-GONZÁLEZ, 2005, SOBCZAK *et al*., 2012, MOHANTY *et al.*, 2000, ZAMPALONI *et al*., 2007).

The production of natural fiber composites uses the same techniques and equipment already in use for traditional composites, whether they are short fibers, long fibers, woven or non-woven mats (FARUK *et al*., 2012). The fibers used can be from many sources, as stated in section 2.1, and many different polymeric matrices can be used. The term “biocomposite” is commonly used, but may have different meanings. So called “true biocomposites” are made with fibers and polymers which are both of biological origin and also both biodegradable. However, the term may also be used to describe non-biodegradable polymers reinforced with lignocellulosic fibers.

Despite of all the benefits of composites reinforced with natural fibers, many problems must be solved before these materials can achieve the optimal properties which are necessary to reach new markets. Poor interaction and bonding between the fibers and matrices is often cited as one of the main issues that must be addressed to improve composites mechanical properties and expand its use into new potential applications (GURUNATHAN *et al*., 2015, PÉREZ *et al*., 2012, SOBCZAK *et al*., 2012, STAMBOULIS *et al.*, 2000). Although many works attempt to address this issue by different strategies, much research is still underway in this field and the mechanisms of fiber-matrix bonding and interactions are not yet fully understood (GURUNATHAN *et* al., 2015, FARUK *et al., 2012*, KARGER-KOCSIS *et al.,* 2015).

Another relevant issue concerning natural fibers is their susceptibility to ambient humidity. Any polymeric matrix composite absorbs water from the environment, which impacts negatively their mechanical properties (AZWA *et al*., 2013). This is intensified in natural fibers composites because of the affinity of cellulose and hemicellulose to absorb water, causing changes in the properties of the fibers themselves (COUSINS, 1978), as well as swelling of the fibers and decrease in load transfer efficiency (AZWA *et al*., 2013). The fiber-matrix interface is also a preferential diffusion path in the material, and it has been shown that improved adhesion between reinforcing phase and polymer reduces the susceptibility to humidity (AZWA *et al., 2013*).

Absorbed humidity can also be problematic during composite processing, since as the fibers are heated and mixed with the polymer, the absorbed humidity is released as water vapor, creating pores and gaps between fibers and matrix. However, this can usually be avoided by drying the fibers before compounding (FARUK *et al*., 2012, HO *et al., 2012*).

2.2.1. Compatibilization between fibers and matrices

The poor fiber-matrix interaction is one of the main issues concerning the fabrication and use of natural fibers reinforced polymers. The most used thermoplastic matrices are hydrophobic while lignocellulosic fibers are hydrophilic, causing poor wettability, low interfacial sheer stress and load transfer, and sometimes agglomeration of fibers during processing (FARUK *et al*., 2012, GURUNATHAN *et al*., 2015). Even when the matrix is also hydrophilic, there is evidence that the interaction between matrix and the fibers is not ideal and can still be greatly improved (ROSA *et al*., 2009, SATYANARAYANA *et al*., 2009, VILASECA *et al*., 2007).

Currently there are many different strategies being researched to improve fiber-matrix adhesion in composites reinforced with natural fibers. Parallels can be drawn between the present situation of natural fibers composites and the beginning of development of glass fibers composites, when the interaction between glass fibers and polymers was also poor until the full development of the silane-based coupling agents, used up to this day to coat glass fibers for use with both thermoset and thermoplastic matrices (KARGER-KOCSIS *et al*., 2015). However, given the great variability of chemical, structural and superficial characteristics of natural fibers, with its many different plant origins, development of a single strategy to improve adhesion is much more complicated in this case.

Two broad categories can be defined when discussing methods to improve fiber-matrix interface: Modification of the matrix chemical character and overall modification of the fibers surfaces, including both physical and chemical modification. Table 2.2 presents some of the results reported in literature for both of these categories, excluding plasma treatments, which will be discussed in section 2.3. Works in the literature which focus in matrix modification deal mostly with additives, of which the most common is maleic anhydride grafted polymers. Such additives consist of a macromolecule equal to the matrix (i.e. polypropylene), but with grafted oxygen-containing polar functional groups (maleic anhydride in this case). This polar group has a good interaction with lignocellulosic fibers, while the unmodified parts of the macromolecule become part of the matrix, promoting bonding. (FARUK *et al*., 2012, LA MANTIA & MORREALE, 2011). However, this can cause a drop in the matrix mechanical properties, especially elastic modulus, among other issues (GUPTA *et al*., 2007, DÁNYÁDI *et al*., 2007, PÉREZ *et al*., 2012)

Table 2.2 – Results of mechanical properties improvement reported for different compatibilization methods.

Reference	Fiber	Matrix	Compatibilization method	Properties change
RAY et al., 2001	Jute	Vinyl ester	NaOH (5%, 4h)	20% increase in flexural strength, 23% increase in flexural modulus
LI, PICKERING, 2008	Hemp	PP	Enzyme treatment	19% increase in tensile strength (both treated and untreated composites had MAPP in the matrix)
DÁNYÁDI et al., 2007	Soft wood	PP	MAPP	Tensile strength increase by 72%
DANYÁDI et al., 2010	Soft wood	PP	MAPP	18%increase in tensile strength
PÉREZ *et al*., 2008	Red pine wood flour	PP	MAPP	68% increase in tensile strength, 33% decrease in E-modulus
HERRERA-FRANCO & VALADEZ-GONZÁLEZ, 2005	Henequen	HDPE	Alkaline (NaOH) followed by silanization	30% increase in tensile strength, no change in E-modulus
SREEKUMAR *et al.*, 2009	Sisal	Isophthalic polyester	Alikaline[1] (NaOH) / Permanganate treatment[2] / Silanization[3]	[36% increase in tensile strength and 53% increase in Young's modulus][1] / [25% increase in flexural strength and 31% increase in flexural modulus][2] / [21% increase in flexural strength and 39% increase in flexural modulus][3]

Modification of the natural fiber surface is one of the most investigated methods to improve the fiber-matrix adhesion and thus the composite properties. Because of the many different approaches researchers use to perform the surface modification, this field is usually classified in one of four broad categories, as discussed by GURUNATHAN *et al.* (2015): chemical (including silane treatment, acetylation and mercerization, also known as alkaline treatment), physicochemical (solvent extraction), mechanical (rolling, swaging, etc.) and physical (plasma, corona, etc.).

Chemical modification is the most common surface treatment, thanks to its relative simplicity. In most cases the fibers are put into a bath of chemical solutions that remove or add components to the surface. Mercerization or alkaline treatment for removal of lignin is the most commonly used (RAY *et al*., 2001, QUIN *et al*., 2008). Replacement of hydroxyl groups from the lignocellulosic fibers by different functional groups is also used to reduce the surface polarity and hydrophilic character. This can be achieved by silanization (XIE *et al*., 2010), esterification, benzylation, among others

(DÁNYÁDI *et al*., 2010). However, chemical modifications present two main problems: Extensive fiber modification beyond the surface, reducing the mechanical properties of the fiber as a whole; and generation of large volumes of wastes, which can't be easily discarded since they are often toxic, harmful to human health and to the environment (DÁNYÁDI *et al*., 2010, FELEKOGLU *et al*., 2009, SREEKUMAR *et al*., 2009). This also increases the cost of these processes due to the necessary steps to neutralize or treat the waste generated.

Among the physical surface modifications technique, plasma discharges are the most explored (KARGER-KOCSIS *et al*., 2015). In this technique, fibers are exposed to a plasma environment (ionized gas), at low or atmospheric pressure, which causes surface reactions and modifications ranging from etching to incorporation of functional groups and changes in surface energy. Plasma treatments are considered the most "eco-friendly" and are able to modify surface chemical composition and physical structure without altering bulk properties (GURUNATHAN *et al.*, 2015, KUSANO *et al*., 2011, MAHLBERG *et al*., 1999). Furthermore, when low pressure is used, the process gas consumption is minimized and the treatment creates little to no process waste (FARUK *et al*., 2012, LI *et al*., 1997, SINHA & PANIGRAHI, 2009, ZHOU *et al*., 2011).

2.3. Plasma surface modification

2.3.1. Cold plasma

Plasma is an ionized gas where free electrons and ions coexist. This can be achieved by heating gasses to extremely high temperatures or by subjecting it to strong electromagnetic fields. Both these processes are able to remove electrons from the atoms and molecules, and these electrons have enough kinetic energy to, in case of a collision, remove further electrons from atoms and molecules. These collisions create a cascading ionization process, creating new ions and electrons, which are balanced by the recombination of these two specimens until the plasma reaches equilibrium. When molecules are present in the plasma, their bonds may also be broken by collisions with electrons or ions, generating new unstable molecules and monatomic specimens, both of which are highly reactive (GOLDSTON & RUTHERFORD, 1995, LI *et al*., 1997).

Laboratory or industrial plasmas, also called "technological plasmas", are generated by electric or electromagnetic fields and usually have low temperature, which can be as low as room temperature, to avoid damage to the materials being

treated. Although high temperatures are needed to maintain ionization, it is possible to keep the perceived temperature of the plasma low with a low degree of ionization. This means that only a fraction (e.g. less than 1% for low temperature plasmas) of all the molecules and atoms in the gas are ionized at any given moment. As a consequence, the average kinetic energy of the molecules, atoms and ions is low, while electrons are accelerated to high velocities thanks to their much lower mass. The result is a so-called “cold plasma”, which is out of thermal equilibrium, i.e. with “hot” electrons and “cold” heavy particles, i.e. atoms, molecules and ions (GOLDSTON & RUTHERFORD, 1995, MUKHOPADHYAY & FANGUEIRO, 2009).

Cold plasma is easier to achieve at pressures bellow the atmospheric, which is the reason why most plasma treatments are made in vacuum, typically between 0.1 to 100 Pa, depending on the application and specific technique used. However, due to simpler operation conditions, atmospheric pressure plasma processes have gained popularity recently, although they have their own drawbacks, like higher consumption of process gas, lower control of the reactions occurring and higher temperatures, due to the higher degree of ionization needed to maintain a plasma discharge at atmospheric pressures (MUKHOPADHYAY & FANGUEIRO, 2009).

For the creation of plasma discharges with electric or electromagnetic fields, many different designs and power sources exist. Interesting for the discussion of this work are two kinds: Glow discharge plasma and radiofrequency (RF) inductively coupled plasma (ICP).

Glow discharge plasma is used in many applications, including fluorescent lamps, being the most widely used type of plasma. To create and sustain a glow discharge, an electric field is applied between two electrodes within a low pressure chamber, as schematically represented in figure 2.6. As free charges (always present due to cosmic rays and other phenomena) are accelerated by the electric field, they collide with neutral specimens (atoms and molecules) in the gas. These collisions will create new electrons and ions, if its energy is sufficiently high, which depend manly on the acceleration from the electric field and mean free path of electrons or ions. The plasma discharge is initiated and becomes stable above a minimum threshold of conditions, dependent on gas composition, reactor geometry, chamber pressure, and others. The intensity of the plasma typically varies according to the electric field combined with the distribution of the charged specimens in the plasma (GOLDSTON & RUTHERFORD, 1995, MUKHOPADHYAY & FANGUEIRO, 2009).

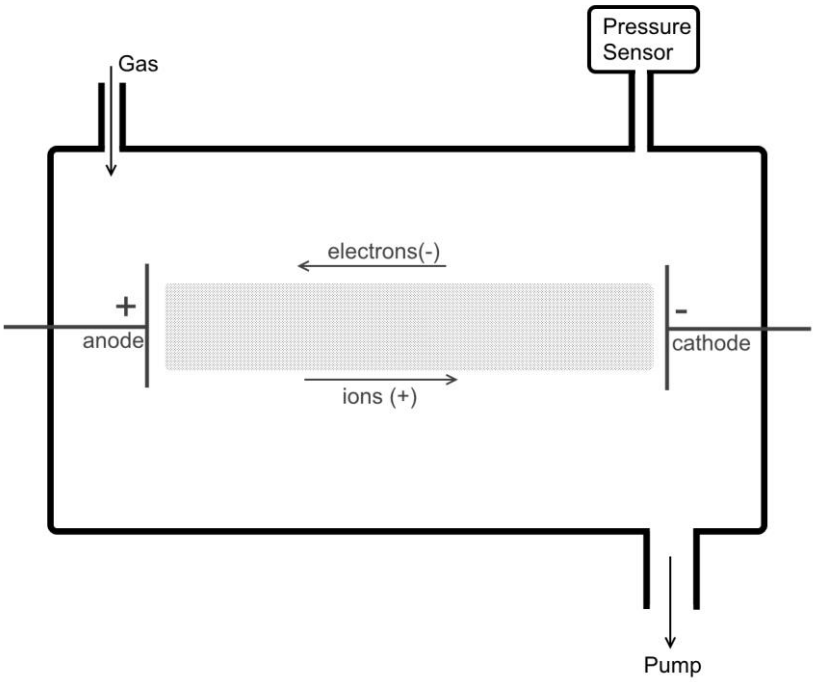

Figure 2.6 – Schematic representation of a simple glow discharge chamber.

In inductively coupled plasmas (ICP), no electrode is present inside the vacuum chamber. Instead, a solenoid or coil is placed outside the chamber with a dielectric material, usually glass, acting as the reactor wall. A radiofrequency (typically 13.56 MHz) current is applied to a coil as the one shown in figure 2.7. This high frequency current induces an alternating magnetic field in the direction Z (indicated), which in turn induces a rotating electric field in the direction θ, as indicated in figure 2.7. This induced electric field is responsible for accelerating the free charges in the chamber and consequently of inducing the gas ionization. Discharge balance between ionizing collisions and recombination happen in an analogous way as in the glow discharge plasma. However, the distribution of electron densities and temperatures, as well as the degree of ionization and energy of collisions follow different patterns than in the glow discharge, and direct comparison between the deposition parameters in different plasma chambers is complex (HUANG *et al.*, 2006, OKUMURA, 2010).

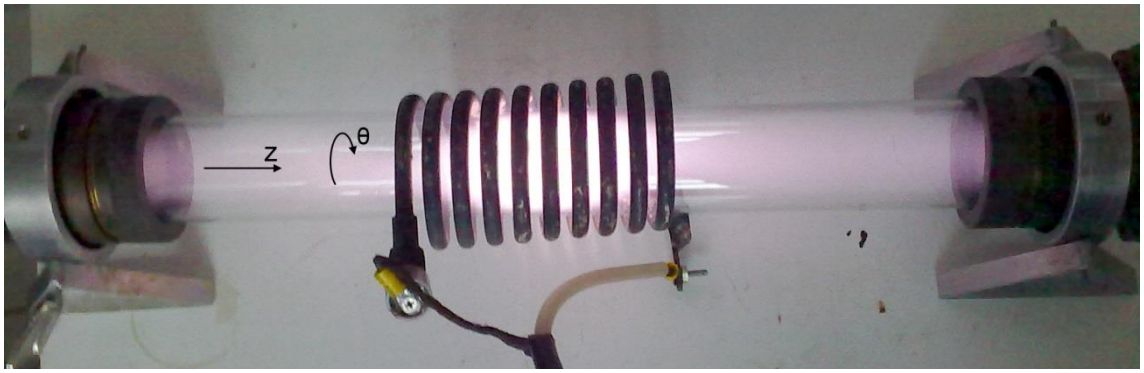

Figure 2.7 – Photo of the inductively coupled plasma system used indicating the directions of magnetic and electric fields induced.

2.3.2. Plasma modification of natural fibers

When plasma of a gas is created it may react with the fibers (or any substrate) in ways that the neutral gas never could, or at rates much higher than could be achieved by heating, for example. This happens due to the many different specimens created in the plasma, which depend on many factors, including gas composition, intensity of electric field, electron temperatures, among others (GOLDSTON & RUTHERFORD, 1995, TEZANI *et al*., 2014). Electrons and ions are just a small part of the plasma environment, which may also include, among others (BOGDANOWICZ, 2008, PAPPAS *et al*., 2006):

a) Molecules or atoms with excited electrons – still bound but at higher energy levels than the ground state, therefore more prone to reaction;
b) Neutral, excited or ionized fragments of molecules (e.g. Figure 2.8a and 2.8b);
c) Neutral, excited or ionized atoms which were broken apart from molecules (e.g. Figure 2.8c and 2.8d);
d) New metastable molecules formed from specimens in the plasma medium, for example, C_2 in H_2/CH_4 plasmas (BOGDANOWICZ, 2008)
e) UV and visible radiation.

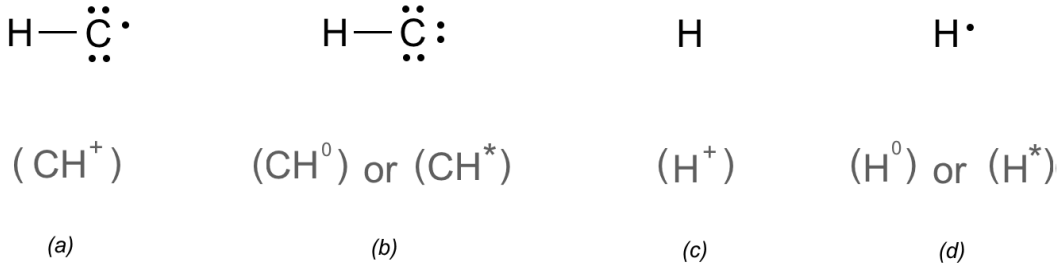

Figure 2.8 – Some examples of specimens that may be present in a H_2/CH_4 plasma environment (BOGDANOWICZ, 2008). The "+" indicates an ionic specimen, "0" a neutral but unstable atom or molecule, while the "*" indicates an excited atom or molecule.

The interaction of the plasma medium with the surface of natural fibers is complex, and many chemical reactions and physical effects can take place simultaneously. As discussed by MUKHOPADHYAY & FANGUEIRO (2009) and RAFFAELEADDAMO *et al*. (2006), processes associated to plasma modification of natural fibers include, but are not limited to:

a) Cleaning - by sputtering or chemical etching of the surface impurities;
b) Ablation - removal of fiber material by physical or chemical means, like erosion, etching, vaporization, sputtering, etc. This usually results in rougher surfaces that can promote higher mechanical interlocking with the matrix;
c) Plasma polymerization – formation of a surface coating from reactions of the gases used, when these have a tendency for polymerization (e.g. methane, ethane, etc.)
d) Surface chemical modification – Incorporation of atoms or functional groups on the surface material itself, usually replacing atoms or fragments of the material removed by the plasma. This can be due to direct reaction or by formation of free radicals followed by reaction with species in the plasma (neutrals or ions) or after exposure to the atmosphere.

The conditions of plasma treatments found in the literature vary greatly due to different techniques, plasma reactor assembly and geometries, gasses used, fibers treated, matrices with which these will be combined and so forth. Throughout the

literature, the expected result reported is always an increase in adhesion between the fibers and the matrix, aiming at better mechanical properties of the resulting composite. Many works have reported improvement in composites tensile strength, elastic modulus or both, as well as in composite flexural and compression strengths (FARUK *et al*., 2012, GURUNATHAN *et al*., 2015, LI *et al.,* 1997, SINHA & PANIGRAHI, 2009, YUAN *et al*., 2004). In annex 1 a table is presented with parameters and results of the most relevant works found in the literature of plasma modification of natural fibers for incorporation in polymeric matrices.

An example of the potential for plasma treatments to promote better interaction between fiber and matrix is the work of ZHOU *et al*. (2011), which used a helium atmospheric pressure plasma system to treat ramie fibers, some of which were pre-soaked in ethanol for 10 minutes. The fibers were then embedded in a polypropylene matrix. It was reported that plasma treatment alone resulted in only a 4% increase in interfacial shear strength (IFSS) due only to roughening of the surface, while fibers soaked in ethanol and then plasma treated had a 50% increase in IFSS, mainly due to the increased hydrophobicity of the fibers, which presented a greater C–C bond concentration and 40% higher contact angle with water.

Of great interest to this thesis are modifications which can turn the natural fibers surfaces hydrophobic. According to SANTOS *et al*. (2012) and SANTOS *et al*. (2013), low pressure SF_6 plasma treatment has led to incorporation of fluorine containing groups on starch, a polysaccharide chemically similar to cellulose. This has changed the starch surface from hydrophilic to hydrophobic, with water contact angle increasing from 45° to almost 120°. SUANPOOT *et al*. (2008) also reported on the potential of SF_6 plasma to increase the hydrophobicity of silk fibers for use in the textile industry. For this reason, SF_6 was chosen as one of the gasses studied in this thesis.

Other works in the literature are discussed in the following sections, which specify the matrices and fibers combinations used in the work presented in this thesis.

2.4. Polypropylene reinforced by wood fibers

Polypropylene (PP) is one of the most produced and consumed polymers in the world thanks to its many advantageous characteristics and properties. It has low cost, simplicity of processing, poses no health issues for workers, can be recycled and may also be burned without generation of toxic emissions (but releasing CO_2 in the process). Polypropylene has low density and good mechanical properties, very good abrasion and fatigue resistances. It is also an excellent electrical insulator and has good water barrier properties. Thanks to all these aspects PP is commonly used in many applications and is also among the most used matrices for composites, including those reinforced with natural fibers (PÉREZ *et al*., 2012, SOBCZAK *et al*., 2012). These natural fiber reinforced PP composites are already in use at various industries, especially automotive and building/construction, where it is used to make products such as fences, decks, outdoor furniture, window parts, roofline product, doors and panels (DÁNYÁDI *et al*., 2007).

As cited in section 2.2.1, nonpolar and hydrophobic matrices like polyolefin, polypropylene included, have poor interaction with natural fibers, which have polar surfaces and are inherently hydrophilic. This causes not only a poor stress transfer between the fiber and matrix, but also difficulty during processing resulting in agglomeration of fibers, pores and defects in the structure (PÉREZ *et al*., 2012, SOBCZAK *et al*., 2012).

Also as noted in section 2.2.1, compatibilization of composites made of polypropylene reinforced with wood fibers can be attempted with many techniques, as reported by PÉREZ *et al*. (2012), such as maleic anhydride modified polypropylene (MAPP) compatibilizer. However, plasma treatments of the fibers have also been reported. Since polypropylene matrices are so predominant, the developments of plasma treatments for compatibilization of natural fibers with this matrix are very relevant and can potentially reach a large market.

YUAN *et al*. (2004) performed low pressure cold plasma treatment on wood fibers with air and Argon plasma, finding improvement in both elastic modulus (20-30%) and tensile strength (10-20%) of the composite with 20 wt% fibers in a polypropylene matrix after treatment at 60 W for 30 seconds at 2 Torr (266 Pa) with air

as the process gas. The improvement was attributed to a rougher surface, leading to better mechanical interlocking.

KIM *et al*. (2013) treated spruce wood powder and waste wood powder with HMDSO (Hexamethyldisiloxane) plasma at atmospheric pressure, using a 3 kV electric field at 17 kHz. The different wood powders were then mixed with polypropylene through extrusion process and the resulting pellets were later injection molded into test specimens. Tensile strength of composites made with waste wood treated with plasma was 21.2 MPa, a 14.6% increase compared to untreated waste wood composites, while elastic modulus increased by 7%. Composites of spruce wood had an increase of 8.8% and 4% in tensile strength and elastic modulus, respectively, after plasma treatment. Using a PVC film as substrate, the authors also report that HMDSO plasma renders the surface hydrophobic due to the decrease in the polar component of the surface energy.

2.5. Polypropylene reinforced by flax fibers

Flax fibers are among the strongest natural fibers in terms of mechanical properties. This is in part due to their high fraction of cellulose combined with low microfibrilar angle (table 2.1). Therefore, they are of great interest in research and industrial application of natural fiber composites. Its elastic modulus is similar to that of E-type glass fibers, and actually superior to glass fibers when comparing specific modulus, even though their ultimate tensile strength is still below that of glass fibers. As MARAIS *et al*. (2005) has shown for composites with unsaturated polyester matrix and untreated fibers, this can be translated to composites of both materials with similar elastic modulus, (40.1 ±4.7) GPa for unidirectional glass fibers (55 wt%) and (42.5 ±3.8) GPa for unidirectional flax fibers (55 wt%). As expected, specific elastic modulus of flax fibers composites was superior to the glass fibers one (31.1 ± 2.8 GPa·cm³/g against 21.2 ± 2.5 GPa·cm³/g).

Few of the works found in the literature deal with plasma treatment of flax fibers, although much research has been made onto this kind of natural fiber (FARUK *et al*., 2012, GURUNATHAN *et al*., 2015). There are also few works in the literature

which report plasma modification of short fibers followed by compounding using high production industrial thermoplastic processing methods, namely extrusion and injection molding. The majority of results reported used single fiber measurements or woven fabrics, where there is a minimum disturbance of the treated surface during composite manufacturing (AGUILAR-RIOS *et al*., 2014, BOZACI *et* al., 2013, LI *et* al., 2013, MAHLBERG *et al*., 1999, SINHA & PANIGRAHI, 2009, SEKI *et al*., 2009, SEKI *et al*., 2010). This preserves the modification caused by plasma and yields high properties improvements. Although these are great methods to study how the plasma treatment changes the interaction of the fibers with the polymer, measuring an optimal improvement, these results cannot be directly used when discussing high volume production techniques.

Extrusion and injection molding cause sheer stresses during flow at high temperatures and can alter or damage the surface, as well as break the fibers to shorter lengths, creating new, untreated surfaces (HO *et* al., 2012, ZAMPALONI *et al*., 2007). The effects of plasma treatment on mechanical properties are somewhat reduced by these mechanisms, but are still detectable and important. Studying the effects of plasma treatment on composites made with high shear stresses during compounding helps to understand the true potential of these techniques on high scale production applications.

The compatibility issues between flax fibers and polypropylene are the same as discussed in sections 2.2.1 and 2.4. The use of MAPP, alkaline treatments, acetylation treatments, among others are reported (FARUK *et al.* 2012). In terms of plasma treatment, BOZACI *et al*. (2013) reported on the treatment of flax fibers with argon and air with atmospheric plasma systems, with later incorporation of the fibers in HDPE (high-density polyethylene) and unsaturated polyester matrices. This treatment increased the adhesion and thus the IFSS (interface shear strength) values in both cases. It was found that plasma treatment increased both the surface roughness and the O/C ratio on the fiber surface, with the addition of the O–C=O functional group. The latter was considered the dominant factor in the increase of adhesion with unsaturated polyester, while the former was the dominant factor for the improved IFSS with a HDPE matrix.

MARAIS *et al*. (2005) performed plasma treatment of nonwoven fabrics of aligned flax fibers in a low pressure, low temperature plasma reactor. Helium was used as treatment gas and the treatment time was 5 minutes with 50 Watts of power. Autoclave treatment was also performed in the nonwoven flax fabric. Composites were

prepared with unsaturated polyester resin (UPR) as matrix by pouring the liquid UPR (with precursor and initiator) onto the fabrics, followed by pressing and later curing. Plasma treatment of the fibers was found to increase elastic modulus by 16%, compared to untreated nonwoven flax, but also led to a reduction of approximately 11% in ultimate tensile strength. The increase in elastic modulus was associated to improved fiber/matrix adhesion due to fewer impurities on the fiber surface. The reduction in tensile strength was related to a decrease in the fibers properties due to damage from the plasma treatment. Meanwhile, autoclave treatment of the fibers has caused both elastic modulus and ultimate tensile strength of the composites to drop by ~8% and ~28%, respectively.

2.6. Thermoplastic starch reinforced by coconut fibers

In general terms, thermoplastic starch (TPS), or plasticized starch, is obtained by disruption of the native granules structure of this material by applying thermomechanical energy in the presence of water and a plasticizer (e.g. glycerol). In this process, the hydrogen bonds between the starch macromolecules (the linear amylose and the larger, ramified amylopectin) are broken and partially replaced by hydrogen bonds with the plasticizer and water. This increases mobility while decreasing crystallinity of the material. As the temperature is reduced below the glass transition temperature, the material becomes rigid again (AVÉROUS & BOQUILLON, 2004).

Since TPS usually has low mechanical properties, the incorporation of a reinforcing phase to create a composite is often desirable. Lignocellulosic fibers are interesting options, since the fibers are also renewable and biodegradable in nature, while also having usually a good adhesion to the matrix (GIRONÈS *et al*., 2012; MÜLLER *et al.*, 2014; WATTANAKORNSIRI & TONGNUNUI, 2014; YU *et al*., 2006).

Although starch matrix and lignocellulosic fibers have a similar chemistry makeup, are both polar and are usually reported as having a good interfacial adhesion (GIRONÈS *et al*., 2012; MÜLLER *et al*., 2014; WATTANAKORNSIRI & TONGNUNUI, 2014; YU *et al*., 2006), other works shows that this is not always the case, and modification of fiber surfaces may lead to better bonding of both phases and improved properties in the composite material (ROSA *et al*., 2009; SATYANARAYANA *et al*., 2009; VILASECA *et al*., 2007). AVÉROUS & BOQUILLON (2004) reported that in

lignocellulosic fibers, the lignin on the surface, which has lower polarity than cellulose, reduces the adhesion and load transfer between the fiber and a TPS matrix, when compared to a cellulose fiber. As a consequence, composites of TPS and lignocellulosic fibers displayed lower mechanical properties than composites made with cellulose fibers of similar aspect ratio and size distribution.

Coconut is an important agricultural product in Brazil, where around 285 thousand hectares are dedicated to its plantation, yielding nearly 2 billion coconut fruits per year (MARTINS & DE JESUS JUNIOR, 2012). The majority of the coconut weight is discarded after consumption or extraction of either the coconut's water or the "meat" (fleshy, white part), creating a large amount of waste that is slow to degrade in nature. Coir fibers can be extracted from the discarded husks, and represent both an economic opportunity and environmental solution to this waste problem (TOMCZAK *et* al., 2007).

In a recent review (GURUNATHAN *et al*., 2015), data regarding coir and other lignocellulosic natural fibers has been compiled. Between the 17 different fibers listed, coir fibers exhibit one of the lowest cellulose content (36 – 43 wt%) and the highest lignin content (41 – 45 wt%). The composition and properties are summarized in table 2.1. This high lignin to cellulose ratio indicates that a surface modification with lignin removal could improve the interaction between a starch matrix and coir fibers, as has been attempted by few authors in the literature.

CORRADINI *et al*. (2006) have shown that a material composed of 35% corn starch, 35% corn gluten, 20% glycerol and 10% coir fiber displays an increase in Young's modulus and ultimate tensile strength of 100% and 76%, respectively, over the matrix without coir fibers. Mercerization (alkaline treatment) of the fibers prior to incorporation in the matrix increased these properties further by 52.2% and 8.3%, respectively.

ROSA *et al*. (2009) reported an increase of about 53% in tensile strength and 17% in tensile modulus for composites made with mercerized coir fibers and a starch/ ethylene vinyl alcohol copolymers blend as matrix, when compared to the same formulation made with untreated fibers. A different treatment of the fibers, bleaching with H_2O_2, has led to lesser improvements, 32% for tensile strength and under 7% for elastic modulus.

3. Materials and methods

The work presented in this thesis was performed initially in Brazil at the Surfaces and Thin Films Laboratory (SFF – *Superfícies e Filmes Finos*), Program of Metallurgical and Materials Engineering (PEMM – *Programa de Engenharia Metalúrgica e de Materiais*) of the Federal University of Rio de Janeiro (UFRJ – *Universidade Federal do Rio de Janeiro*). The compounding of the composites and tensile testing was done at a partner institution in the state of São Paulo, Brazil, the Federal University of ABC (UFABC – *Universidade Federal do ABC*). The materials and methods of these two facilities are presented here in subsection 3.1.

The author has participated in a research exchange program (PDSE-CAPES) and has performed several of the experiments presented here in Germany, at the Department of Lightweight Structures and Polymers Processing (SLK - *Struktur Leichtbau und Kunststoffeverarbeitung*) of the Technical University of Chemnitz (TUC – Technische Universität Chemnitz). The materials and methods used in this institute are described in subsection 3.2.

3.1. Brazil

3.1.1. Materials used

From the natural fibers used, wood fibers type HBS 150-500 were supplied by LIGNOCEL GmbH, Germany. According to the material data sheet supplied by the manufacturer, these fibers are made from selected softwood and have particle sizes in the range of 200 to 400 µm. A random sample of this material was analyzed on a scanning electron microscope and the sizes were measured from the obtained image. The sizes measured ranged from 100 µm to 400 µm in length, with width varying from 20 to 100 µm. The average dimensions calculated were 190 µm (Standard deviation: 63 µm) in length and 50 µm (standard deviation: 19 µm) for width.

A flat wood sheet from the same softwood was also supplied by LIGNOCEL GmbH, Germany, from which sheet samples of 1 cm x 1 cm were cut for further analysis by XPS (section 3.1.7) and water contact angle (section 3.1.9).

The coir fibers, extracted from the mesocarp of the green coconut fruit, were gracefully donated by PROJETO COCO VERDE. These were knife milled and

classified by vibration sieving and the fraction retained in the 125 μm sieve, having passed the 250 μm sieve, was used on this work.

Polypropylene was obtained from BRASKEM PETROQUÍMICA SA. Thermoplastic starch was prepared by a mixture of 70% AMIDEX® 3001 starch powder supplied by CORN PRODUCTS BRASIL and 30% Glycerol.

Sulfur hexafluoride (SF_6) gas with 99.95% purity was supplied by WHITE MARTINS PRAXAIR INC. Oxygen 5.0 (99.999% pure) was acquired from WHITE MARTINS PRAXAIR INC. Methane (CH_4) with 99.95% purity was supplied by WHITE MARTINS PRAXAIR INC. When air treatment is cited throughout this work, no standard pressurized mixture was used. Instead, air from the atmosphere was directly leaked into the reactor through a valve.

3.1.2. Reactor construction in Brazil

The plasma reactor used for the treatments in the Laboratory of Surfaces and Thin Films (SFF), UFRJ, was developed in-house and is shown in figure 3.1. It consists of an RF-induction solenoid or coil (A) around a borosilicate glass tube (B), inside of which the vacuum atmosphere may be controlled by the inflow of gases (C) and restriction of the pump throughput by a valve (D). Inside this outer glass, a second, partially open tube (E) containing the fibers is placed and rotated by an internal step engine (G) for the whole duration of the treatment. Due to the low pressure and low power of this process, the plasma did not caused the surfaces in contact with it to heat excessively, being the glass tube only lukewarm to touch. Therefore, no thermal degradation or burning of the fibers occurred.

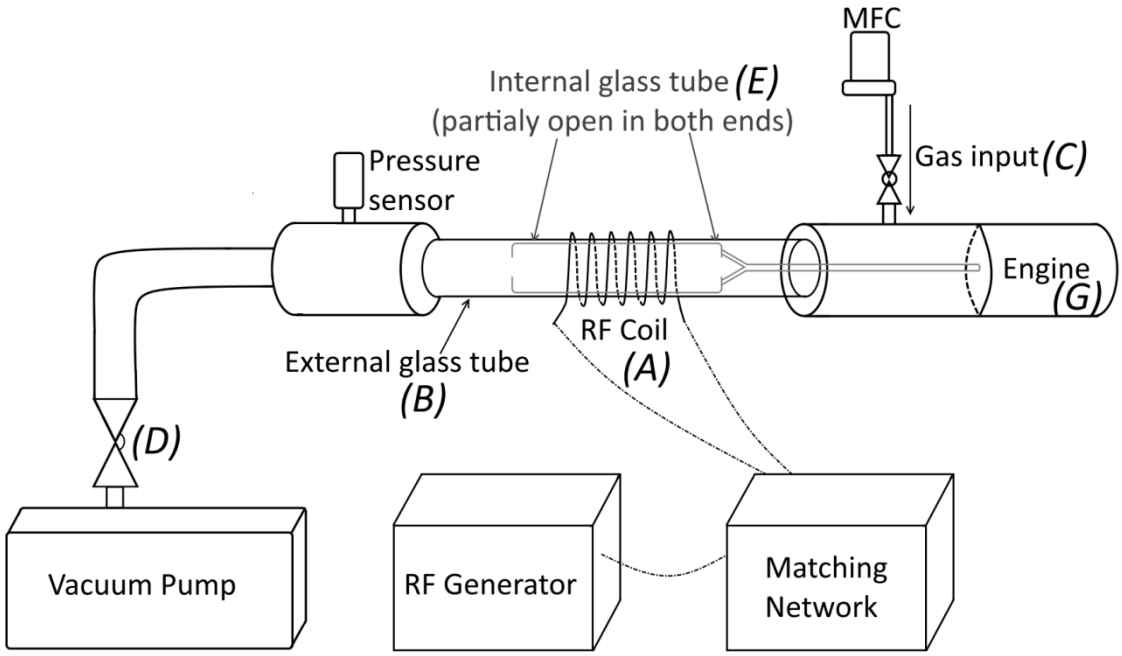

Fig. 3.1. Schematic representation of the plasma reactor built in-house for fiber treatment.

It was possible with such a system to expose to plasma all surfaces of a batch (~5 g) of short fibers. As shown schematically in figure 3.2, while a static system (2.a) would have exposed only one face of the top fibers to the plasma environment, in a rotating system (2.b) the fibers exposed to the plasma were constantly changing in such a way that all sides of all fibers eventually came in contact with the plasma.

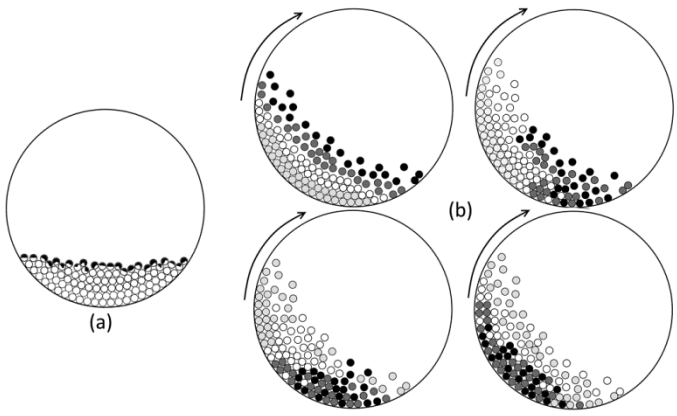

Figure 3.2 (a) Reactor without movement, with only fibers in the black regions being exposed to the plasma. (b) Schematics of movement of the fibers during reactor rotation, color coded to represent the movement.

Given the irregularities of the natural fibers and the differences between the many types of available fibers, a numerical modeling of the complex tumbling movement inside the reactor was not feasible. However, the tumbling motion of fibers inside the reactor can be compared to that of a ball mill used widely in the mineral processing industry. As it has been shown in many works (AGRAWALA *et al*., 1997, MALEKI-MOGHADDAM *et al*., 2013), such a simulation is complex, but there is no indication of stagnation of the balls inside the mill for speeds bellow a critical value. Therefore, given a sufficiently long treatment time compared to the time of a single rotation, it can be assumed that, on average, all fibers are exposed to the plasma for similar times.

A simplified model is presented in equation 3.1, which yields the ratio of volume of fibers exposed at a given moment over the total volume of fibers in the reactor. It is important to note that the movement in the reactor was fast enough to allow fibers to rise and fall in a tumbling motion, but the geometry of the stacked fibers remained approximately like that schematically shown in figure 3.3a. The total volume of fibers in the cylindrical sample holder was calculated as the length (l) multiplied by the area of the circle segment occupied by the fibers, given as a function of the cylinder radius (R) and the height of the fibers (h), as shown in equation 3.2. Equation 3.3 represents the exposed fibers volume, calculated as a rectangular cuboid with the following dimensions: length (l) of the tube; chord length (a), shown in figure 3.3a; and plasma “penetration depth” (d) into the fibers. Since the interaction of the plasma specimens are limited to the very surface of the exposed materials (at the power levels used in this work), the “penetration depth” is actually related to the roughness of the surface formed by the fibers aggregate. Considering the broad distribution of fiber sizes and aspect ratios, as well as the constant change of the apparent surface due to sample holder rotation, the determination of a precise value for the variable “d” is not practical. Therefore, for the purpose of approximation, the value is assumed to be half the average length of the fibers. As shown schematically in figure 3.3b as it is believed that fibers would “stick out” from the apparent surface, but if they are too far up they would fall.

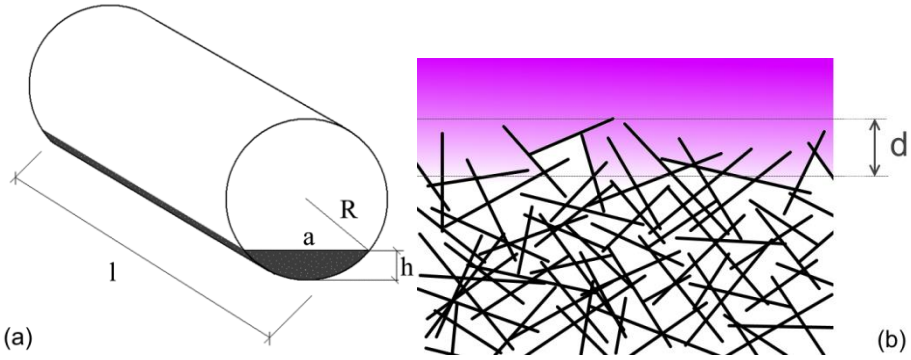

Figure 3.3 – Schematic representation of the geometry of sample holder with fibers (a) and schematic representation of the plasma "penetration" in the stacked fibers (b)

$$\frac{V_{exposed}}{V_{total}} = \frac{d.2.\sqrt{h(2.R-h)}}{R^2\cos^{-1}\left(\frac{R-h}{R}\right)-(R-h)\sqrt{h(2R-h)}} \quad (3.1)$$

$$V_{total} = l\left(R^2\cos^{-1}\left(\frac{R-h}{R}\right) - (R-h)\sqrt{h(2R-h)}\right) \quad (3.2)$$

$$V_{exposed} = l.d.2.\sqrt{h(2.R-h)} \quad (3.3)$$

Considering the continuous movement and assuming that the treatment time is long enough to allow thorough and homogeneous mixing, it can be said that a single fiber will have occupied all possible positions inside the moving cylinder. If that is the case, then the ratio 'time exposed/time not exposed' for one given fiber is approximately the same as the ratio 'volume of exposed fibers/volume of non-exposed fibers'. Thus, the effective treatment time (t_{eff}) for each fiber in a batch is given by equation 4.

$$t_{eff} \cong t_{total} \times \frac{V_{exposed}}{V_{total}} \quad (3.4)$$

The radiofrequency power source used was an RFN600A with 13.56 MHz frequency from ADVANCED ENERGY, USA, connected to a matching network built in-house using two variable capacitors. The vacuum pump used was a PASCAL 2010SD from ADIXEN (ALCATEL ®) and the pressure sensor was a Pirani-type SENSIFIL DW100P from SENSUM, Brazil.

3.1.3. Plasma treatment conditions

The procedure for treatment was as follows:

a) First, the inside of the reactor glass tube and the sample holder were cleaned with a compressed air pistol and later isopropyl alcohol to avoid any cross contamination of the vacuum and plasma. Nitrile gloves were worn at all times to avoid contamination of the parts exposed to the vacuum with sweat, skin fat and so on.
b) Approximately 5 grams of fibers were weighted and then added to the sample holder (internal glass tube, as in figure 3.1). This was inserted in the reactor and attached to the engine axis, so it could be rotated later.
c) The reactor was closed and then pumped using a rotary vane (mechanical) vacuum pump. The pump was connected to the reactor chamber by a diaphragm valve, which was opened slowly at first to stop the fibers from being sucked by the strong pressure drop.
d) Once the pressure dropped below 10 Pa (10^{-1} mbar), the engine was started, causing the sample holder to rotate and the fibers to fall in a tumbling movement. This caused a temporary rise in pressure due to release of trapped gas.
e) The chosen process gas was inserted in the chamber by a needle valve or mass flow controller (MFC), rising the pressure to nearly 10^2 Pa (1 mbar) while still pumping. This pressure was maintained for 2 minutes, and then the gas input was closed. After 2 to 5 minutes of further pumping, this procedure was repeated. This helped the pressure to drop faster, carrying the humidity which constantly desorbs from the fibers at first, and ensured that leftover gasses would contain manly the desired gas. The system was then pumped to a base pressure near 10^{-1} Pa (10^{-3} mbar).
f) Once base pressure was reached, the desired gas was inserted in the system by the valve/MFC, while still pumping, up to a pressure of 10 Pa (10^{-1} mbar) for air, SF_6 and CH_4. For oxygen, a pressure of 5 Pa was used, since at this pressure the intensity of the plasma was visibly higher. The gas flow was kept for 5 minutes to guarantee its stability and the purity of the atmosphere in the reactor.
g) The plasma source was turned on and the matching network was adjusted for minimal reflected power. The value of “load power”, as

displayed in the power source, was controlled and used as the parameter for plasma treatment.

h) Once the desired time was elapsed, the power source was turned off. Gas flow was maintained for another 5 minutes, to carry away any undesired reaction products.

i) Gas flow was closed and shortly after the vacuum pump valve was also closed.

j) The vacuum was broken slowly with a needle valve, to avoid blowing the fibers out of the sample holder. Once atmospheric pressure was reached, the reactor was opened, the sample holder removed and the treated fibers were collected.

The first tests of plasma treatment of wood fibers had the goal to evaluate how SF_6 would compare to other gases at the same conditions. Two other gases were used, with very distinct effects: air plasma for etching, increasing surface roughness and contact area to the matrix; and methane (CH_4) for surface polymerization, creating a hydrocarbon-like coating, chemically similar to the polypropylene, chosen as the matrix material. The plasma treatment conditions were 50 Watts and 30 minutes, based on previous experiments in the reactor. These samples of treated wood fibers (table 3.1) compounded with PP are called “Group 1” throughout this work.

Table 3.1 – Plasma treatment conditions for the “group 1” samples of wood fibers.

Material	**Power (W)**	**Time (minutes)**	**Gas**
Wood fiber (HBS 150-500)	50	30	SF_6
Wood fiber (HBS 150-500)	50	30	Air
Wood fiber (HBS 150-500)	50	30	CH_4

After SF_6 plasma was found to have greater effectiveness in increasing mechanical properties of the composite (as will be discussed in sections 4.1 and 5.1), a factorial experiment design was made to evaluate the effect of treatment time and power in these properties. The condition of 50 W for 30 minutes was also repeated for confirmation of the results found. Table 3.2 presents the conditions of the experimental design, as well as the repeated condition for confirmation of the results. This group of treatment conditions on wood fibers and the resulting composites with PP matrix are called “Group 2” throughout this work.

Table 3.2 – Plasma treatment conditions for the “group 2” samples of wood fibers.

Material	Power (W)	Time (minutes)	Gas
Wood fiber (HBS 150-500)	50	30	SF_6
Wood fiber (HBS 150-500)	30	10	SF_6
Wood fiber (HBS 150-500)	60	10	SF_6
Wood fiber (HBS 150-500)	30	40	SF_6
Wood fiber (HBS 150-500)	60	40	SF_6

For wood sheet samples, the procedure for plasma treatment was analogous to that of wood fibers, but the samples were placed in a glass slab, which in turn was inserted in the plasma reactor. Also, the engine was not activated, since nothing was attached to it. The sheet samples were plasma treated at 60 W power for 4, 10 and 40 minutes, being two samples treated in each condition. Because these were laid on the reactor with no movement, the surface was exposed during the whole treatment time to the plasma, in contrast to the treatment of the fiber samples as described in subsection 3.1.2. Thus, the 4 minutes treatment was performed as an approximation to the actual effective time on the fibers treatment, aiming at similar level of modification. It was expected that, due to similar chemical and structural characteristics, these samples would respond similarly to the plasma treatment.

Treatments of coconut fibers followed the same procedure described here on items (a)-(j). Different plasma conditions were used to evaluate the effect of power and effective treatment time in the modification of coir fibers, which are summarized in table 3.3. The batches, which will be called “standard batches” here, had approximately 5 grams, with each fiber being exposed to the plasma for approximately 12% of the total time, as described in section 3.1.2. To further study the effect of the plasma treatment on the fibers, 60 minutes treatments were carried out on a reduced amount of fibers (0.1g) for both gases using 50W and 80W power (table 3.3). That way, surfaces would be exposed to the plasma for nearly the entire duration of the treatment, revealing more clearly the morphological and chemical effects of plasma etching. These will be addresses as “micro batch”.

Table 3.3 – Plasma treatment conditions for coir fibers in the Standard and Micro batches.

Condition name	Gas	Treatment time (minutes)	Plasma power (W)	Batch	Fiber amount (g)	Effective treatment time (minutes)
[Air/60min/50W]	Air	60	50	Standard	5	7.2
[µ/Air/60min/50W]	Air	60	50	Micro	0.1	60
[Air/60min/80W]	Air	60	80	Standard	5	7.2
[µ/Air/60min/80W]	Air	60	80	Micro	0.1	60
[O_2/60min/50W]	Oxygen	60	50	Standard	5	7.2
[µ/O_2/60min/50W]	Oxygen	60	50	Micro	0.1	60
[O_2/60min/80W]	Oxygen	60	80	Standard	5	7.2
[µO_2/60min/80W]	Oxygen	60	80	Micro	0.1	60

3.1.4. Composites preparation

Untreated and treated wood fibers from “Group 1” and “Group 2” (refer to section 3.1.3) were compounded with polypropylene pellets. No additives were used. A total of 40 grams of material was inserted in the mixer MH-50H from M.H. EQUIPAMENTOS, Brazil, being 33.20 grams of PP pellets and 6.80 grams of wood fibers, i.e. 17wt% of fibers in the polymer. The mixer was closed and activated at low rotation (1800 RPM) for 15 seconds, followed by another 15 seconds at high rotation (3600 RPM). After shut down of the mixer, the melted mass was removed and placed between two flat steel plates with a 2 mm spacer on the borders and placed in a hot press, also from M.H. EQUIPAMENTOS. The melted mass was pressed for 15 seconds at 60°C temperature with 8 Tons force, resulting in a disc with thickness of approximately 2 mm. These were later cut using a cutting tool and hydraulic press into tensile test specimens with working area of 15 mm x 5.3 mm x 2 mm, according to ASTM D1708-6a standard. Figure 3.4 shows pictures taken during some of the steps described.

It was observed in preliminary test that specimens cut in the radial direction had higher mechanical properties. This was associated with the partial orientation of the fibers with respect to the flow direction of melted polymer during compression molding, as observed by visual inspection. As the polymer flows from the central fused mass towards the borders of the mold, the fibers become partially oriented in the radial

direction. Given this consideration, samples analyzed here were cut in the radial direction or as close to it as possible, to reduce data dispersion.

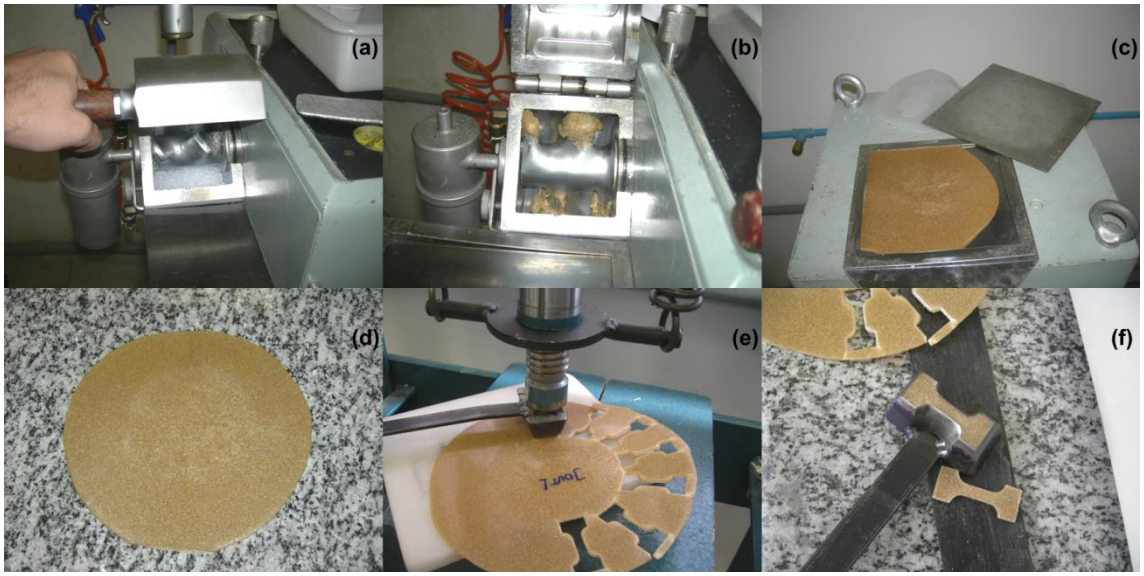

Figure 3.4 – Picture illustrating the composite fabrication procedure. (a) pellets inside the mixer; (b) melted mass after mixing; (c) and (d) disc formed by compression molding and; (e) and (f) cutting of the tensile test specimens with cutting tool and press.

Coir fibers composites with thermoplastic starch matrix were processed in the same machines and procedure described here. The differences are:

a) The matrix material (thermoplastic starch or TPS) was a mixture of 70% starch and 30% glycerol (plasticizer).
b) 20wt% of coir fibers was added to the TPS matrix when making the composites.
c) Before cutting, the compression molded 2 mm thick discs were conditioned under controlled air humidity of 50% for 30 days.

3.1.5. Mechanical testing

All tensile specimens (pure polymers and composites) were of the ASTM D 1708-6a standard, with the gauge section measuring 15 mm x 5.3 mm x 2 mm. Tensile testing was performed in an INSTRON 3369 tensile testing machine with a load cell of

50 kN and the load speed used was 10 mm/minute. Between 7 and 10 samples of each condition were tested, according to how many good samples could be cut from each composite disc.

The results of elastic modulus and ultimate tensile strength were analyzed for the null hypotheses ("do the means differ?") by one-way ANOVA with significance level of 0.05 (α=0.05 or 95% confidence interval). Calculations were done in the software Minitab 16.1 statistical Software, from Minitab Inc.

3.1.6. FTIR

Infrared spectroscopy (FTIR) spectra were obtained in the range of 400 to 4000 cm^{-1} with a NICOLET 6700 spectrophotometer from THERMO SCIENTIFIC, using 64 scans averages for each spectrum. Data processing was done according to the procedure explained by PANDEY & PITMAN (2003), where the area of cellulose related peaks are used as reference and analyzed compared to lignin peaks. The areas were measured using the software "OMNIC Spectra" from THERMO SCIENTIFIC.

3.1.7. XPS

X-ray photoelectron spectroscopy (XPS) analysis were carried out in a SPECS assembly with a XR50 X-ray source with an aluminum anode ($K\alpha_{1/2}$= 1486.6 eV) and PHOIBOS 100 hemispherical energy analyzer. Due to the susceptibility of carbon-fluorine bonds to X-rays, as reported by FERRARIA *et al*. (2003), the acquisition sequence was as follows:

1) High-resolution spectrum of carbon, scanning binding energies from 280 to 300 eV;

2) Full spectrum, scanning binding energies from 0 to 1200 eV;

3) High-resolution spectrum of oxygen, scanning binding energies from 526 to 540 eV.

Analysis and quantification of elements found was carried out using CasaXPS, software provided by the spectrometer manufacturer. The full spectra were used to calculate the atomic fractions of each element present in the samples, as well as the

elemental ratios, like oxygen-to-carbon (O/C). High-resolution spectra were deconvoluted into Gaussian shaped components, each representing different chemical bonding states of the element analyzed. This can be done since the atoms to which a certain element is bonded cause a change in the bonding energy of the core electrons, which in turn is seen as a shift in the energy of the electron, as detected by XPS. For example, a fluorine atom bonded to a carbon atom will attract the shared electron pair more strongly, due to fluorine high electronegativity. This reduces the effective negative charge around the carbon atom, meaning that the nucleus positive charge will draw all core electrons slightly "closer" to it. This results in an increase of the measured binding energy, which in this example, is shifted from 284.6 eV to 289.5 eV. Analyzing the shifted components which make up a certain elements XPS peak, it is possible to quantify the fraction of such atoms in the sample which are bonded to certain other atoms, as shown by FERRARIA *et al*. (2003), LI & JINJIN (2007), YUN *et al.* (2007) and others.

3.1.8. SEM

To evaluate changes to the surface morphology of the fibers after plasma treatment, these were observed by scanning electron microscopy (SEM). The fibers were placed over a conducting adhesive tape and coated with a thin film of gold, to make the fibers surface conductive.

The microscope used was a JSM-6460LV from JEOL, USA. Secondary electron imaging was used with electron acceleration of 20 kV or 15 kV, according to the fibers sensitivity to damage by the electron beam.

The fracture surfaces of the tested tensile specimens were also observed under scanning electron microscopy (SEM) to evaluate changes in the fracture mechanism. The fractured samples were fixated in a stub sample holder and coated with a thin film of gold, to ensure conductivity of the observed surface. The microscope used and the analysis conditions were the same as in the case of the fibers.

3.1.9. Contact Angle

The water contact angle measurements for natural fibers are challenging. Although the Washburn method can theoretically be used for measurements of

compacted small fibers (YUAN & LEE, 2013), this requires a known and regular pore structure in the compacted fiber structure. This is nearly impossible to guarantee with natural fibers, given the already discussed variability in size, aspect ratio, surface energy and so on.

To measure the effect of plasma treatment on wood fibers, a flat sheet of the same kind of wood was obtained from the same manufacturer. These were cut into 1 cm x 1 cm squares and plasma treated according to section 3.1.3. The water contact angle of these sheet samples were then measured by the sessile drop method (YUAN & LEE, 2013) in a NRL A-100-00 RAME-HART Goniometer. The contact angle value was measured in both sides of the drop profile for 10 seconds, acquiring 100 points which were then averaged. This was repeated at least 5 times for two samples for each condition. One measurement lasting 5 minutes was also performed to evaluate the diminishing contact angle due to absorption of the droplet.

3.2. Germany

3.2.1. Materials used

For the plasma treatments and composites made at SLK-TUC, different materials were used. Flax fibers of two different kinds were used. The first was a technical fiber “TechnoFlax”, which are chopped short fibers from the plant bast or stem, supplied by SachsenLeinen e.V. The fibers lengths are not regular, but most fall between 3 and 4 mm (as will be shown in section 4.2.1). The second was a micronized flax fiber supplied by Texilis. The fibers are mostly ribbon-like in shape and their size distribution was measured by SEM as 450(±170) µm x 25 µm x 3 µm (also shown in section 4.2.1).

Wood flour type JELUXYL WEHO 500 s were supplied by JELIPLAST, Germany. The wood flour particles had sizes between 100 µm and 200 µm and were produced from spruce and fir wood, according to the manufacturer.

Sisal fibers type VF 4160 were supplied by SACHSEN-LEINEN e.V., Germany. These were extracted from the bole (i.e. trunk) of the plant and had lengths of 2 mm to 4 mm, according to the manufacturer.

For composites made with polypropylene matrix, pellets of BE170M0 from BOREALIS, Austria, were used. PLA matrix composites used INGEO™ 4043D pellets from NATUREWORKS.

All gases used in the plasma reactor at SLK-TUC were supplied in pressurized cylinders by PRAXAIR GmbH, Germany. Argon gas had 99.998% purity (Also known as 4.8 purity), oxygen had 99.999% purity (5.0) and sulfur hexafluoride (SF_6) had 99.9% purity (3.0).

3.2.2. Plasma Reactor PICO

Plasma treatments were performed in a cold plasma reactor model PICO VERSION C from DIENER ELECTRONIC GmbH, Germany, configured as shown in figure 3.5. The provided rotary drum for powder samples was used, which consisted of a square cross-section glass laboratory bottle, as also shown in figure 3.5. Each treatment batch consisted of 6.5 grams of fibers, which were rotated inside the glass bottle for the whole treatment, exposing different fibers to the plasma at each moment, analogous to the reactor used at SFF-UFRJ described in section 3.1.2. As is the case of the Brazilian reactor, it is expected that, given the long treatment time in relation to the rotation period, all fibers had a similar average exposure time. In this case, this is estimated to be in the order of 10% or less of the total treatment time.

Figure 3.5 Low pressure plasma system PICO from DIENER ELECTRONIC GmbH and details of the plasma chamber with the squared section glass bottle (sample holder).

The power source had a 40 kHz frequency with adjustable power varying from 0-500 W. One of the electrodes was located at the bottom of the chamber, where the opening of the glass bottle would touch. The other electrode was a long tube, which also served as gas entrance, covering most of the length of the glass bottle. The two were separated by approximately 3 centimeters of insulating material. This arrangement is shown schematically in figure 3.6.

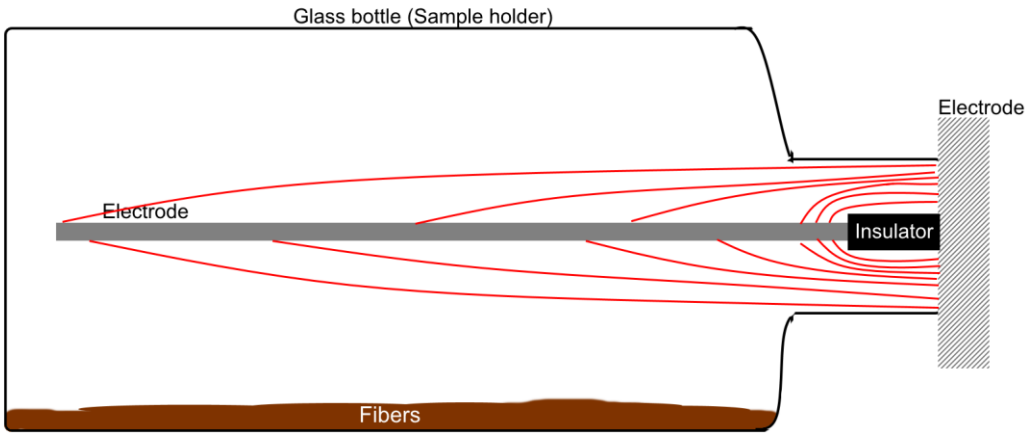

Figure 3.6 – Side view cut from the plasma reactor chamber, showing the main components in the system and a schematic approximation of the electric field distribution (red lines)

Feeding of the gas was done by a needle valve for SF_6 and by mass flow controllers (MFCs) for argon and oxygen. The system was automated, meaning that a program could be created and that the plasma system would maintain the desired conditions and change from one step to the other automatically as the programed variable was reached (pressure, time, etc.). The chamber could also be heated from resistors build around the walls. The vacuum pump was a LAYBOLD D16BCS rotary vane pump.

3.2.3. Plasma treatment conditions

On the time working in the Techniche Universtität Chemnitz (TUC), many series of experiments have been performed. Table 3.4 summarizes the different series presented here, listing the fibers treated and the range of parameters as well as gasses used. Other series of treatments were also performed, but the results were not always relevant and in some cases not all conditions were tested, due to limited time. These are presented in annex 2.

Table 3.4 Different series of plasma treatments performed at TUC.

Series name	Fiber type	Plasma power	Treatment time	Gases used
'A-B Series'	Wood, Sisal, Technical flax, Micronized flax.	150-200W	30-180min	SF_6, O_2, O_2 followed by SF_6.
'E Series'	Wood, Micronized flax.	200W	120-180 min	SF_6 (73%) combined with Ar (27%).
'L Series'	Wood, Sisal, Technical flax, Micronized flax.	200W	120-180 min	SF_6, O_2, O_2 followed by SF_6.

The plasma system available at TUC was operated following the procedure described in the steps bellow.

a) While wearing nitrile gloves, 6.5 grams of the fibers to be treated were placed inside the sample holder (glass jar), which was previously cleaned with pressurized air and isopropyl alcohol.
b) The sample holder was placed inside the reactor, the door was closed and the system was pumped down. The chamber is simultaneously heated to 50°C to speed up, even if slightly, the desorption of gases and humidity inside the system.
c) To help remove residual gas trapped between the fibers, the rotation of the sample holder is started at a pressure of approximately 10^3 Pa (10 mbar). The system is then further pumped until a pressure of 50 Pa ($5x10^{-1}$ mbar) or lower was reached.
d) The chosen gas for the treatment was inserted in the chamber until a dynamic pressure of $5x10^2$ Pa (5 mbar) was reached, then this gas flux was maintained for 2 minutes and the gas input was closed after the time elapsed. After 2 to 5 minutes of further pumping, this procedure was repeated. This helped the pressure to drop faster, carrying the humidity which constantly desorbs from the fibers at first, and ensured that leftover gasses would contain manly the desired gas. The system was then pumped to a base pressure near 20 Pa ($2x10^{-1}$ mbar).
e) Once base pressure is reached, the automatic program was started.
f) The first step of all treatments consisted of a cleaning step with argon, which also helped speed up the removal of water from the fibers. The conditions were:

a. Gas: Argon (100%)
b. Pressure: 42 Pa (0.42 mbar)
c. Time: 7 minutes
d. Power: 125 W
e. Rotation: 40 seconds on, 10 seconds off
f. Wall heating: off

g) Once complete, the plasma and gas input was turned off and the system was pumped further until reaching a base pressure of 10 Pa (10^{-1} mbar). When the pressure was reached, the next step automatically started.

h) The conditions were varied according to the desired treatment, as further detailed in tables 3.4, 3.5 and 3.6. A maximum time of 1h was stipulated, to avoid damage to the electrode, so treatments with 2 or 3 hours consisted of repetitions of the following program with 15 minutes interval for cool down (in vacuum).
   a. Gas: SF_6 (100%) / O_2 (100%) / SF_6 (73%) and Ar (27%)
   b. Pressure: 30 Pa [SF_6] / 39 Pa [O_2] / 55 Pa [SF_6+Ar]
   c. Time: 30-60 minutes
   d. Power: 150-200 W
   e. Rotation: Always on
   f. Wall heating: off

i) Once the treatment was complete, plasma and gas input were turned off and the system was left under vacuum for 10 minutes, to allow the electrode to cool down and for any undesired products to be pumped out.

j) The vacuum was broken slowly with a needle valve, to avoid blowing the fibers out of the sample holder. Once atmospheric pressure was reached, the reactor was opened, the sample holder removed and the treated fibers were collected.

Tables 3.5, 3.6 and 3.7 show the plasma treatment conditions and names for the samples of the A-B series, E series and L series, respectively.

Table 3.5 Treatment conditions of fibers of the “A-B series” prior to compounding.

Sample name	Fiber type	Gas	Plasma power	Treatment time
TF1	Technical flax	-	*Untreated*	*Untreated*
TF2	Technical flax	SF_6	150W	30 min
TF3	Technical flax	SF_6	200W	60 min
TF4	Technical flax	SF_6	200W	180 min
MF1	Micronized flax	-	*Untreated*	*Untreated*
MF2	Micronized flax	SF_6	200W	60 min
MF3	Micronized flax	SF_6	200W	180 min

Table 3.6 Treatment conditions of fibers of the “E series” prior to compounding.

Sample name	Fiber type	Gas	Plasma power	Treatment time
MF-E0	Micronized flax	-	*Untreated*	*Untreated*
MF-E1	Micronized flax	SF_6+Ar	100W	30 min
MF-E2	Micronized flax	SF_6+Ar	200W	30 min
MF-E3	Micronized flax	SF_6+Ar	200W	180 min

Table 3.7 Treatment conditions of fibers of the “L series” prior to compounding.

Sample name	Fiber type	Gas	Plasma power (watts)	Treatment time (minutes)
PLA-L1	(pure polymer)	-	-	-
HW-L1	Wood flour	-	*Untreated*	*Untreated*
HW-L2	Wood flour	O_2	200	120
HW-L3	Wood flour	SF_6	200	120
HW-L4	Wood flour	O_2/SF_6	200	120 (O_2) + 60 (SF_6)
SI-L1	Sisal	-	*Untreated*	*Untreated*
SI-L2	Sisal	O_2	200	120
SI-L3	Sisal	SF_6	200	120
SI-L4	Sisal	O_2/SF_6	200	120 (O_2) + 60 (SF_6)
FL-L1	Technical flax	-	*Untreated*	*Untreated*
FL-L2	Technical flax	O_2	200	120
FL-L3	Technical flax	SF_6	200	120
FL-L4	Technical flax	O_2/SF_6	200	120 (O_2) + 60 (SF_6)
MF-L1	Micronized flax	-	*Untreated*	*Untreated*
MF-L2	Micronized flax	O_2	200	120
MF-L3	Micronized flax	SF_6	200	120
MF-L4	Micronized flax	O_2/SF_6	200	120 (O_2) + 60 (SF_6)

3.2.4. Composites preparation

A HAAKE MINI-LAB micro-extruder with co-rotating screws (figure 3.7) was used to mix the fibers and polymers to prepare the composites at SLK-TUC. This machine worked together with a HAAKE MINI-JET II mini-injection molding machine (figure 3.8). The material leaving the micro-extruder (figure 3.8-A) was loaded directly into the hot cylinder (figure 3.8-B) until filled. This was then placed over the mold (figure 3.8-C) and a pneumatic piston pressed and injected the material.

Figure 3.7 – Mixing chamber with capillary channel and screws of the HAAKE MINI-LAB micro-extruder. “v” indicates the valve that controls the melted material flux and “e” indicates the exit opening.

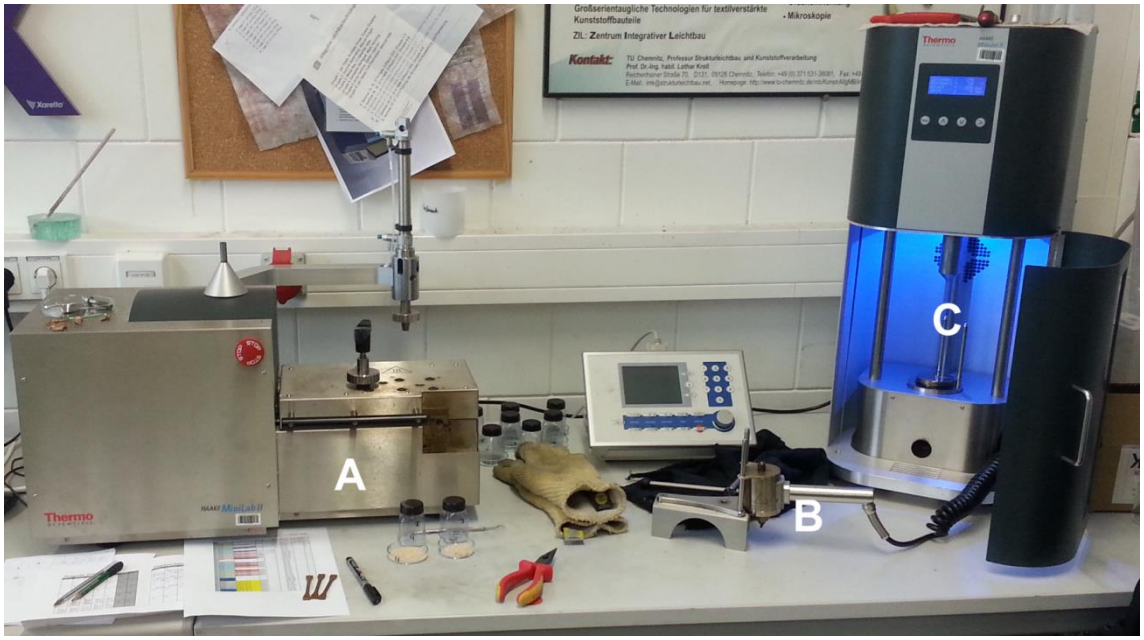

Figure 3.8 – Experimental bench at SLK-TUC, showing the HAAKE MINI-LAB (A), the hot cylinder of the HAAKE MINI-JET II (B) and the injection molding machine's main body, with the piston at the top and mold on the bottom (C).

The fibers and polymer pellets are added through the feeding opening and pressed manually into the system. The rotation of the screws drives the mixture forward and then in the capillary cannel that takes back to the base of the screws, as can be seen in figure 3.7. The material remained in the closed loop circuit until the mixing time was completed, then the valve at the end of the screws channel (indicated as "v" on figure 3.7) was switched from "cycle" to "flush", and the melted mass left the chamber through a fontal opening (indicated as "e" on figure 3.7). The hot cylinder of the MINI-JET II was placed at this exit point, where it was filled. The hot cylinder was then placed over the mold that was maintained at a controlled temperature. The pneumatic cylinder applied the injection pressure for a specified amount of time, followed by a post injection pressure for another specified time. Once finished, the mold was removed from the machine and opened. In all experiments reported here a mold of the tensile specimen ISO/DIN-527-2 was used.

A preliminary study was performed to select the compounding and injection conditions, based on manufacturer recommendations. For the A-B series, the following parameters were used:

a) Micro-extruder
    a. Temperature: 190 °C
    b. Screw rotation: 50 RPM
    c. Mixing time: 7 minutes
b) Mini-injection molding
    a. Hot cylinder temperature: 190 °C
    b. Injection pressure: 690 bar
    c. Injection time: 5 seconds
    d. Mold temperature: 50°C
    e. Post injection pressure: 300 bar
    f. Post injection time: 15 seconds

The composites made in the “E series” used the same parameters, except the mixing time, which was 2 minutes.

For the L series, the following parameters were used:

a) Micro-extruder
    a. Temperature: 180 °C
    b. Screw rotation: 50 RPM
    c. Mixing time: 7 minutes
b) Mini-injection molding
    a. Hot cylinder temperature: 180 °C
    b. Injection pressure: 950 bar
    c. Injection time: 5 seconds
    d. Mold temperature: 65 °C
    e. Post injection pressure: 200 bar
    f. Post injection time: 15 seconds

3.2.5. Mechanical testing

All tensile specimens (pure polymers and composites) were of the ISO/DIN-527-2. Tensile testing was performed in a Zwick/Roell Z010 machine with a 10 kN load cell, deformation rate of 1mm/min in the elastic regime and 5mm/min during plastic deformation. The lower deformation rate at the elastic regime was used to improve the sensitivity of the test to measure the elastic modulus of the materials. The longer

deformation time was not enough to cause deviation in the elastic region due to viscoelastic behavior. For reference, annex 3 shows some of the typical stress-strain curves obtained for different materials.

The results of elastic modulus and ultimate tensile strength were analyzed for the null hypotheses (“do the means differ?”) by one-way ANOVA with significance level of 0.05 (α=0.05 or 95% confidence interval).. Calculations were done in the software Minitab 16.1 statistical Software, from Minitab Inc.

4. Results

In this section the most relevant results obtained are presented, organized by sub-sections that will later be discussed in section 5. Throughout the research for this thesis, many more results were obtained, but not all were as significant. Thus, they are presented at the end of the text in the annex 2.

4.1. Wood fibers for incorporation in PP matrix

Plasma treatments of softwood fibers (LIGNOCEL® HBS 150-500) were performed using three distinct gasses (air, methane and sulfur hexafluoride) in a single set of conditions, as described in section 3.1.3, here called the “Group 1”. After compounding the treated and untreated fibers with polypropylene matrix, tensile tests were carried out. The elastic modulus results are presented in figure 4.1 and the ultimate tensile strength can be found in the table 4.1.

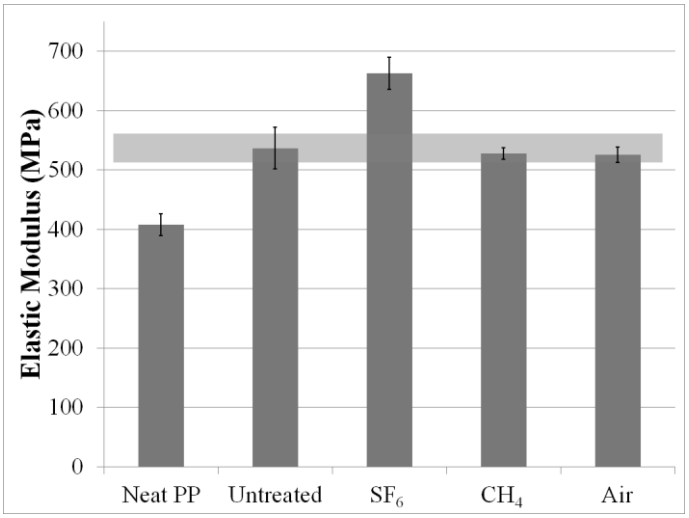

Figure 4.1 – Elastic modulus results of the composites made with the Group 1 wood fibers before and after plasma treatment (30 minutes, 50 W) in different gases.

Table 4.1 – Ultimate tensile strength (U.T.S.) of composites made with the Group 1 wood fibers before and after plasma treatment (30 minutes, 50 W) in different gases.

	U.T.S (Mpa)	S.D.
Neat PP	21.2	2.10
Untreated	24.5	2.21
SF_6	24.3	1.22
CH_4	23.5	1.56
Air	24.3	0.76

The addition of 17 wt% of untreated wood fibers in the polypropylene matrix has caused a 32% increase in elastic modulus, from 408 MPa to 537 MPa. Ultimate tensile strength also seems to improve by 15%, but due dispersion in the data, this is not statistically significant. It is also clear from table 4.1 that ultimate tensile strength of the composites had no significant change between the different plasma treatments and the untreated fibers.

Compared to composites made with untreated fibers, the ones made with methane (CH_4) and air treated fibers show no significant change, as indicated by the gray horizontal bar in figure 4.1, which represents the 95% confidence interval as calculated by ANOVA. Composites made with SF6 treated fibers, however, present a distinctive 23% increase in elastic modulus compared to composites of untreated fibers. Compared to the samples of pure polypropylene, the increase is of 63%, from 408 MPa to 663 MPa.

The “Group 2” samples, which tested composites of fibers treated with different plasma parameters of power and time while using only SF_6 as gas, confirmed the results for the “30 minutes, 50 W” condition, as seen in figure 4.2. The “Group 1” results are combined in the graphic to highlight the similar tendency. It can be seen that the treatment condition with the highest levels (60 W for 40 minutes) shows the best results with an elastic modulus of 655 MPa versus 527 MPa for untreated fibers, a 24% increase.

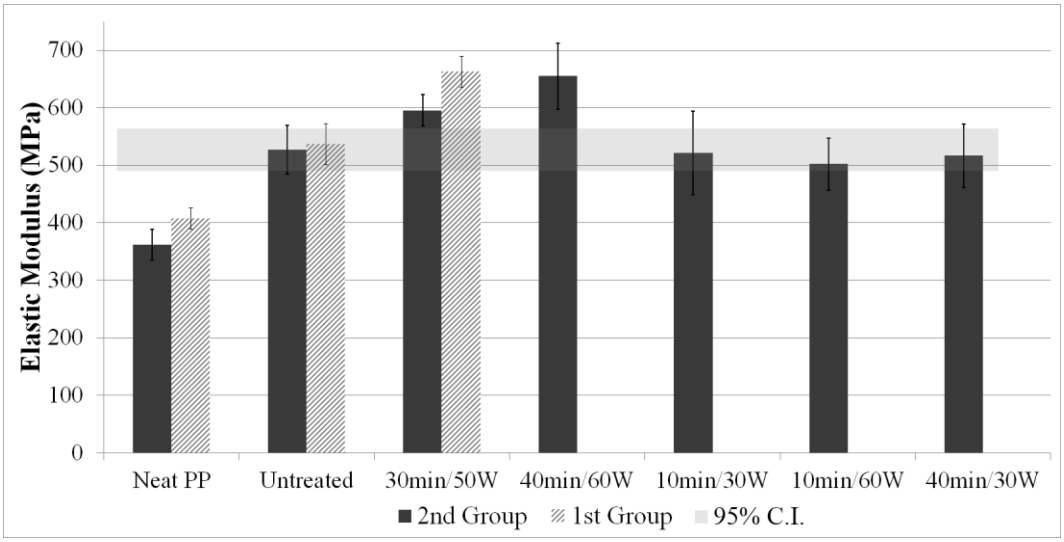

Figure 4.2 – Elastic modulus results of the composites made with the Group 2 wood fibers before and after plasma treatment with SF_6 in different treatment conditions.

Fibers treated at lower powers and for shorter times than 50 W and 30 minutes resulted in composites with no significant change in elastic modulus. This indicates a minimum threshold for these two conditions to introduce effective changes on the fibers' surfaces. The Analysis of Variance (ANOVA) on the factorial experiment design indicates that the effect on the elastic modulus is influenced by both time ($F=9.16$; $p=0.007$) and power ($F=6.86$; $p=0.016$), as well as the combination of both factors ($F=10.34$, $p=0.004$).

As for the composites from "Group 1", the addition of 17 wt% of wood fibers in the matrix resulted in an increase in ultimate tensile strength, when compared to the pure polypropylene. Results are presented in table 4.2, and in this group of samples, the improvement of U.T.S. from pure polypropylene to the composites is statistically significant. The variation between the composites U.T.S., however, is not significant.

Table 4.2 – Ultimate tensile strength (U.T.S.) of composites made with the Group 2 wood fibers before and after plasma treatment with SF_6 in different plasma conditions.

	U.T.S (Mpa)	S.D.
Neat PP	20.9	2.18
Untreated	25.9	1.52
30min/50W	24.9	0.79
40min/60W	24.6	1.58
10min/30W	25.6	1.25
10min/60W	25.7	1.75
40min/30W	25.2	0.64

Scanning electron microscope images were obtained from the tensile test fracture surfaces of composites reinforced with untreated fibers (figure 4.3) and with fibers treated for 30 minutes at 50 W from Group 2 (figure 4.4). It can be observed that the wood fibers were pulled-out from the matrix of the composites made with untreated fibers. This can be seen in figure 4.3 as bare fibers with no evidence of adhesion to the polypropylene and as holes in the matrix, some with striations showing the texture of the fibers that were pulled out. The only way that such marks could be visible is if no attachment between the fiber and matrix occurred. Some of these low adhesion signatures are indicated by the white arrows, and all of these are known to signal little interaction between the fibers and the matrix, as explained by MARAIS *et al.* (2005) and YUAN *et al*. (2004).

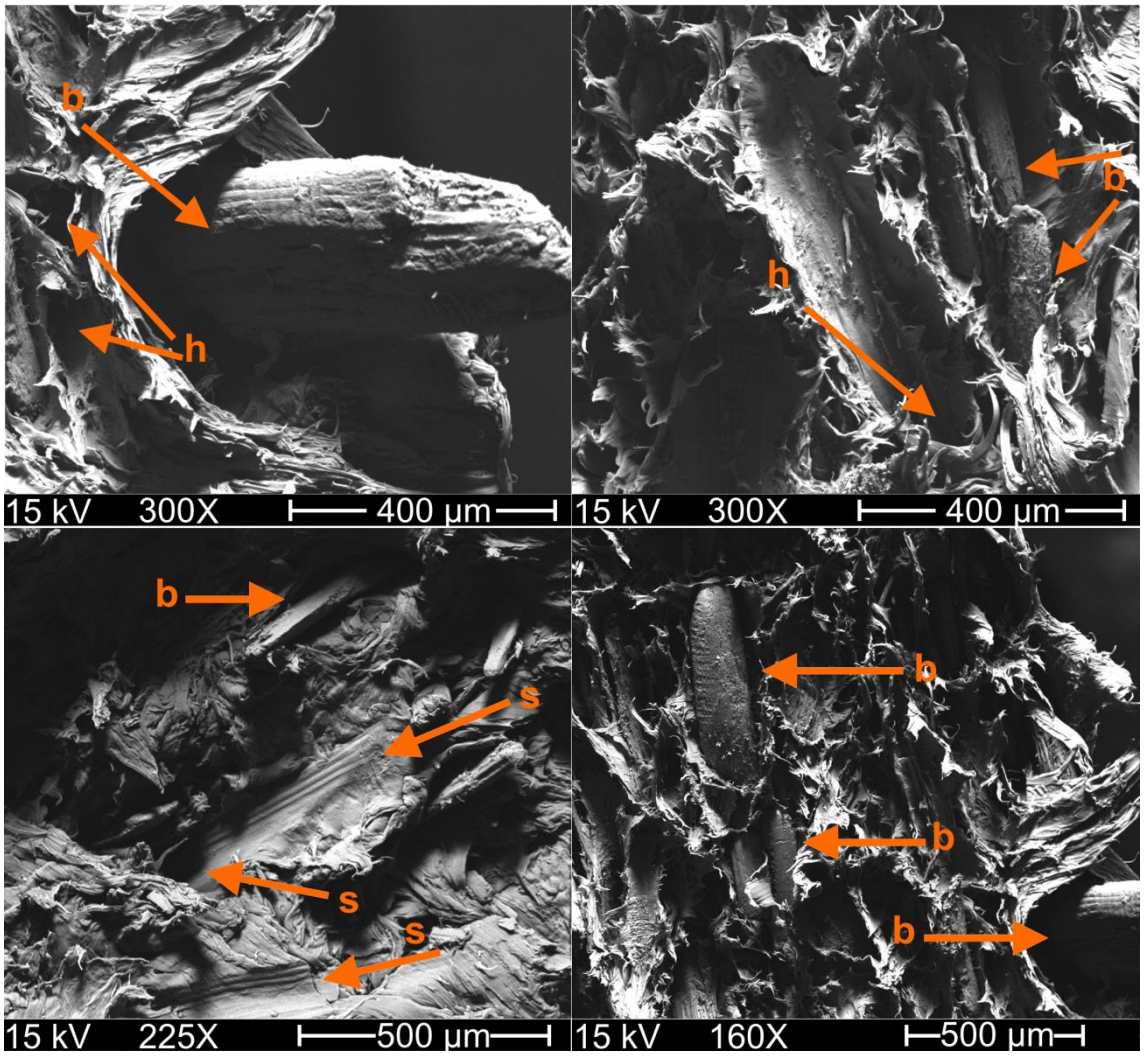

Figure 4.3 SEM micrographs of tensile test fracture surface of composite made with untreated fibers. Arrows indicate pull-out holes (‘h’), striations (‘s’) left by sliding fibers and bare fiber surfaces (‘b’) with no PP adhered.

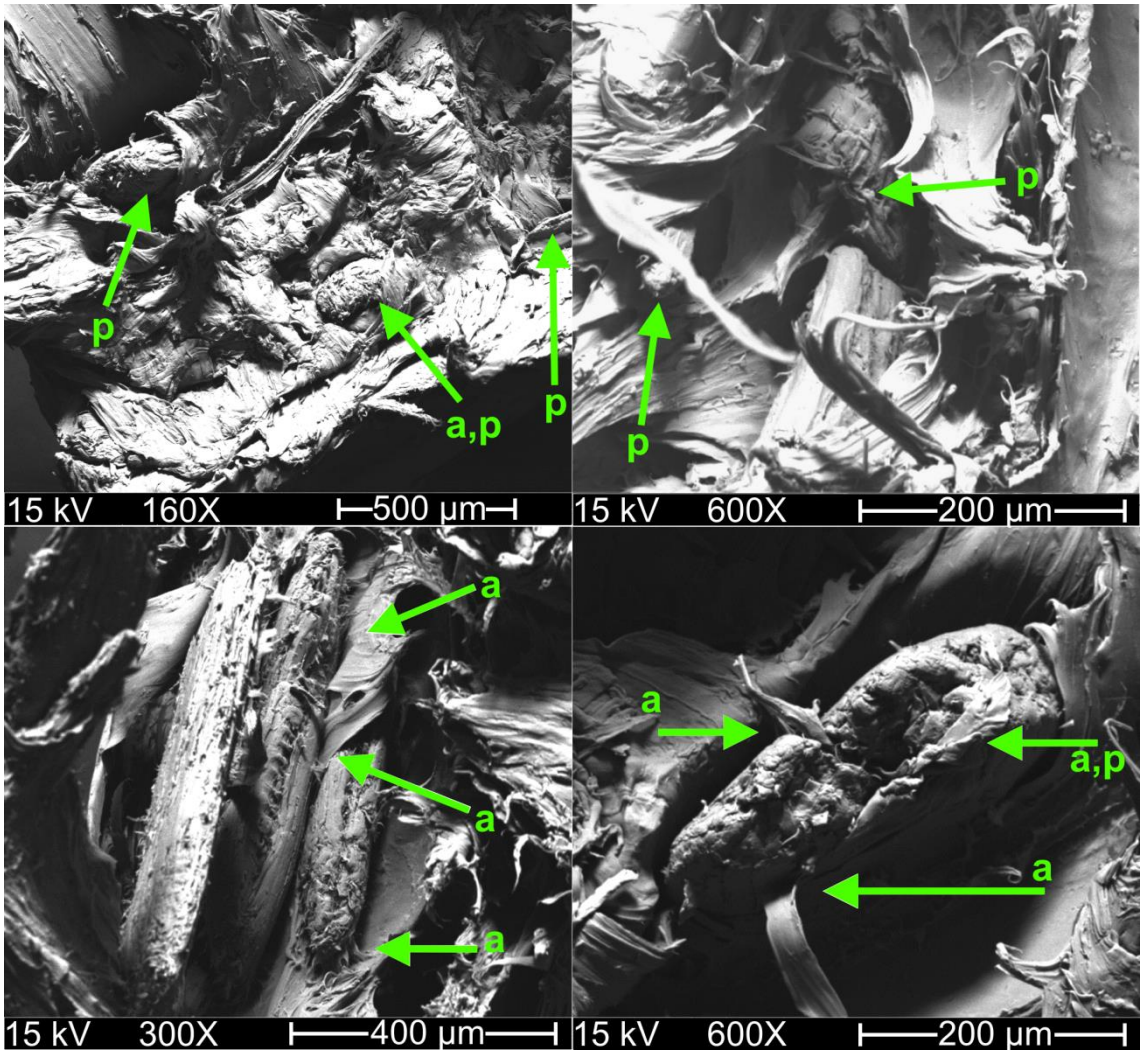

Figure 4.4 SEM micrographs of tensile test fracture surface of composite made with fibers treated for 30 min at 50 W under SF_6 plasma. Arrows indicate places where the PP matrix remained attached to the fiber (a) and fibers with short pull-out lengths (p).

As seen in figure 4.4, fracture surface of composites made with wood treated with SF_6 plasma show a different behavior, with fewer apparent fibers, smaller pull-out lengths, as mosr fibers are seen mostly contained inside the matrix. More importantly, no striated slide paths or holes were visible on the fracture surface, and in many places it was possible to see the polymer highly deformed and attached to the fibers, as if the interface had held together all of the way to fracture. All of these are signatures of higher interfacial shear strength and, consequently, stronger interaction between fibers and matrix (MARAIS *et al*., 2005, YUAN *et al.*, 2004).

To better analyze the surface morphology of the fibers themselves, SEM images were made of the wood fibers before compounding with PP. Natural fibers are

known to have great variability in mechanical properties and surface structure, especially after the comminution process to achieve the sizes typically used (FARUK *et al.*, 2012, GURUNATHAN *et al.*, 2015). Due to this great variety of surface morphologies on the fibers, no conclusive change due to plasma treatment could be detected by SEM, as illustrated in figure 4.5. Higher magnifications were also used, but the variations observed could not be associated to the plasma treatment. If the plasma treatment caused any morphological change, it was not in a pattern detectable above the natural variation in the fibers surface.

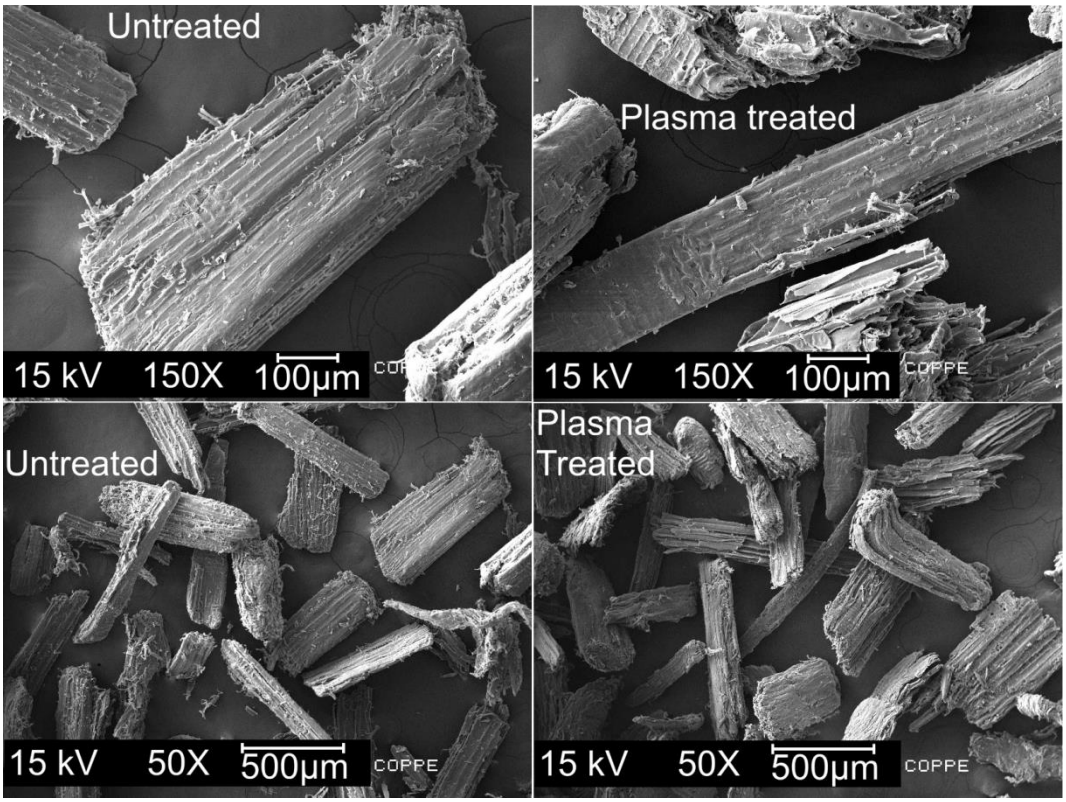

Figure 4.5 - SEM images of fiber surface morphology before (left) and after plasma treatment with SF_6 for 30 minutes at 50 W power (right)

Surface chemical characterization was performed by XPS of untreated and treated fibers, and the resulting spectra are presented in figure 4.6. XPS analysis of untreated fibers shows clear peaks of carbon and oxygen, as would be expected for the polysaccharide-rich surface of wood. In contrast, after plasma treatment with SF_6 plasma for 30 min at 50 W power, additional peaks can be seen, indicating the presence of fluorine (18.8 at%) and sulfur (1.6 at%) on the treated surface. The O/C ratio, however, increased only slightly from 0.31 to 0.35.

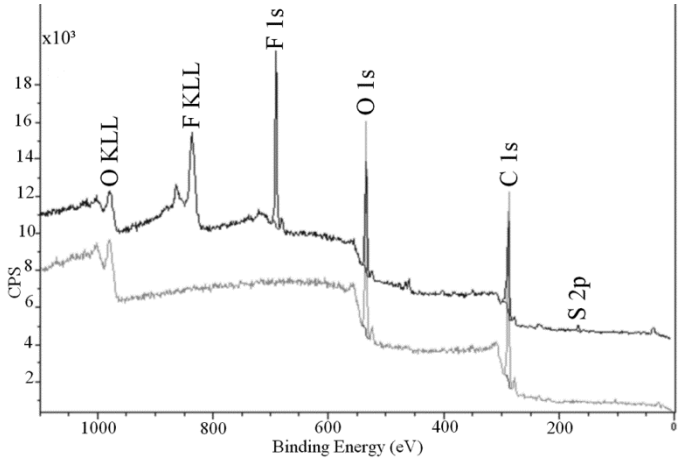

Figure 4.6 - XPS Spectra of wood fibers untreated (gray spectrum) and plasma treated for 30 minutes at 50 W power with SF_6 as process gas (black spectrum).

High-resolution spectra of the carbon and oxygen peaks are shown in figure 4.7. From the carbon 1s deconvoluted spectrum, it is clear that fluorine was incorporated on the surface covalently bound to carbon, as indicated by the C-F, C-F_2 and C-F_3 peaks representing carbons bonded to one, two and three fluorine atoms, respectively. Combined, they represent 17% of all surface carbon atoms.

Oxygen peaks show an initial domination of R-O-R/R-OH chemical states (oxygen bound either as a hydroxyl group or between carbon radicals/chains), with later increases in R-C=O (carbonyl) and O=RC-OH (carboxylic acid). Table 4.3 show the quantification of the deconvoluted peaks for fiber samples as well as for wood sheet samples (refer to section 3.1.1), treated for a similar effective treatment time (refer to section 3.1.2) with 60W power. It can be seen in the table that the same trends of increase or decrease are observed for most peaks when comparing the fiber and sheet samples. For example, C-C decreases, C-O/C-F- remains constant and O-C-O/C=O decreases, etc.This is an indication that the chemical modifications occurring in both kinds of surfaces is similar, corroborating the results of the fiber analysis.

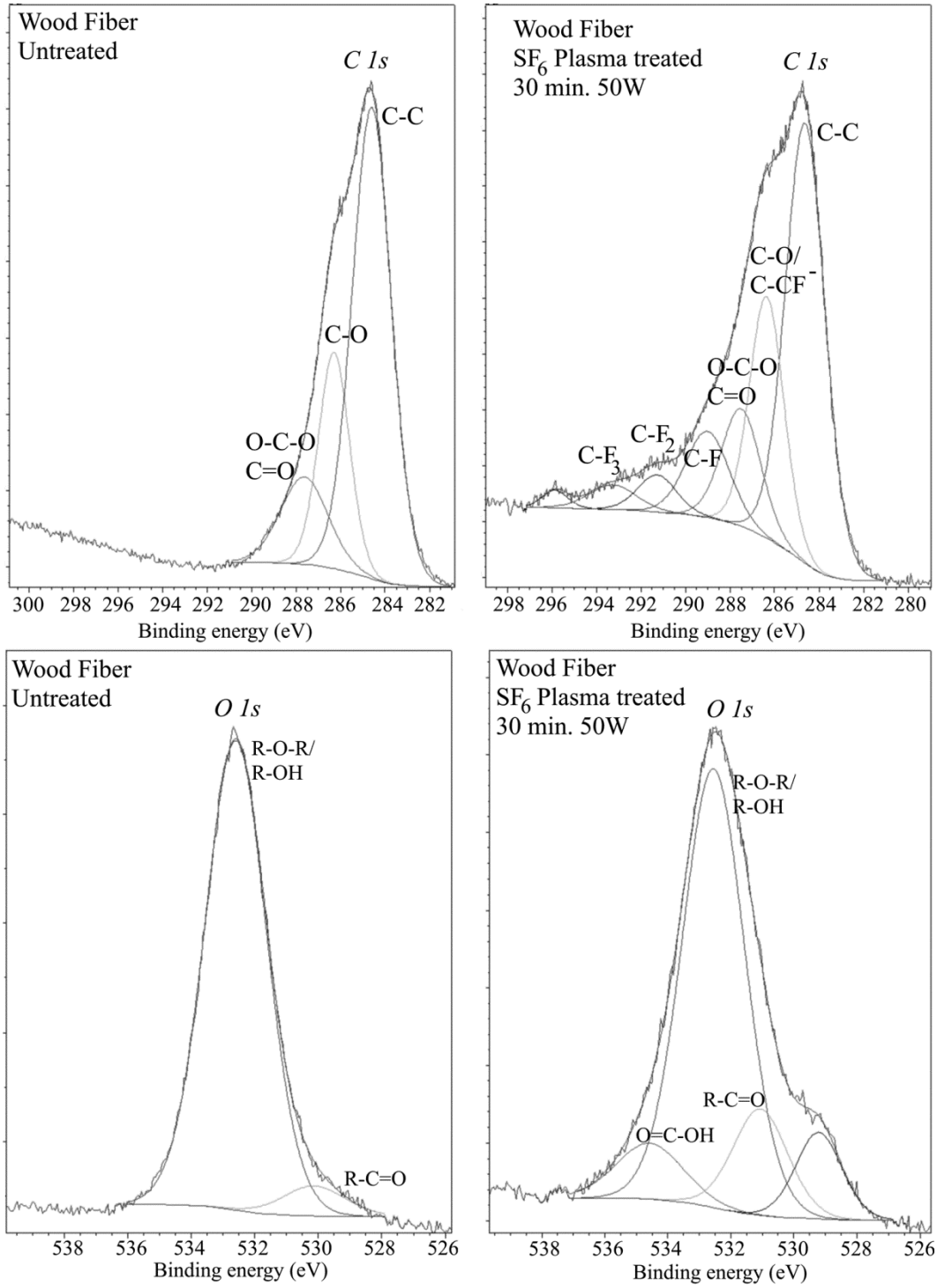

Figure 4.7 - High-resolution XPS spectra of carbon and oxygen peaks from untreated and SF_6 treated wood fibers.

Table 4.3 - XPS analysis of untreated and treated wood samples

	Fibers Untreated	Fibers 30 min / 50W	Sheet Untreated	Sheet 4 min / 60W
Carbon	76.1%	59.2%	73.1%	54.4%
Oxygen	23.9%	20.4%	26.3%	17.1%
Fluorine	0.0%	18.8%	0.0%	25.9%
Others	0.0%	1.6% (S)	0.7% (Ca)	1.6% (Ca)
O/C	0.31	0.35	0.36	0.31
F/C	-	0.32	-	0.48
F/O	-	0.92	-	1.51
C-C	63.0%	46.8%	61.5%	32.6%
C-O / C-CF	22.9%	22.4%	25.6%	25.6%
O-C-O / C=O	14.1%	12.5%	12.9%	9.9%
C-F	-	10.1%	-	12.4%
$C-F_2$	-	3.9%	-	12.6%
$C-F_3$	-	3.2%	-	6.9%
592.2	-	9.8%	-	-
R-C=O	6.1%	14.2%	8.0%	2.6%
R-O-R / R-OH	93.9%	66.9%	92.0%	82.0%
O=C-OH	-	9.2%	-	15.4%

The wood sheet samples were also used to measure water contact angle before and after treatment, as it was expected that the incorporation of fluorine would cause changes to this property. The results are shown in table 4.4.

Table 4.4 - Contact angle measurements of water droplet on wood sheet samples.

Condition	Mean	S.D.	Observations
Untreated	24.1°	6.7°	Quickly absorbed, falling from ~40° to below 20° in under 1 min
4 min	89.6°	2.2°	Slowly absorbed, falling from ~90° to ~85° in 5 minutes
10 min	131.7	5.6°	<2° variation over 5 minutes of observation
40 min	121.3°	13.9°	Slight absorption, falling from 115° to 110° after 5 minutes

For untreated wood specimens, the absorption of the drop was quick and the contact angle was difficult to measure in time. Plasma treatment of wood in mild conditions led to a substantial increase in contact angle, reaching 90° after only 4 minutes of treatment, and 130° with 10 minutes, showing little or no absorption in the observation time frame (up to 5 minutes). However, 40 minutes of exposure to plasma led to a slight decrease in contact angle and increased data dispersion, in comparison to the result obtained for 10 minutes. It should be noted that for these samples, the treatment time is the same as the effective treatment time t_{eff} (refer to section 3.1.2). This means that the 4 minutes conditions for the wood sheet samples are approximately equivalent to treating the wood fibers for 40 minutes (t_{eff}≈9% of treatment time).

4.2. Flax fibers for incorporation in PP matrix

4.2.1. Treatments of "technical" flax fibers

Short flax fibers, also known as "technical" fibers, were plasma treated according to the procedure described in section 3.2.3 and then compounded with polypropylene in a micro-extruder followed by micro-injection, as described in section 3.2.4. The first noticeable effect of the compounding process is a decrease in the apparent fiber size, as illustrated by figure 4.8 and quantified by table 4.5, which was done by measuring the fibers visible in the pictures of figure 4.8. It can be seen that the average fiber length is reduced from over 3mm to less than 1mm, a nearly 75% reduction. This is important to point out, since it shows that fibers break throughout the compounding process, creating new surfaces which were not treated by plasma, as will be discussed later in section 5.3.

Figure 4.8 – Photos of flax fibers before incorporation into the matrix and of the composite, showing reduced fiber sizes.

Table 4.5 – Estimated sizes of the technical flax fibers based on photos like the ones presented at figure 4.8. All sizes in millimeters (mm).

Before compounding				In the composite			
Untreated		Plasma treated		Untreated		Plasma treated	
3.00	3.68	2.92	4.41	1.07	0.83	0.77	0.58
5.06	2.00	2.78	1.81	0.79	1.10	1.35	0.68
7.35	3.19	2.89	2.92	0.79	0.79	0.74	0.94
3.61	2.68	2.78	3.35	0.83	0.79	0.81	0.58
4.26	3.90	2.30	2.59	0.93	0.66	1.10	0.71
2.74	3.71	2.59	2.97	1.17	0.62	0.90	0.55
2.39	1.81	3.24	2.24	1.31	0.86	0.68	0.97
2.45	2.16	3.38	4.32	0.62	0.93	1.13	1.00
4.55	1.97	3.59	3.22	0.59	0.90	0.55	0.65
2.48	2.61	3.24	3.11	0.97	0.52	0.84	0.77
2.10	5.42	3.03	3.86	1.03	0.66	0.39	1.03
5.26	2.26	3.08	2.30	0.90	0.55	0.71	0.89
2.55	3.42	3.65	1.89	0.93	0.69	0.84	1.16
3.52	5.97	3.43	2.51	0.66	1.00	0.74	0.97
3.94	5.77	3.89	3.76	1.31	0.34	0.77	0.87
5.26	2.87	2.68	1.03	0.79	0.97	0.97	0.90
4.39	3.26	6.59	2.68	0.97	0.86	0.45	0.58
3.90	3.74	3.05	2.65	1.07	0.59	0.68	0.90
3.87	4.84	2.86	2.43	0.90	0.59	1.16	0.68
2.77	2.42	3.46	2.59	0.79	0.59		
3.13	3.19	3.32	2.76	0.72	1.00		
5.87				0.66	0.66		
				1.52	0.62		
				1.00	1.07		
				1.76	1.17		
				0.76	1.34		
				1.07	1.00		
				1.10	0.72		
				1.07	1.17		
				0.79	0.83		
Average	S.D.	Average	S.D.	Average	S.D.	Average	S.D.
3.61	1.29	3.05	0.86	0.89	0.26	0.82	0.21
Average		Standard Deviation		Average		Standard Deviation	
3.34		1.13		0.86		0.24	

Mechanical testing of the composites revealed that composite's Young's modulus increased only after one hour of SF_6 treatment of the fibers (TF3) with 200 W power (figure 4.9). The condition with longer treatment time (180 min/200 W) had the same result for Young's modulus, indicating a plateau has been reached in this range of conditions. Treatment for 30 minutes at 150 W power (TF2) has caused no statistically significant change in Young's modulus compared to untreated fibers.

For ultimate tensile strength, however, smaller changes were observed, and only conditions TF2 (30 min/150 W) and TF4 (180 min/200 W) presented a statistically significant drop in this property, although of only 4%.

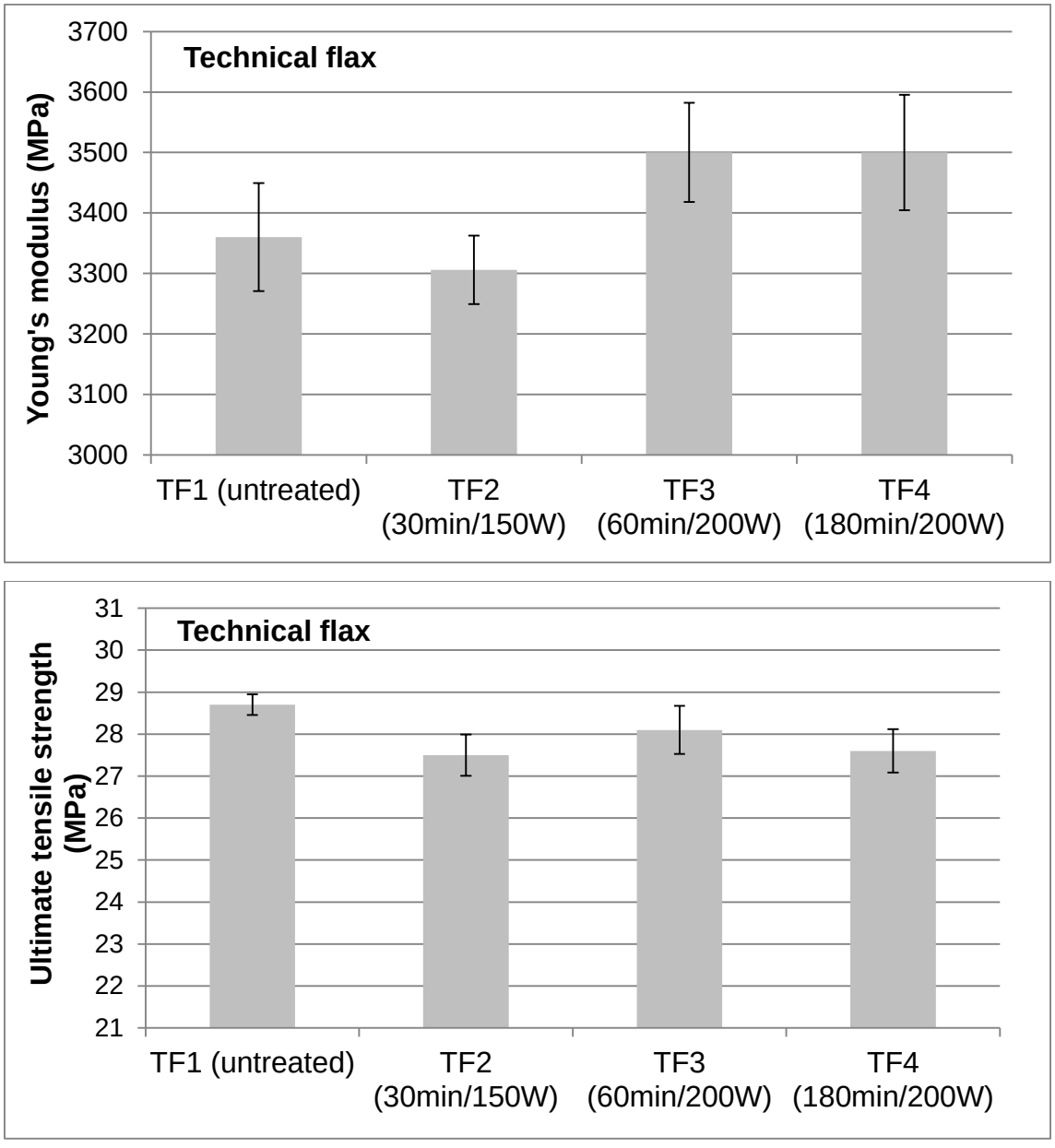

Figure 4.9 - Tensile testing results for composites made with technical flax fibers.

The fracture surface of composites made of untreated technical flax fibers and polypropylene matrix display clear signs of a poor interfacial adhesion, with large areas of exposed fibers with no polymer attached to it, long pull-out lengths, holes where fibers have slid out with little to no deformation of the matrix, large gaps between fibers and polymer and even imprinted texture of the fibers, which can only happen when a fiber with no adhesion to the matrix is pulled out by the tensile test (MARAIS *et al.*, 2005, YUAN *et al.*, 2004). These features are pointed by black arrows in figure 4.10.

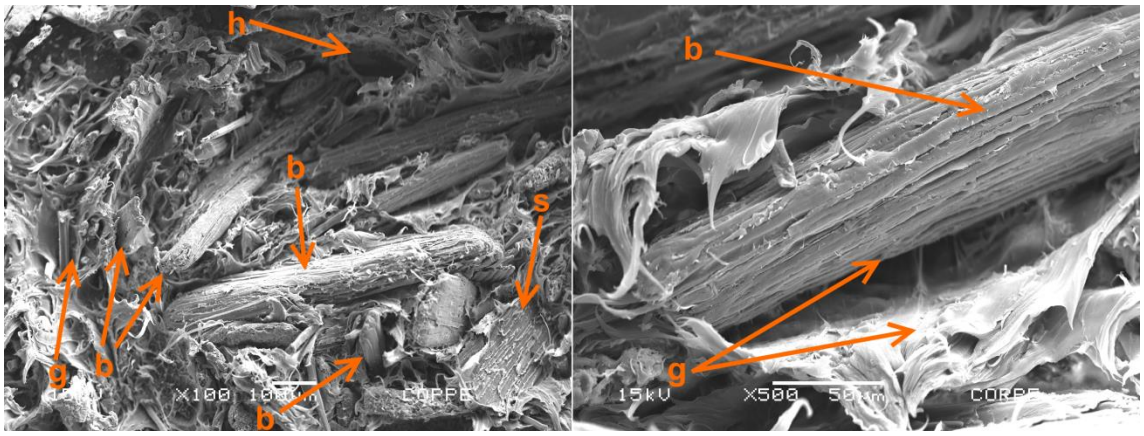

Figure 4.10 - SEM micrographs of tensile test fracture surface of composite made with untreated technical flax fibers. Arrows indicate some of the pull-out holes ('h'), striations ('s') left by sliding fibers, large gaps between fiber and matrix ('g') and bare fiber surfaces ('b') with no matrix adhered.

Composites made of technical flax fibers treated for 3h at 200W in SF_6 plasma display some differences in the fracture surface, as seen in figure 4.11. Shorter pull-out lengths are observed, much smaller or no gap can be seen between matrix and fiber, fewer holes are seen and there is evidence of fibers breaking on the fracture surface (especially on the micrograph on the right side), which are indications of improved interfacial bond between the two phases (MARAIS *et al.*, 2005, YUAN *et al.*, 2004). These surface features are pointed by black arrows in figure 4.11.

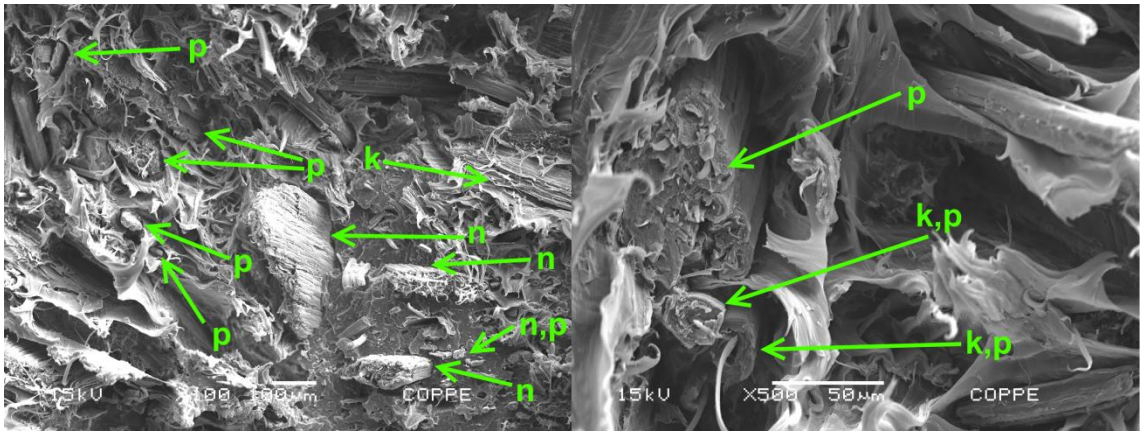

Figure 4.11 - SEM micrographs of tensile test fracture surface of composite made with technical flax fibers treated by SF_6 plasma for 3 hours and 200 W power. Arrows indicate some of the places where there is no gap between fiber and matrix (‘n’), fibers with short pull-out lengths (‘p’) and broken fibers (‘k’).

Scanning electron microscopy was also used in an attempt to detect morphological modifications on the surface of technical flax fibers, prior to compounding with PP. However, no significant distinction could be observed, partially due to the natural variability of surface morphologies present in the untreated fibers, in the first place, illustrated in figure 4.12.

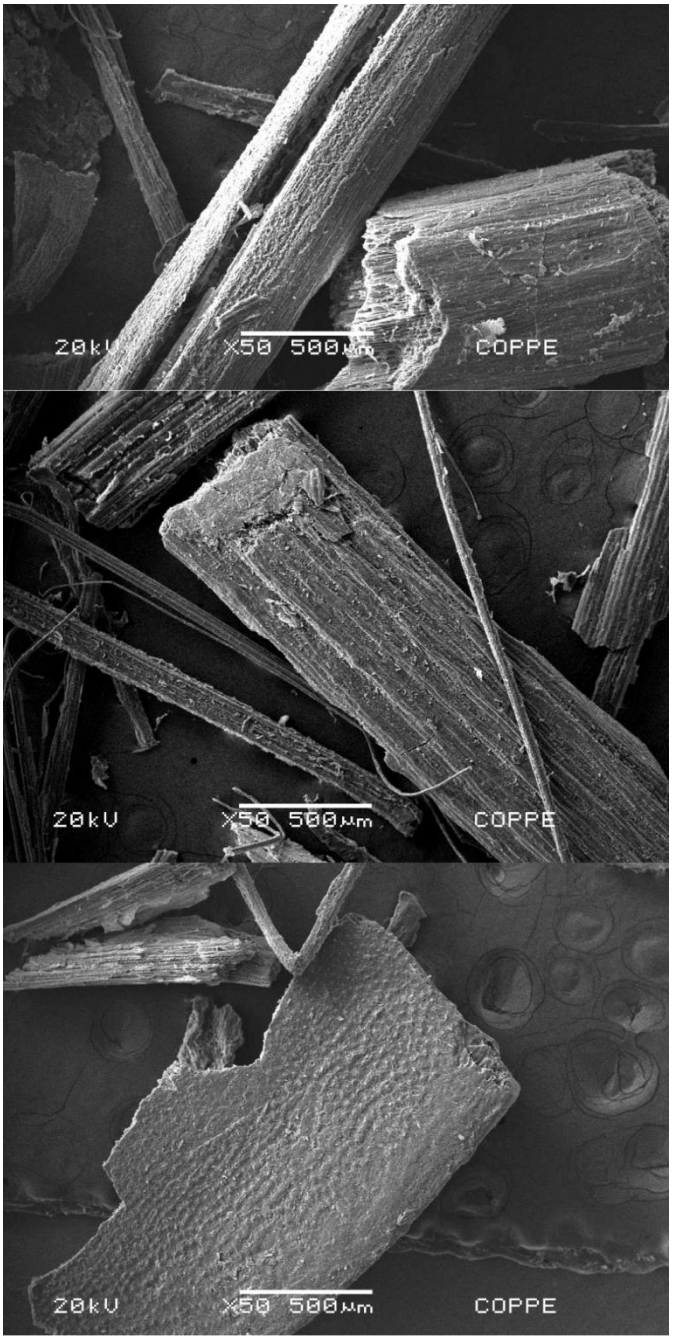

Figure 4.12 - Examples of morphological variability in untreated technical flax fibers.

The surface chemical makeup of these fibers has been studied by XPS and the results of the complete survey and the high resolution spectra of C1s and O1s peak are presented in tables 4.6 and 4.7, respectively. Table 4.6 shows that plasma treatment incorporates fluorine on the surface, and longer treatment times increase the amount of fluorine, while carbon atomic concentration decreases. A small increase in oxygen concentration was also observed after plasma treatment, but the surface

concentration of this atom remained stable for longer treatment times. The steady increase in O/C ratio observed with increasing treatment time is a result mainly of the decrease in carbon.

Table 4.6 - Surface atomic concentration and ratios between main elements obtained by XPS.

	TF1 (untreated)	**TF3 (60min/200W)**	**TF4 (180min/200W)**
Carbon	79%	63%	52%
Oxygen	18%	23%	24%
Fluorine	-	9%	18%
Others	3%	4%	5%
O/C	0,23	0,36	0,47
F/C	-	0,15	0,35
F/O	-	0,41	0,75

Table 4.7 - Proportions of different chemical bonds obtained from the deconvolution of high resolution XPS spectra of C1s and O1s peaks.

		TF1 (untreated)	**TF3 (60min/200W)**	**TF4 (180min/200W)**
C 1s	**C-C**	70%	74%	64%
	C-O / C-CF^{-}	21%	13%	21%
	O-C-O / C=O	9%	9%	8%
	O=RC-OH	-	-	-
	C-F	-	~4.5%	~7%
	C-F_2	-	N/A	N/A
	C-F_3	-	N/A	N/A
O 1s	**592.2 eV**	12%	3%	7%
	R-C=O	9%	22%	19%
	R-O-R / R-OH	79%	62%	61%
	O=C-OH	-	12%	14%

From the high resolution spectra com carbon 1s peak, it can be seen that plasma treatment with SF_6 has led to the formation of covalent bonds between carbon and fluorine. Only carbons bonded to a single fluorine atom could be analyzed though, since the presence of potassium (K) impurity created a peak which overlapped with the higher energies of the C-F_2 and C-F_3 peaks, making their identification impossible.

Other superpositions of peaks are typical for the XPS analysis of this material, notably the C-O (Carbon bonded to a single oxygen atom and three hydrogen or carbon atoms)/ C-CF^- (Carbon bonded to a fluorine atom, having the bond an ionic character) and the R-O-R (Oxygen bonded to two organic radicals, typically in between carbon atoms) /R-OH (Hydroxyl radical bonded to an organic radical, typically a carbon chain) (HAN *et al*., 2011, LI & JINJIN, 2007, TOUZIN *et al.*, 2008). Due to these facts, interpretation of the results is not trivial, and will be done at the Discussion section (5.2.1).

4.2.2. Treatments of micronized flax fibers

Micronized flax fibers, supplied by TEXILIS, had a different morphological aspect and size distribution, as it can be seen in figure 4.13 and table 4.8. In these fibers, high aspect ratios are observed and ribbon-like fibers are predominant. In some cases, a bundle of ribbon-like fibers can be seen.

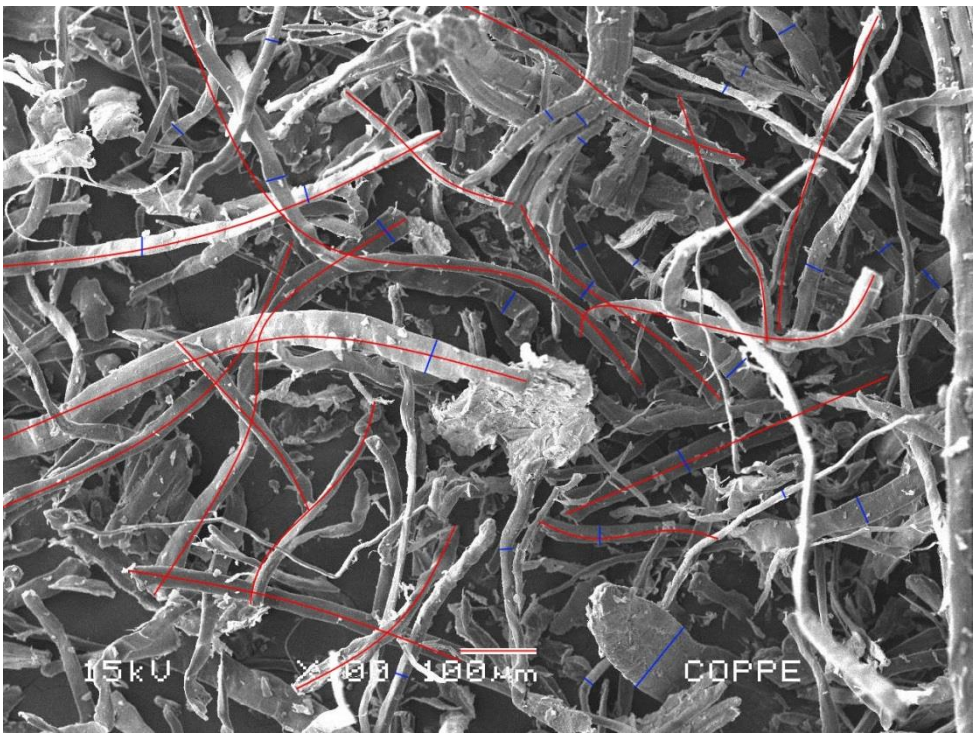

Figure 4.13 – SEM image of untreated micronized flax fibers. Red and blue lines are curved approximations used for measuring the fiber length (red) and width (blue).

Table 4.8 – Approximated lengths and widths measured as indicated in figure 4.13.

Length (µm)						Width (µm)					
461	460	482	860	243		18	18	24	37	32	
310	353	490	286	616		20	25	14	28	21	
456	272	692	322	673		17	33	24	15	26	
542	725	254	254			26	19	24	18	15	
628	433	411	278	**Average**	**460**	20	47	38	32	**Average**	**24**
439	373	385	716	**S.D.**	**171**	38	17	13	11	**S.D.**	**9**

Figure 4.14 presents the mechanical properties of the composites produced with 30wt% of plasma treated micronized flax fibers and PP matrices. It can be observed that a 10% increase in both Young's modulus and ultimate tensile strength (MF3 – 180 min/200 W) could be obtained for composites produced with plasma treated fibers when compared to the ones containing untreated fibers (MF1). Young's modulus of the composites increased after one hour of treatment of the fibers at 200 watts (MF2). Longer treatment times did not further increased Young's modulus and this property had the same value after 3 hours of treatment, compared to 1 hour of treatment. On the other hand, ultimate tensile strength only improved significantly after 3 hours of treatment, where values increased up to 10%. It is important to note that due to the conditions in the plasma reactor, as explained in section 3.2.2, individual fiber treatment time is actually much less than total treatment time, in the order of 10% or less.

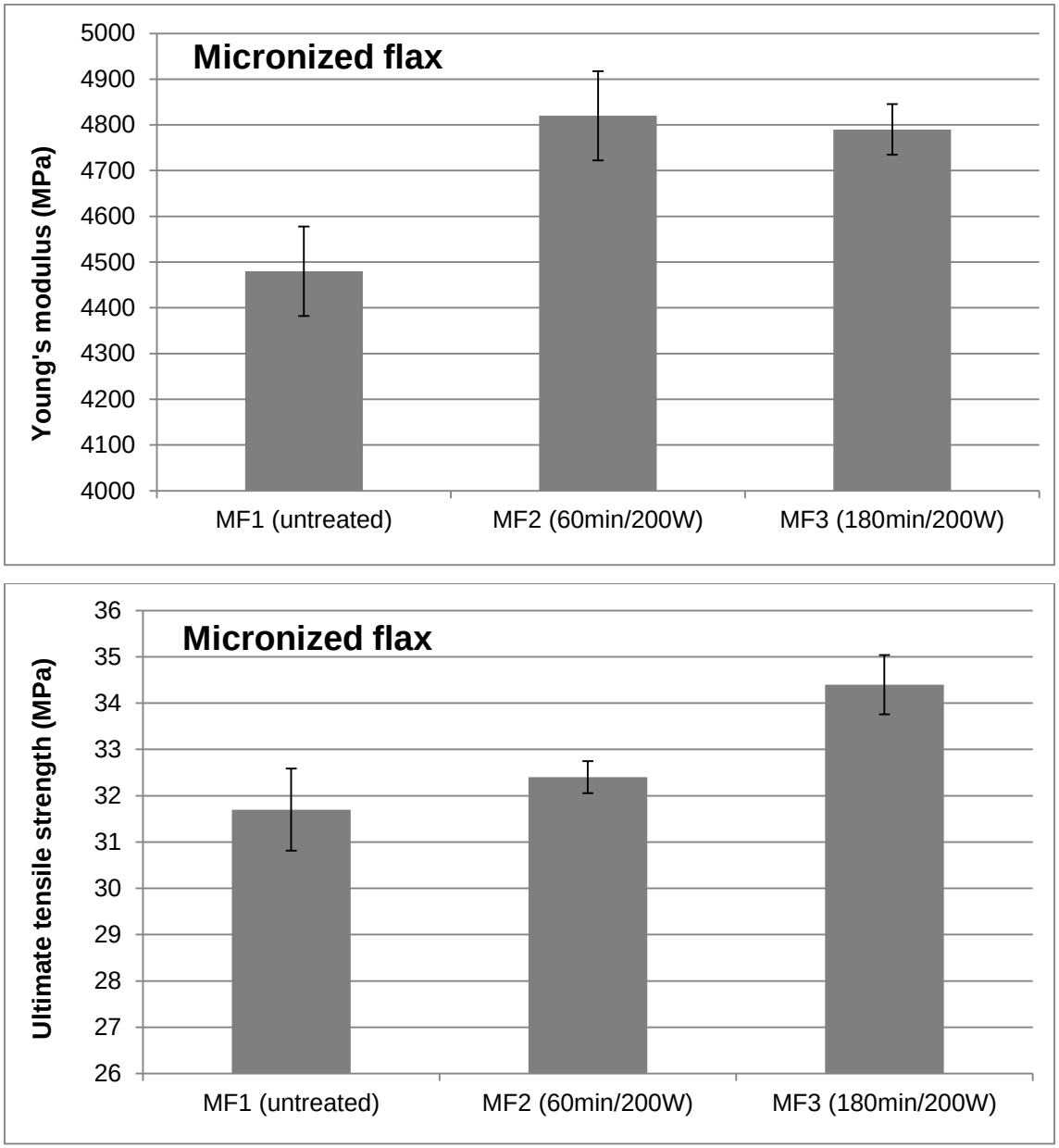

Figure 4.14 - Tensile testing results for composites made with micronized flax fibers and PP matrix.

Fracture surface of the tensile test specimens have been observed under SEM, and are presented in figure 4.15 and 4.16, for composites made with untreated and treated micronized flax, respectively. It can be observed on figure 4.15 that the untreated micronized flax fibers are exposed on the surface with no apparent adhesion to the matrix. Many fibers show a long pull-out length (~100 µm) and holes are visible from where fibers have slid out without significantly deforming the matrix around it.

Some of these features are pointed by black arrows and these are all known indications of low interfacial shear stress (MARAIS *et al.*, 2005, YUAN *et al.*, 2004).

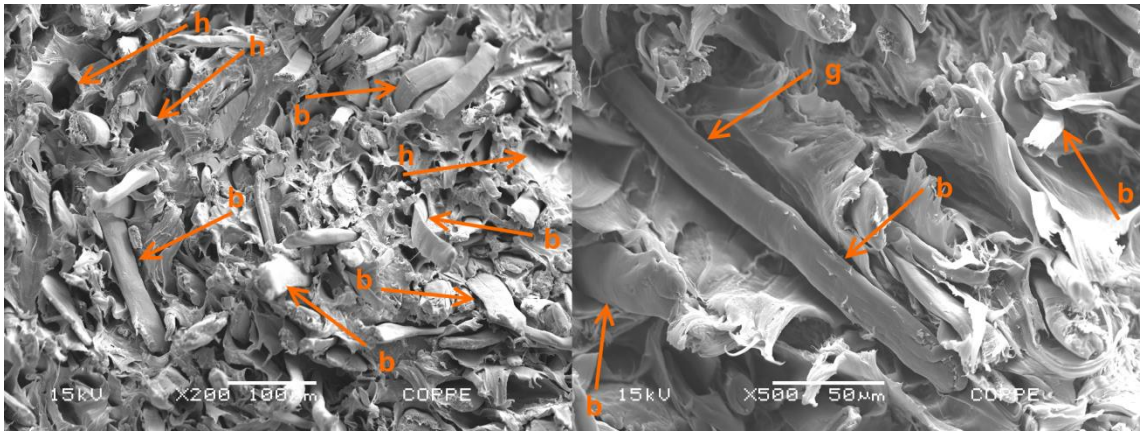

Figure 4.15 - SEM micrographs of tensile test fracture surface of composite made with untreated micronized flax fibers. Arrows indicate some of the pull-out holes ('h'), large gaps between fiber and matrix ('g') and bare fiber surfaces ('b') with no matrix adhered.

After plasma treatment of the fibers, the fracture surface (figure 4.16) shows some distinct differences. Fiber pull-out length is much shorter, with fibers breaking approximately at the same height as the matrix. The polymer also seems to attach closer to the fibers in most regions, with smaller gaps between both, as pointed by the white arrows. Some exposed fibers and slide holes are still visible, similarly to the untreated sample, but their concentration is much lower.

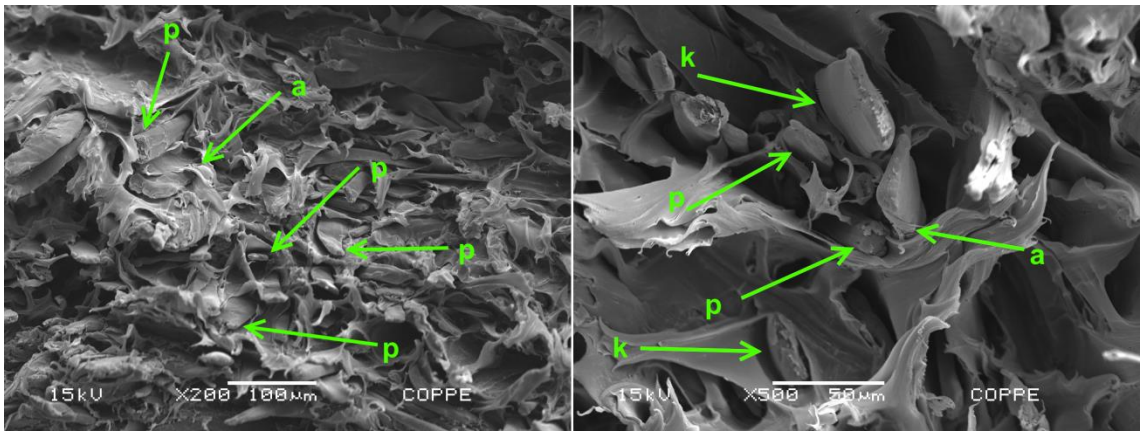

Figure 4.16 - SEM micrographs of tensile test fracture surface of composite made with micronized flax fibers treated with SF_6 plasma for 3 hours at 200 W power. Arrows indicate places where the PP matrix remained attached to the fiber ('a'), fibers with short pull-out lengths ('p') and broken fibers ('k')

Morphological analysis of the micronized fibers, prior to compounding, before and after plasma treatment does not indicate any significant change in surface roughness with magnifications up to 5000x (figure 4.17). Treated surfaces actually seem less rough than untreated ones, although it is inconclusive, due to the natural variability that all plant based fibers present.

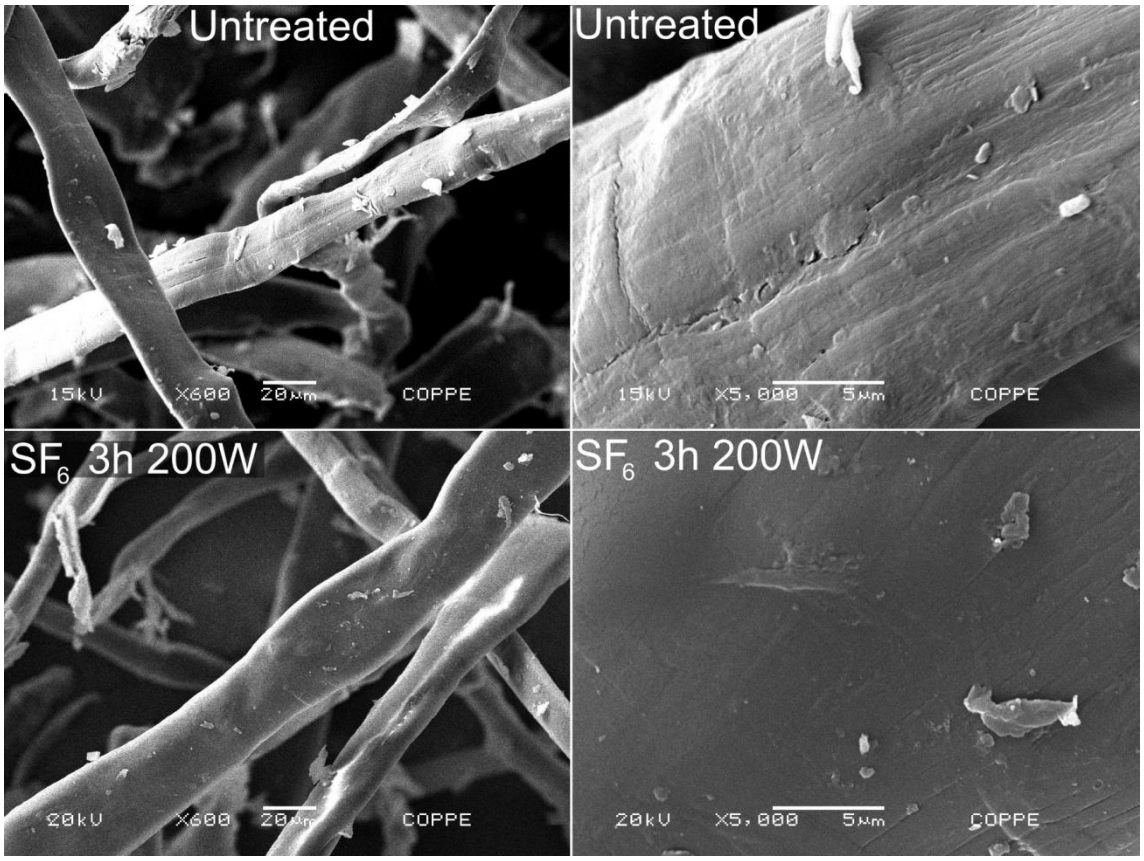

Figure 4.17 - SEM images of micronized flax fiber surface before and after plasma treatment

XPS surveys were performed to evaluate the changes in chemical state of the fibers surfaces. Figure 4.18 shows a comparison between the high resolution carbon 1s (C1s) peak of untreated micronized flax fibers and technical fibers. It is clear that, although derived from the same plant, the two kinds of fibers display very different surface compositions. It is important to note that XPS is a surface analysis technique, and the data obtained comes from the first atomic layers of the material, typically on the lower end of the range from 1 nm to 10 nm.

As discussed by JOHANSSON *et al*. (1999), the fraction of carbon bonded to other carbons or to hydrogen (C-C peak) is a good indicator of the fraction between

surface cellulose and lignin. It is clear from the deconvolution of the C1s peak that micronized flax has very little C-C bonds, and this is a good indication that the surface is composed mostly cellulose, while technical fibers display a C-C fraction above 50%, meaning that lignin is present on the surface.

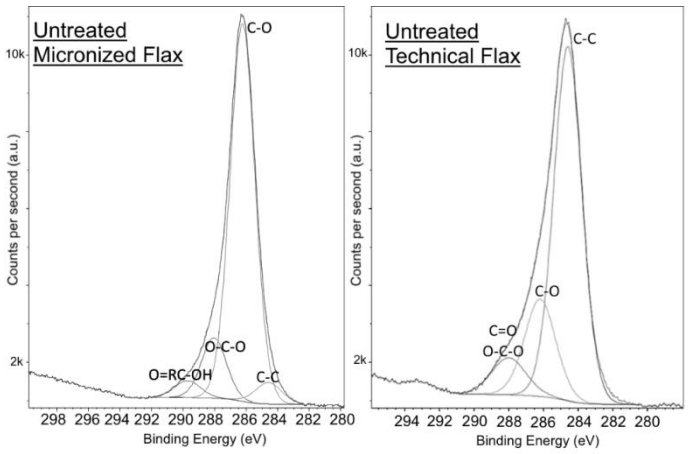

Figure 4.18 - High resolution XPS spectra of carbon 1s peak of micronized flax and technical flax fibers.

Table 4.9 shows the atomic concentrations and their ratios for micronized fibers and also for technical fibers (as seen in table 4.6) for comparison. It is clear that longer treatment times lead to greater fluorine content, as would be expected. The fluorine to carbon (F/C) and fluorine to oxygen (F/O) both increase with time in all fibers, indicating that fluorine incorporation is the predominant phenomena. The atomic concentration of carbon in the surface is the only that decreases, while oxygen increases slightly.

Table 4.9 - Surface atomic concentration and ratios between main elements obtained by XPS for micronized and technical flax, before and after plasma treatment

	Technical fibers			Micronized fibers		
	TF1 (untreated)	**TF3 (60min/ 200 W)**	**TF4 (180min/ 200 W)**	**MF1 (untreated)**	**MF2 (60min/ 200 W)**	**MF3 (1800min/ 200 W)**
Carbon	79%	63%	52%	91%	77%	67%
Oxygen	18%	23%	24%	10%	13%	19%
Fluorine	-	9%	18%		5%	10%
Others	3%	4%	5%		5%	3%
O/C	0,23	0,36	0,47	0,10	0,16	0,29
F/C	-	0,15	0,35		0,07	0,16
F/O	-	0,41	0,75		0,43	0,54

Table 4.10 presents the results of deconvolution of the high resolution spectra of the peaks C 1s and O 1s of untreated and treated micronized flax, also with the technical fibers results (table 4.7) for comparison. For carbon, the most important shift observed is the decline of C-O with increased treatment time and concomitant increase in the C-F, C-F_2 and C=O peaks, all proportional to treatment time. In the oxygen peak it is noticeable that the R-O-R/R-OH peak (oxygen between carbons or hydroxyl group) decreases after treatment, but remains stable for longer treatment times. Meanwhile both R-C=O (Carbonyl) and O=C-OH (Carboxyl group), which were not present in untreated samples, increase proportional to treatment time.

Table 4.10 - Proportions of different chemical bonds obtained from the deconvolution of high resolution XPS spectra of C 1s and O 1s peaks.

		Technical fibers			Micronized fibers		
		TF1 (untreated)	**TF3 (60min/ 200 W)**	**TF4 (180min/ 200 W)**	**MF1 (untreated)**	**MF2 (60min/ 200 W)**	**MF3 (1800min/ 200 W)**
C 1s	**C-C**	70%	74%	64%	5%	2%	2%
	C-O / C-CF$^-$	21%	13%	21%	79%	67%	54%
	O-C-O / C=O	9%	9%	8%	13%	20%	27%
	O=RC-OH	-	-	-	4%	-	-
	C-F	-	~4.5%	~7%	-	9%	14%
	C-F_2	-	N/A	N/A	-	1%	2%
	C-F_3	-	N/A	N/A	-	-	-
O 1s	**592.2 eV**	12%	3%	7%	17%	22%	-
	R-C=O	9%	22%	19%	-	6%	18%
	R-O-R / R-OH	79%	62%	61%	83%	63%	64%
	O=C-OH	-	12%	14%	-	8%	18%

Another series of composites made with plasma treated micronized flax was made. Although a full analysis as of the “A-B series” could not be performed, the mechanical results of “E series” is presented in figure 4.19, and it confirms that plasma treatment with SF_6 plasma is effective in increasing the mechanical properties of the composites of micronized flax reinforced with polypropylene. Again it can be seen that elastic modulus increases even with a small power (100 W) and time (30 minutes), and further treatment brings only small improvements (10.5% increase at 30 min/100 W and 12.5% increase at 180 min/200 W).

The tensile strength improvement is again dependent on the treatment time, as well as on the treatment power. While 30 min/100 W causes only a marginal increase of 2%, 30 min/200 W improves tensile strength by 5% and 180 min/200 W by 10.5%. Different from the elastic modulus, tensile strength does not reach a plateau and increases constantly in the range of conditions tested.

While the A-B series used 30 wt% of fibers in the composite, the E series used 20 wt%, which explains the lower values of elastic modulus. On the other hand, the E series ultimate tensile strength was slightly higher than those of A-B series. This could indicate that even with the plasma treatment, the adhesion is still not ideal, meaning that adding more fibers will not reinforce the material further (in terms of ultimate tensile strength). Fibers with poor interaction can act as defects, since unattached surfaces can act like crack initiation points. A higher concentration of fibers also increases the chances of agglomeration, thus further increasing the chances of unattached surfaces and voids in the matrix.

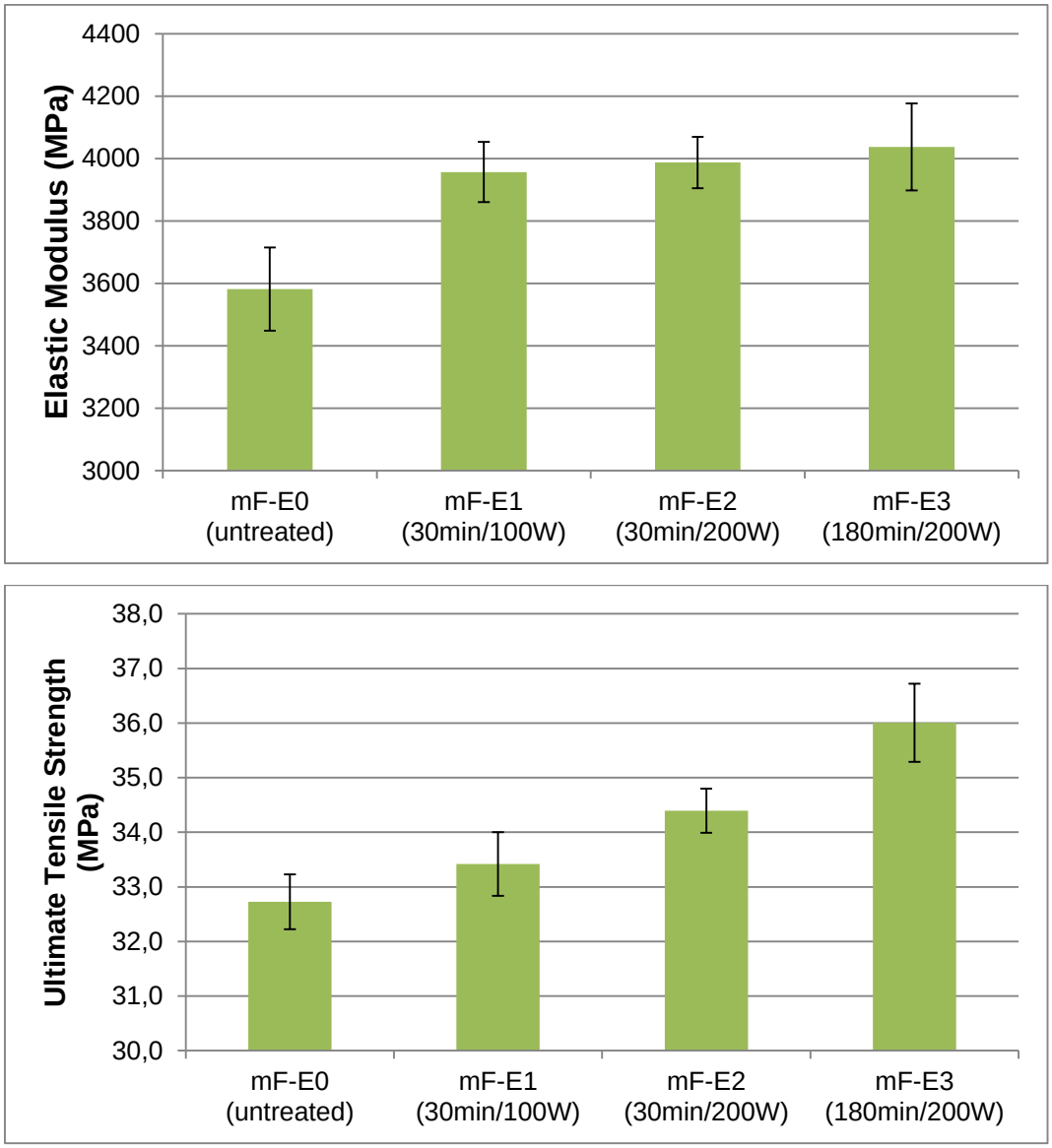

Figure 4.19 – Mechanical properties results for the E Series.

4.3. Multiple fibers for incorporation into PLA matrix

Four different kinds of fiber were treated by plasma according to the procedure described in section 3.2.3, and later incorporated in a PLA (Polylactic acid) matrix by micro-extrusion followed by micro-injection molding into tensile test specimen, as described in section 3.2.4. The tensile test results are presented in figures 4.20 for elastic modulus and 4.21 for ultimate tensile strength. The table 3.7 is presented again here to make easier the understanding of the conditions used for these results. It can be seen, comparing only untreated fibers, that each kind of fiber had a distinct effect in the mechanical properties. Micronized flax fibers had the best results, increasing elastic

modulus by 80% and maintaining the ultimate tensile strength at the same level (65 MPa compared to 63.6 MPa of pure PLA). All other fibers decreased the tensile strength by 8% (to 58.3 MPa) and increased the elastic modulus by varying degrees.

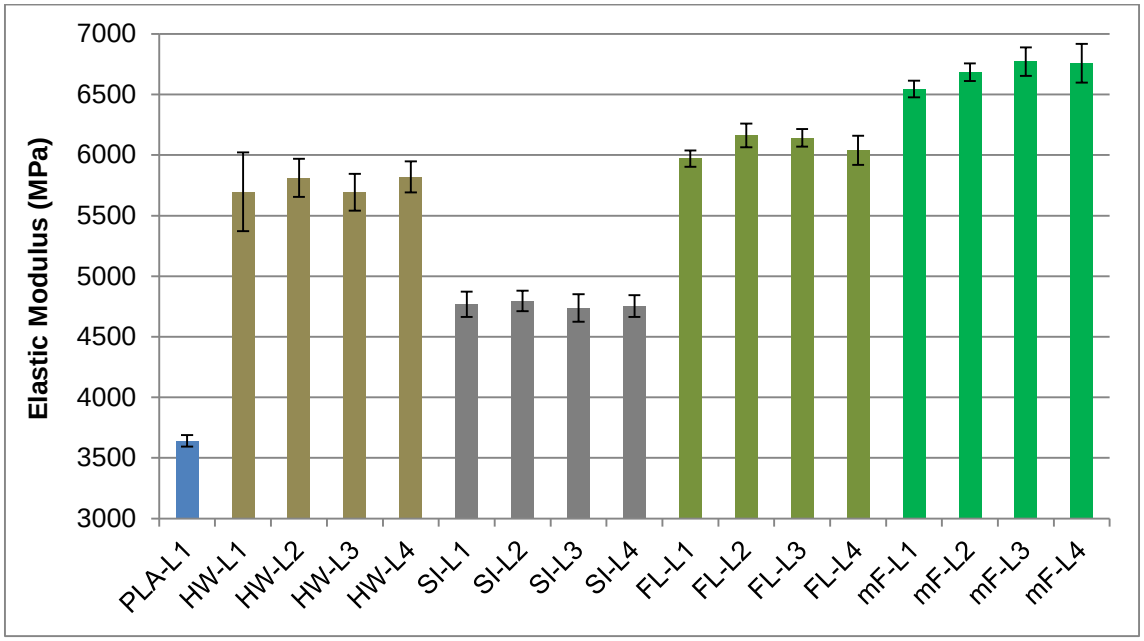

Figure 4.20 – Tensile test results of elastic modulus for composites of PLA matrix and different untreated and treated fibers.

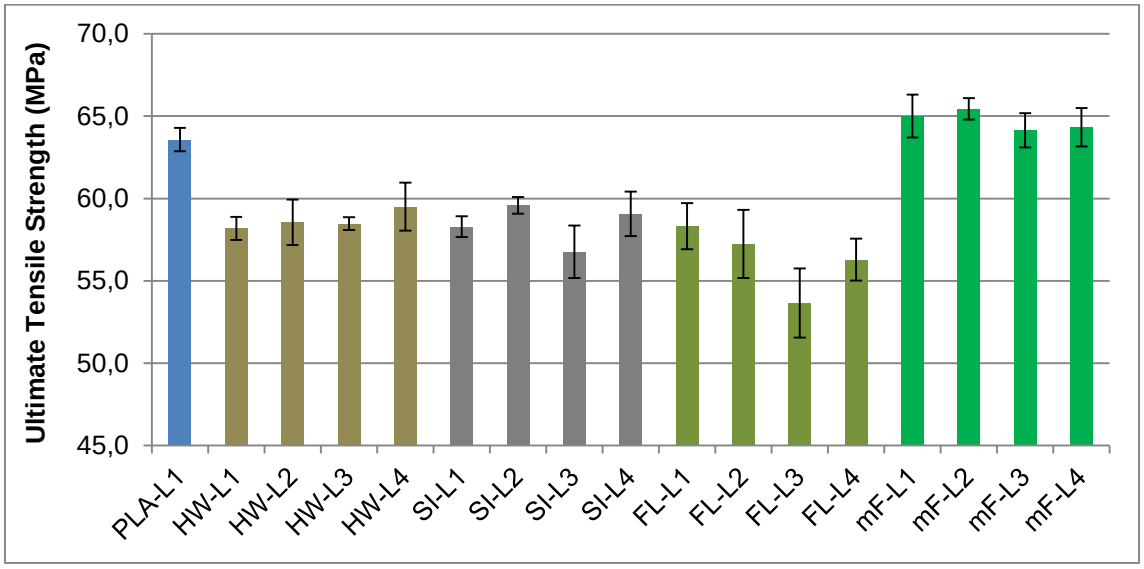

Figure 4.21 – Tensile test results of ultimate tensile strength for composites of PLA matrix and different untreated and treated fibers.

Table 3.7 Treatment conditions of fibers of the “L series” prior to compounding.

Sample name	Fiber type	Gas	Plasma power (watts)	Treatment time (minutes)
PLA-L1	(pure polymer)	-	-	-
HW-L1	Wood flour	-	*Untreated*	*Untreated*
HW-L2	Wood flour	O_2	200	120
HW-L3	Wood flour	SF_6	200	120
HW-L4	Wood flour	O_2/SF_6	200	120 (O_2) + 60 (SF_6)
SI-L1	Sisal	-	*Untreated*	*Untreated*
SI-L2	Sisal	O_2	200	120
SI-L3	Sisal	SF_6	200	120
SI-L4	Sisal	O_2/SF_6	200	120 (O_2) + 60 (SF_6)
FL-L1	Technical flax	-	*Untreated*	*Untreated*
FL-L2	Technical flax	O_2	200	120
FL-L3	Technical flax	SF_6	200	120
FL-L4	Technical flax	O_2/SF_6	200	120 (O_2) + 60 (SF_6)
MF-L1	Micronized flax	-	*Untreated*	*Untreated*
MF-L2	Micronized flax	O_2	200	120
MF-L3	Micronized flax	SF_6	200	120
MF-L4	Micronized flax	O_2/SF_6	200	120 (O_2) + 60 (SF_6)

Plasma treatment of the different fibers had very little effect in the mechanical properties, with all variations of properties below 4%. Most changes are not statistically significant, when comparing to the composite made with untreated fibers of the same kind. Worth noting is the drop in tensile strength on sisal (SL-L3), technical flax (FL-L3) and micronized flax (mF-L3), when the fibers were treated with SF_6 plasma. This was expected, since the matrix is hydrophilic and, as shown previously in section 3.1, SF_6 plasma treatment tends to make the surface hydrophobic.

4.4. Coir fibers for incorporation in starch matrix

Coir fibers extracted from Brazilian green coconut were plasma treated according to the procedure explained in section 3.1.3 and later incorporated into a thermoplastic starch matrix according to the procedure described in section 3.1.4.

4.4.1. Effects of plasma treatment on the coir fibers

As described in section 3.1.3, a small amount of fibers, approximately 0.1 gram, were treated with oxygen and air plasma to evaluate the effect on the fiber surface for longer exposure times. Fibers treated under these conditions are named here “micro batch” and were used only for surface analysis, since the amount was too

small to produce composites. With the longer times in the “micro batch” it was expected that the modifications caused by plasma would be easier to detect and analyze, improving the understanding of the mechanisms involved and improving the analysis of the “normal batch”. Figure 4.22 compares the morphology observed by SEM of untreated and treated fibers under different conditions. Untreated fibers have generally a smooth surface, which resembles an amorphous layer with light striations that reflect the internal cell structure.

Plasma treatment of the fibers for 60 minutes has led to a strong modification of surface features. Exposure of the coir surfaces to 50 W power for 60 minutes has led to partial removal of the surface amorphous layer, revealing an underlying structure of long valleys and peaks aligned with the fiber length. Especially in the oxygen treated fibers, it can be observed that the surface layer is thinned and that holes opened on it. For both gases, the final result of a long exposure at an 80 W power is an extremely rough surface, with deep canals between sharp crests, as well as smaller scale roughness where parts of the outer layer still remain, or where the inner structure was latter also etched (figure 4.22d and 4.22f). Oxygen might be more effective at etching the outer layer, as the inner structure is more clearly seen (figure 4.22e and 4.22f). Air treated fibers at the same power level, on the other hand, seem to have higher amounts of the now roughened outer layer (figure 4.22c and 4.22d).

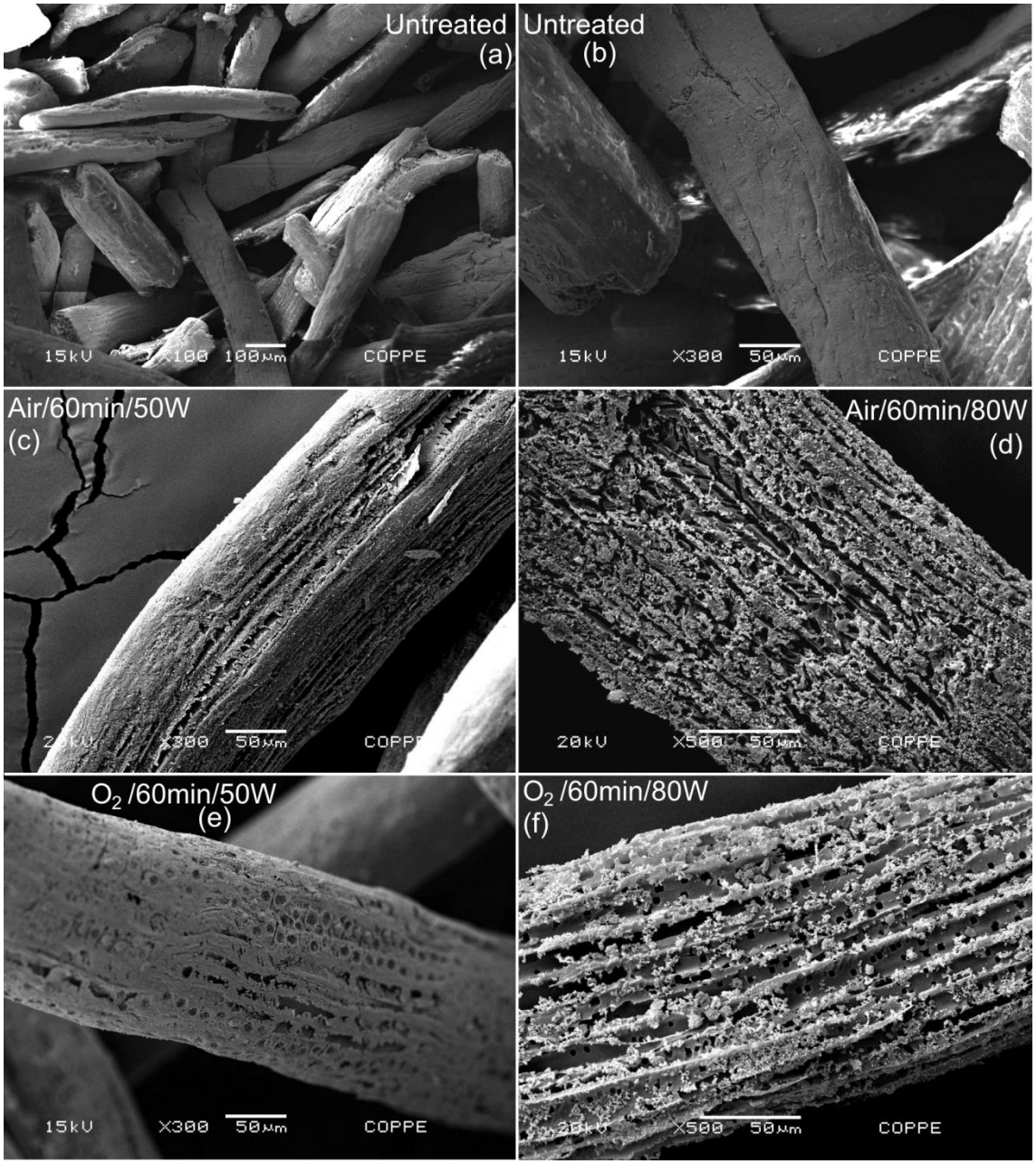

Figure 4.22 - SEM images of the coir fibers surface before treatment (a & b), after air plasma treatment (c & d) and after oxygen plasma treatment (e & f).

When performing the plasma treatment on a normal batch (approximately 5 g of fibers), each individual coir fiber is treated for approximately 12% of the total time, as explained in section 3.1.3. Consequently a less intensive effect is expected for processes done with the same total time. Figure 4.23 presents the SEM images of coir fibers treated in normal batches for 60 minutes at 80 W power for both air and oxygen plasma. Untreated fibers are shown again for comparison. Although the effect is not as visible as in figure 4.22, the same pattern of change can be observed, with the surface

amorphous layer becoming rougher and displaying the elongated striations associated with the internal structure of the fiber.

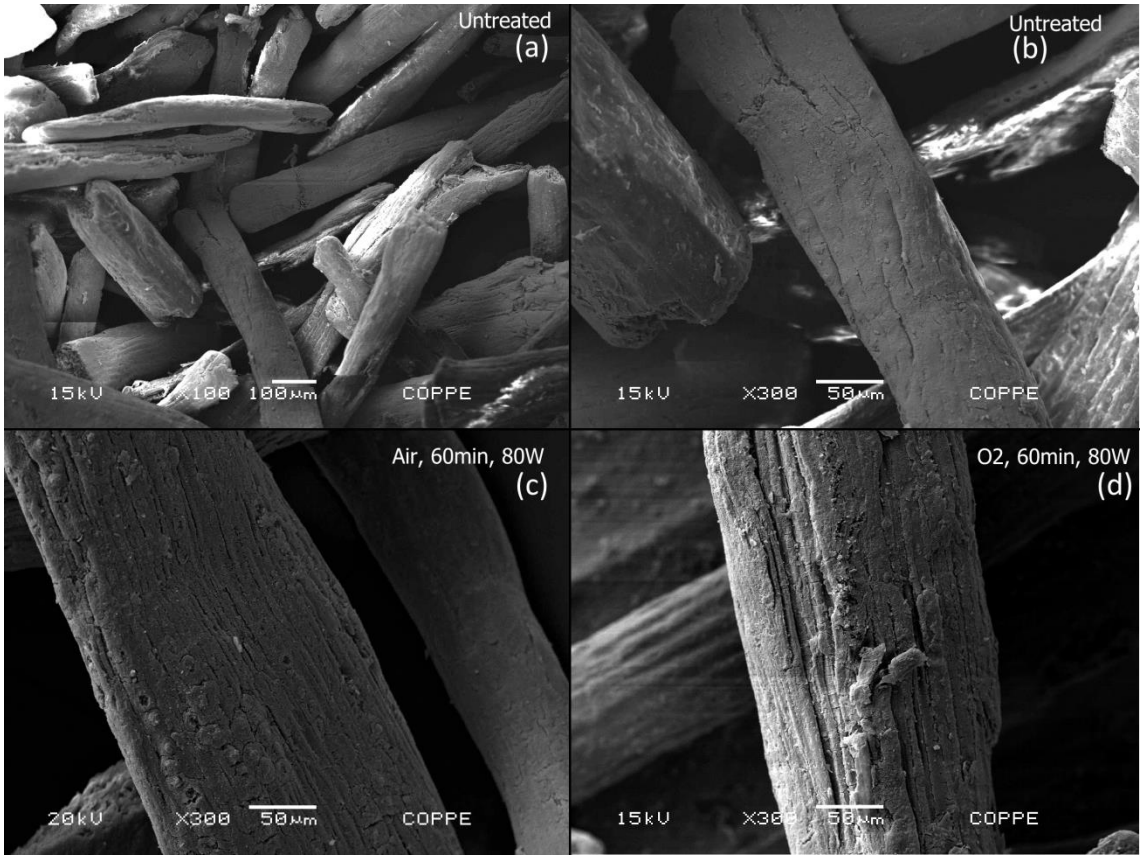

Figure 4.23 – SEM images of the coir fibers surface before treatment (a & b), after air (c) and oxygen plasma treatment (d) in the normal batch.

FTIR analyses were made on the micro batch to evaluate modifications of surface chemistry on the fibers. The spectrums for the fibers treated for 60 min at 50W are practically identical to untreated fibers, and thus are not shown here. The same is true for all treatments done on “standard batches”, with 5 grams of fibers, where no conclusive difference from the untreated samples can be pointed. However, with 60 minutes and 80W of treatment, changes are finally detectable by FTIR. Figure 4.24 shows the whole spectrum acquired for untreated, air treated and oxygen treated coir fibers under the mentioned conditions, and figure 4.25 shows details of two regions associated with cellulose.

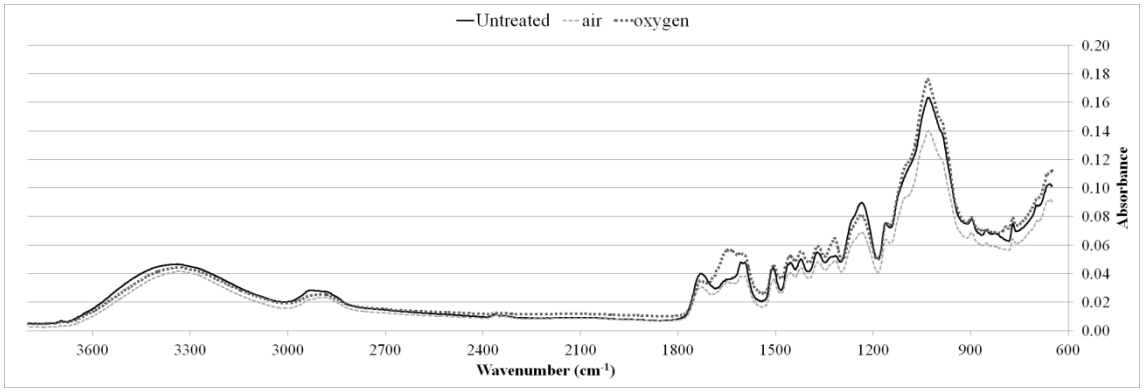

Figure 4.24 - FTIR spectrum of untreated and treated fibers for 60 minutes at 80W power in the micro batch.

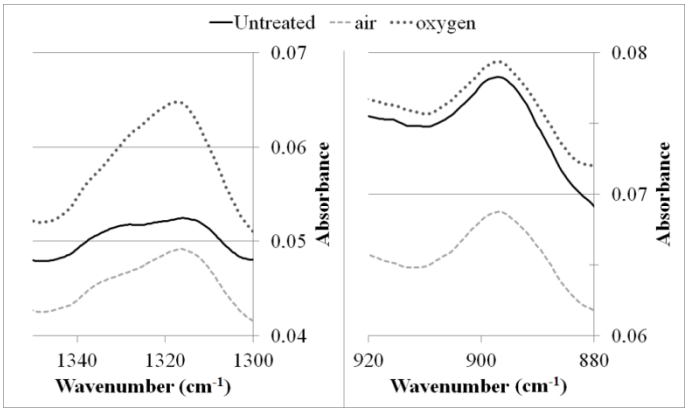

Figure 4.25 - Detail of FTIR spectrum, showing two of the peaks associated with cellulose.

Although no significant change can be seen on the 898cm^{-1} peak, there is a clear increase in the area of the peak at 1317cm^{-1}, such that untreated fiber has the smallest area (measured from the baseline), with a higher and more well defined peak after air treatment, followed by a much higher peak after oxygen treatment. This visual increase is confirmed by calculating the area ratio of the peaks of lignin and hemicellulose to the peaks of cellulose, as described by PANDEY & PITMAN (2003). The peaks at 1602cm^{-1} and 1508cm^{-1} were used for lignin, 1728cm^{-1} for hemicellulose and 1317cm^{-1} and 898cm^{-1} for cellulose. As mentioned before, this last peak had no significant change, but it was used in the calculations as a control standard, to verify if the ratio change was due to modification only in the 1317cm^{-1} peak, or also from the other peaks compared. Table 4.11 shows the calculated results.

Ratio changes for the control 898cm^{-1} peak are within experimental errors and can be considered non-significant, meaning that the lignin and hemicellulose peaks did not changed significantly with the plasma treatment. It is then clear that the statisticaly significant changes observed in the lignin/cellulose and hemicellulose/cellulose ratio are due to the increase in the cellulose peak at 1317cm^{-1}. The ratios which exhibited change are marked in bold fonts in table 4.11 and the relative increase of the cellulose peak is between 16 and 25 fold.

Table 4.11 - Ratios of areas for different peaks of cellulose, hemicellulose and lignin, before and after treatment for 60 minutes at 80W power.

	Lignin/Cellulose ratio		Lignin/Cellulose ratio		Hemicellulose/Cellulose ratio	
	1508 cm^{-1} / 898 cm^{-1}	*1508 cm^{-1} / 1317 cm^{-1}*	*1602 cm^{-1} / 898 cm^{-1}*	*1602 cm^{-1} / 1317 cm^{-1}*	*1728 cm^{-1} / 898 cm^{-1}*	*1728 cm^{-1} / 1317 cm^{-1}*
Untreated	3.65 ± 0.41	**16.21 ± 1.02**	0.28 ± 0.03	**1.23 ± 0.06**	6.95 ± 0.95	**30.83 ± 3.08**
Air	3.61 ± 0.22	**1.61 ± 0.08**	0.25 ± 0.03	**0.11 ± 0.01**	5.59 ± 0.71	**2.51 ± 0.39**
Oxygen	4.17 ± 0.16	**0.99 ± 0.06**	0.27 ± 0.02	**0.06 ± 0.01**	5.03 ± 0.50	**1.19 ± 0.17**

4.4.2. Effects of fiber modification on composites properties

Coir fibers treated in the normal batches (section 3.1.3 and 4.4.1) were compounded with thermoplastic starch (TPS) matrix in a ratio of 20wt% fibers to 80wt% TPS. Tensile test results are presented in figure 4.26.

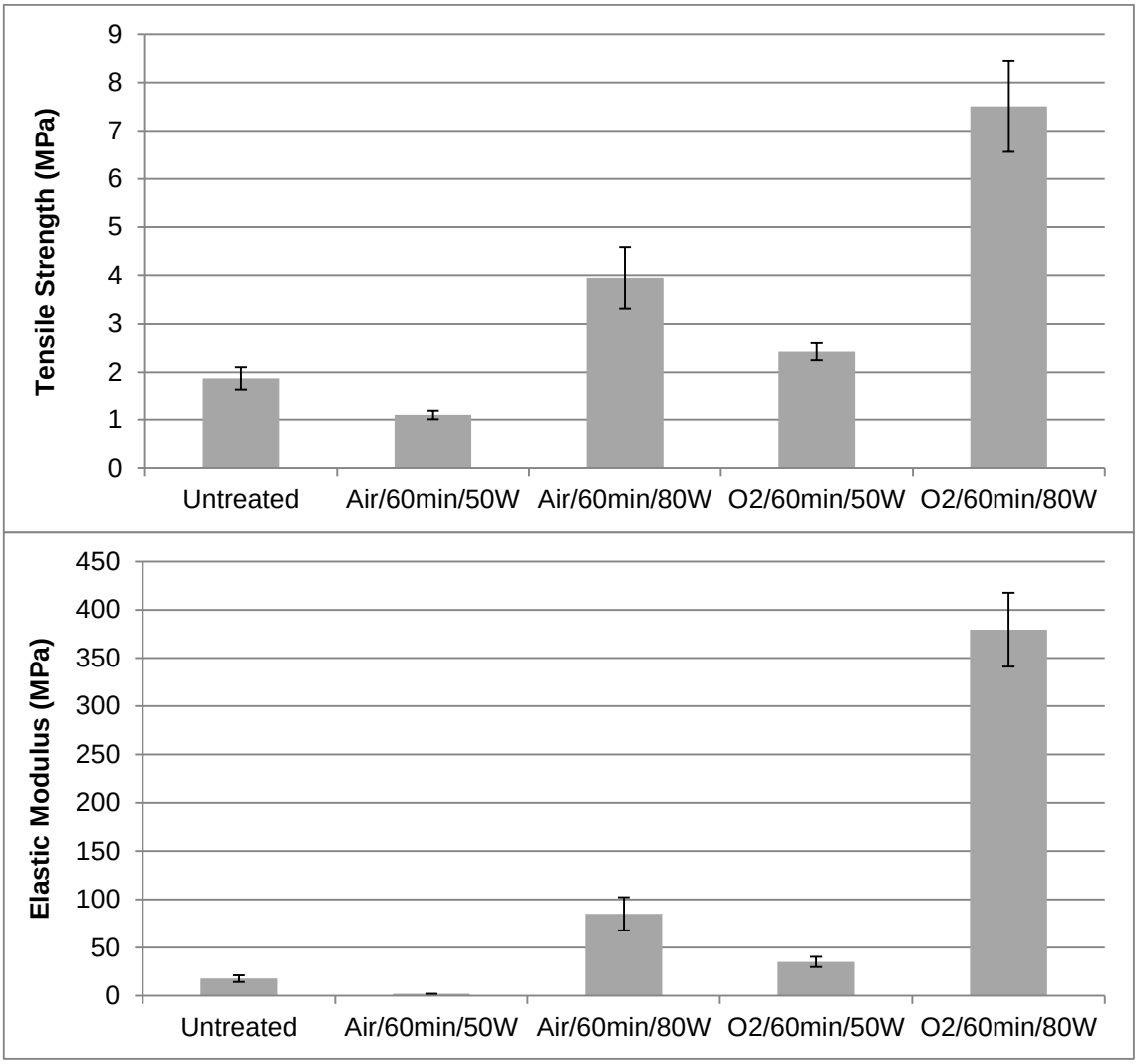

Figure 4.26 - Tensile test results for composites containing 20 wt% coir fibers in starch matrix.

Tensile strength of composites made with treated fibers suffers a reduction only in the case of lower power air treatment (60 minutes, 50 W). In all other cases, considerable increases were observed, peaking at 300% for fibers treated with pure oxygen for 60 minutes at 80 W plasma power. Two clear trends can be seen on the results when isolating the variable effects. Keeping the time and power condition constant, oxygen plasma is more effective (i.e. causes a greater increase in mechanical properties) in all conditions. Looking at the results of each gas separately, it is clear that 80 W power is significantly more effective than 50 W, with the properties increasing many-folds when changing this parameter.

The change in elastic modulus in the composites made with untreated and treated fibers show the same trends as described before, with oxygen plasma being more effective than air plasma, and higher power (80 W) yielding the best results after compounding. The effect in elastic modulus, however, is much more intense. Fiber treatment with [Air/60 min/80 W] more than tripled the elastic modulus compared to untreated fibers, from 17.9 MPa to 84.9 MPa (375% increase), and oxygen treated fibers [O_2/60 min/80 W] resulted in a composite 20 times stiffer (379.4 MPa, 2022% increase).

The fracture surface of the composites also show significant change, following the trends verified for the mechanical properties. Figure 4.27 shows the fracture surface of the composites before (a) and after treatment with oxygen (b, c and d) in different power conditions. It can be clearly seen that without treatment most fibers slipped out of the matrix, leaving their texture imprinted in the unaltered TPS surface bellow, as indicated by white arrows. This can only happen if nearly no attachment exists, as any deformation on this surface would distort or destroy the imprinted texture. Other fibers can be seen laying on the surface with little or no matrix attached to it, frequently with a gap between it and the starch, also pointed in figure 4.27a. After the most intense plasma treatment [O_2/60 min/80 W], the fracture surface displays many fibers which were broken during the tensile test, as portrayed in figure 4.27c, where a fiber has broken in half in the longitudinal plane, and in figure 4.27d, where there is also no gap between the fiber and the matrix. The intermediate oxygen plasma treatment [O_2/60 min/50 W] has a surface fracture with a combination of both, with loose and unattached fibers combined with fibers that are covered by the starch (figure 4.27b). The matrix also shows sign of deformation during the fracture process. All these features are pointed at figure 4.27, where orange arrows indicate the signs of low adhesion and green arrows the signs of good adhesion.

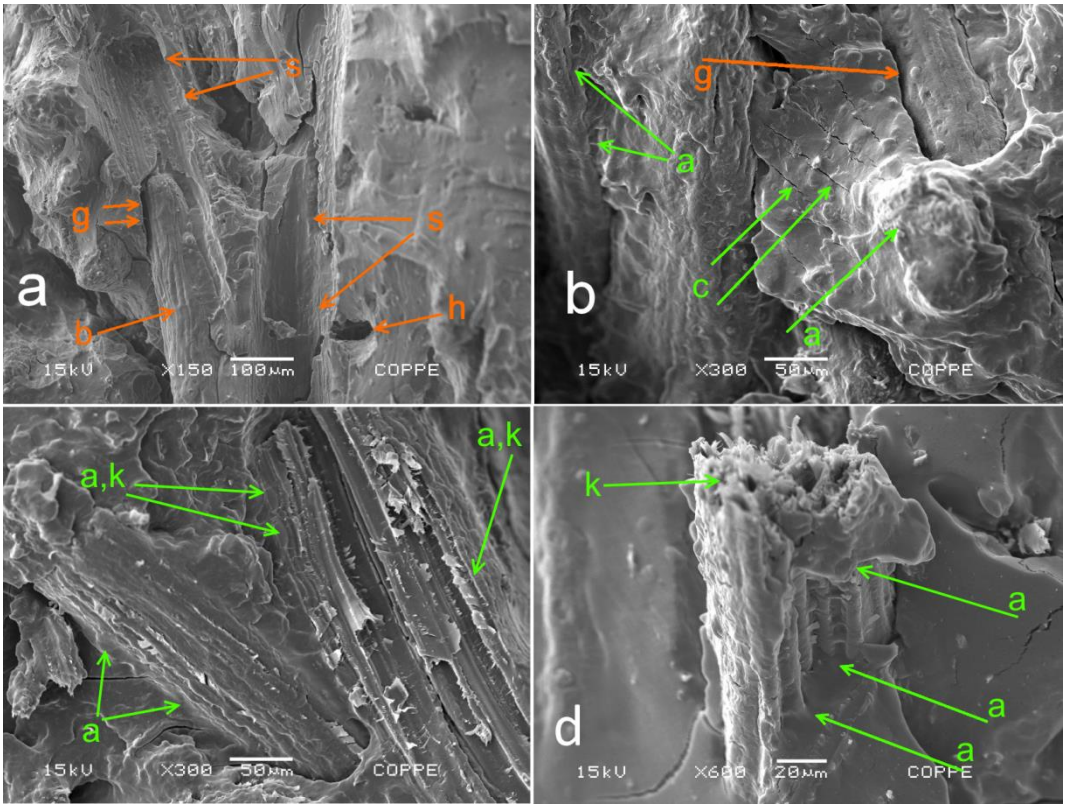

Figure 4.27 - SEM of starch composites with untreated (a), [O_2/60 min/50 W] (b) and [O_2/60 min/80 W] (c, d) treated fibers. Arrows indicate some of the pull-out holes (‘h’), large gaps between fiber and matrix (‘g’), striations (‘s’) left by sliding fibers, bare fiber surfaces (‘b’) with no matrix adhered, broken fibers (‘k’), matrix attached to the fibers (‘a) and cracked matrix pulled by the fiber (‘c’).

5. Discussion

5.1. Wood fibers for incorporation in PP matrix

5.1.1. Choice of gas

From the results shown in section 4.1 it can be seen that between all the gases used for plasma treatment, only SF_6 had a significant effect on mechanical properties of composites made with wood fibers and polypropylene, even if the effect could only be detected in the elastic modulus.

When comparing the different gases used (figure 4.1), it is clear that neither methane (CH_4) nor air had any detectable effect on the mechanical properties. This does not mean, however, that these gases cause no change in the surface, nor that they would be ineffective in other treatment conditions. What can be concluded from the results presented in figure 4.1 is that any modification caused by methane and air in the plasma treatment conditions used was insufficient to cause a change in the mechanical properties. It is possible that different treatment conditions of power and time would render good mechanical results for composites made with fibers treated with these gases. But since in the conditions chosen, no change was observed, it was assumed that much longer time or power would be necessary to reach the same improvement already achieved with sulfur hexafluoride (SF_6) plasma, and possibly SF_6 would have even better results at these conditions.

Considering the results from the “group 2” of samples and the contact angle results from table 4.4, it can be inferred that more intense plasma conditions, either in time or power, could reach better properties for composites made with SF_6 plasma treated wood fibers and polypropylene matrix. This means that the treatment conditions can be optimized to reach even better results with SF6, This indicates that for longer treatment times and powers, even if methane or air showed improvements, SF6 would show higher improvements than the ones presented in this work. This was expected considering the way each gas modifies the fibers surface and how this modification changes its interaction with the matrix. While air plasma is based in etching of the surface constituents and increased surface roughness (SEKI *et. al*., 2009), retaining the hydrophilic nature of the fibers (BOZACI *et. al.,* 2013), CH_4 and SF_6 modify the chemical characteristics of the fibers, making them hydrophobic and thus more similar

to the polypropylene matrix (KIM *et al*., 2013, ZHOU *et al*., 2011). Both mechanisms are reported to promote better mechanical properties by improvement of the fiber-matrix interface, but the chemical modification is not as explored as the morphological modification, and the use of SF_6 has not yet been reported for this application. Given the knowledge of its effect on polysaccharide surfaces, turning them highly hydrophobic (SANTOS *et al*., 2012, SANTOS *et al*., 2013), this gas was the most interesting choice for exploration in this thesis work.

5.1.2. Effects of SF_6 plasma treatment on wood fibers and its composites

Neither the “group 1” nor the “group 2” samples displayed statistically significant changes in ultimate tensile strength, as shown in table 4.1, where only the neat PP samples have a different value, as they have no reinforcing phase. The lack of significant variation of tensile strength between composites might be explained by the presence of large fibers in the relatively small tensile specimen, with the fibers acting as critical-sized flaw, inducing premature failure, as reported by PÉREZ *et al*. (2012). Possible failure mechanisms may be the growth of a crack from a flawed fiber/matrix interface or from a flaw inside the wood fiber itself, since it is not a unitary fiber, i.e. they are constituted of a bundle of smaller units (plant cells) that may not be properly adhered after the composites thermo-mechanical processing.

Nevertheless, the variation in elastic modulus is statistically significant and is reproducible, as can be seen in the graph from figure 4.2. There seems to be, however, a minimum threshold of plasma parameters, bellow which no detectable effect in mechanical properties of the composite can be seen. Although 60 watts power is sufficient to cause increase in elastic modulus of the composite when the fibers are treated for 40 minutes, if the time is shorter (10 minutes), no variation occurs. The same can be said for the treatment time of 40 minutes, which causes modifications when a power of 60 watts is applied, but not when 30 watts is used. As seen from the ANOVA results, the combination of both parameters has a stronger influence ($F=10.34$, $p=0.004$) than the isolated power ($F=6.86$; $p=0.016$) and time ($F=9.16$; $p=0.007$) parameters.

The power is important, as it determines the ion and electron kinetic energy in the plasma, and thus the types and density of ionic and excited species formed in the

plasma, as well as the collision energy of these species with the surface. It was already reported that the sulfur and fluoride incorporation by plasma treatment is dependent on the power of the plasma (SANTOS *et al.*, 2012, SANTOS *et al.*, 2013). The effect of time is straightforward, as more time allows for greater changes to occur on the surfaces as well as for a larger area to be affected. This is especially important due to the rough surface of the natural fibers, where valleys are less likely to be struck by exited specimens than protruding peaks. Another factor to be taken into account in this specific experimental arrangement is that each individual fiber was exposed for only a fraction of the total treatment time, as explained previously in subsection 3.1.2. Without the proper combination of sufficient exposure time paired with ionic specimens and energies, changes on the fiber surface are too small to be detected as a modification of mechanical behavior of a resulting composite.

The surface morphology of the fibers was not seen to have changed, as shown in figure 4.5. Still, the fracture surface of composites changed when using untreated or treated fibers. This can be seen in figures 4.3 and 4.4, respectively for composites of untreated fibers and of fibers treated for 30 minutes at 50 watts. These changes are pointed and are related to how the interaction between fiber and matrix influences the fracture surface of a composite, as discussed by MARAIS *et al.* (2005) and YUAN *et al.* (2004). It must be noted, though, that the treatment in the plasma reactor is not homogeneous on all fibers surfaces due to their movement. The average exposure is in the order of 10% of the total treatment time, but some regions or some fibers likely remain for a longer or shorter time in the plasma. So it is expected that while some fibers display signs of good adhesion, others may still behave as the untreated fibers, with the fracture surface showing a mixture of both behaviors, as in figure 4.4.

As noted, the fibers' surface morphology was not noticeably modified, but the surface chemistry is clearly changed by the SF_6 plasma treatment, as can be seen from the XPS results presented in figures 4.6 and 4.7, as well as in tables 4.3 and 4.4. As pointed in the section 3.1, fluorine was incorporated on the surface covalently bound to carbon, as indicated by the C-F, C-F_2 and C-F_3 peaks representing carbons bonded to one, two and three fluorine atoms, respectively.

As can be seen in table 4.3 for the carbon 1s high resolution deconvoluted peak, the total number of carbons covalently bonded to fluorine (C-F, C-F_2 and C-F_3) is comparable to the reduction in C-C atoms (carbon bonded solely to other carbons and/or hydrogen), with a smaller decrease observed in O-C-O/C=O atoms (carbon

bound to two oxygen atoms or doubly bonded to one). Because neither cellulose nor hemicellulose have carbon atoms bonded only to other carbons or hydrogen (JOHANSSON *et al.*, 1999), the drop in C-C bonded atoms is associated mostly with breakage in lignin with possible contributions from minor components and contaminants in this wood fiber sample. Similarly, because lignin does not contain carbon atoms bound to two oxygen atoms or doubly bound to a single one, the reduction in O-C-O is largely attributed to the breaking of cellulose or hemicellulose chains. In both cases, the broken bonds are replaced mostly by fluorine.

The high-resolution XPS of the oxygen 1s peak indicates that the presence of carbonyl groups (R-C=O) increased in treated fibers, compared to untreated fibers, accompanied by the appearance of carboxyl groups (O=C-OH). These can be formed directly during the plasma treatment by using extra oxygen atoms ripped from the material itself or from leftover humidity or air retained in the fibers. Another explanation for the carboxyl groups is the formation of acyl fluoride groups (F-C=O) during treatment, which readily react with humidity upon contact with atmosphere. The fluorine is then replaced by a hydroxyl group and the acyl fluoride becomes a carboxyl group, as demonstrated by EBNESAJJAD (2000). The appearance of a peak at 529.2 eV, which is usually associated with metallic oxides, is not clearly understood. It might be correlated with the presence of fluorine on the sample surface, due to its strong electronegativity, influencing the molecular orbitals of neighboring oxygen atoms without being directly bounded to them.

The C-O/C-CF^- peak shows no sign of reduction with plasma treatment, but this peak is the overlap of the signal from carbon bonded to hydroxyl groups (C-OH) and carbon bounded to fluorine with an ionic character (C-CF^-), as discussed by TOUZIN *et al.* (2008). Combining this information of the carbon 1s peak with the oxygen 1s peak, where a strong decrease in the R-O-R/R-OH peak is seen, it can be inferred that hydroxyl groups have been removed by the plasma treatment and replaced with a similar proportion of ionically bound fluorine.

Given these data, a reaction mechanism to partially explain the changes in cellulose is proposed and described in figure 5.1. The cellulose structure is used in this example, but the same reactions may also occur in hemicellulose. Bond breakage leading to a decrease in the O-C-O peak can only happen in two places, as indicated. Incorporation of fluorine from the plasma could only happen on the carbon containing side of the broken chain, and the free oxygen would most likely react with free

hydrogen also present in the plasma, forming a hydroxyl group. This or other hydroxyl groups can also be broken and replaced by either covalent or ionic fluorine.

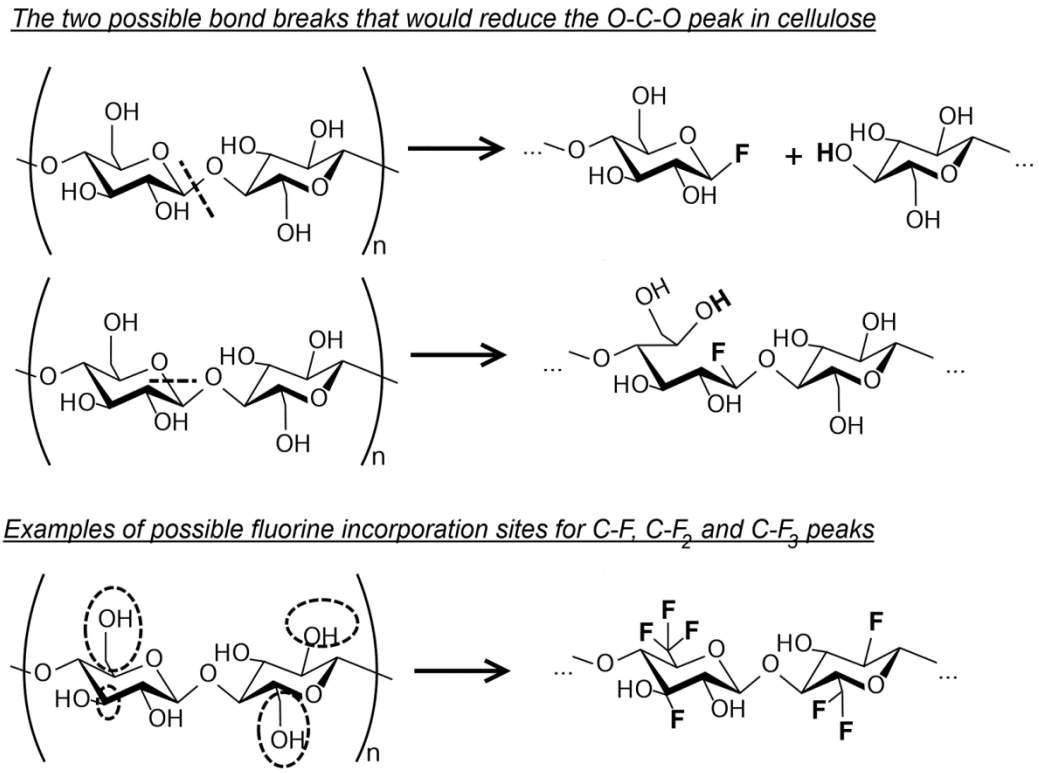

Figure 5.1 - Proposed plasma reaction mechanisms between SF_6 plasma and cellulose structure

The modification of the wood sheet sample due to plasma for a similar time (effective time, as explained in section 3.1.2) follows a very similar trend as the fibers, with the noticeable exception of the R-C=O peak, in the oxygen 1s deconvoluted peak, which decreases instead of increasing. Possible hypothesis for this difference may be the constant exposure of the sheet surface, in contrast to multiple short exposures of fibers, or a lower concentration of residual oxygen in the plasma, since the sheets have much lower surface area than a batch of fibers, making the removal of adsorbed humidity much easier in the vacuum.

The water contact angle results shown in table 4.4 can be explained by the presence of fluorine on the surface of the wood sheet samples, especially the covalently bound C-F, C-F_2 and C-F_3 groups, creating a PTFE-like surface and making the wood highly hydrophobic (SANTOS *et al.*, 2012, SANTOS *et al., 2013,*

SUANPOOT *et al*., 2012). This hydrophobic characteristic is thought to be the main responsible for the improved fiber-matrix adhesion, as the matrix is also hydrophobic. This leads to better wetting of the fibers by the polypropylene, increasing the amount of secondary bonds that can be formed while at the same time reducing the chance of pores and defects between both phases (KIM *et al*., 2013, LI *et al*., 2013).

5.2. Flax fibers for incorporation in PP matrix

As presented in section 4.2, plasma treatment with SF_6 plasma of flax fibers had a positive influence on mechanical properties of composites made with polypropylene matrix. However, the extent of improvement on mechanical properties was dependent on the type of fiber used.

5.2.1. Effect of SF_6 plasma on flax fibers

Morphological changes on the surface, mostly due to etching by plasma treatment, are known to influence fiber-matrix adhesion through increased surface area and mechanical interlocking (KARGER-KOCSIS *et al*., 2015). Many works in the literature report improvement in mechanical properties of composites due to increased surface roughness, which is achieved by plasma treatments with etching gasses like oxygen, air or argon (AGUILAR-RIOS *et al*., 2014, BOZACI *et al.*, 2013, SEKI *et al.*, 2010, SINHA *et al.*, 2009, YUAN *et al*., 2004). In this work, however, plasma treatment with SF_6 on micronized flax has led to no significant change in surface roughness, as presented in figure 4.17. Even so, composites made with treated fibers had better ultimate tensile strength and elastic modulus, compared to composites made with untreated fibers. This is further confirmed by the changes observed in the fracture surface morphology, which indicate an improved fiber-matrix adhesion (figures 4.15 and 4.16). This makes clear that improvement in mechanical properties occurs not due to improved mechanical interlocking, but is mainly, maybe exclusively, a result of chemical modification of the fiber surface, which has direct influence on the wettability and bonding of fiber and matrix.

This chemical modification is seen by the XPS analysis (figure 4.18 and tables 4.9 and 4.10). Being composed mostly of cellulose, reactions occurring on micronized flax during plasma treatment are simpler to interpret, although the overlapping of important peaks makes this task still challenging. From table 4.10, the most important

shift observed in the C 1s deconvolution is the decline of C-O and concomitant increase in both C-F and C=O. This is a clear indication that surface hydroxyl groups have been replaced both by fluorine (covalent or ionic) and carbonyl radicals.

Combining the information on the change of the C-O/C-CF^- carbon peak and the change in the R-O-R/R-OH oxygen peak, it can be concluded that most replacement of hydroxyl groups happened within the first hour of treatment, and the latter change of ionic fluorine into covalent fluorine is the probable explanation for the further decrease of the C-O/C-CF^- peak.

With technical flax fibers, a similar behavior is observed for the R-O-R/R-OH peak, indicating that hydroxyl groups are also partially removed due to the plasma treatment within the first hour (TF3), then this peak remains stable for up to 3 hours of treatment (TF4). C-O/C-CF^- is also reduced after 1h of treatment, like with micronized flax, but increases after 3 hours in the plasma (TF4). Combining the information from both peaks it is clear that new hydroxyl bonds were not formed, so the increase can be solely due to ionic fluorine incorporation (C-CF^-). As the inverse behavior was observed with the micronized flax, which is composed mostly of cellulose, it is hypothesized that the ionic fluorine results from incorporation in the lignin portion of the technical fiber. This assumption is supported by the fact that the C-C peak, which can only occur due to the presence of lignin, only decreases on the 3-hours treatment (TF4), indicating that lignin reacted with the plasma between 1h and 3h of exposure. Simultaneously, an increase in covalent bonded fluorine is observed, but a detailed analysis is further complicated by the presence of potassium (K) impurities in the sample, which partially overlap with the higher energies carbon components (C-F_2 and C-F_3).

The decrease in hydroxyl groups and especially the presence of fluorine in the surface contribute to changing the flax surface from hydrophilic to hydrophobic (SANTOS *et al.*, 2011, SANTOS *et al.*, 2012, SUANPOOT *et al.*, 2008, ZHOU *et al.*, 2011). This is the same modification as observed on the wood surface, which had its water contact angle measured and was found to become hydrophobic, as reported in section 4.1. Also as in the case of the wood fibers, this change in surface chemistry is believed to be responsible for making flax fibers more compatible with the hydrophobic polypropylene matrix, promoting better wetting and closer contact between both phases, increasing intermolecular forces and reducing the concentration and sizes of interfacial defects.

5.2.2. *Effect of the size and type of flax fiber*

A distinctive difference can be seen when comparing the mechanical behavior of composites made with technical flax and micronized flax. Besides the fact that micronized flax has overall better properties, it is noticeable that while micronized fibers treated with plasma experienced an increase in ultimate tensile strength (figure 4.14), technical flax experienced a decrease in this property after plasma treatment (figure 4.9).

Two factors are thought to play a role in these results on the technical fibers. The first is the breaking of the fibers during micro-extrusion. Since the dimensions of the micro-extruder channels and screw spacing are smaller than the fibers, they break while mixing with the molten polymer, as it has been also reported by BOS *et al.* (2006). This effect reduces the mean length from over 3mm to under 1mm, a nearly 75% reduction in length, as shown in section 4.2.1. As the treated fibers break, new surfaces are created, which were not treated by the plasma. As a result, only a fraction of the fiber-matrix interfaces in the composite may present the beneficial effects of the plasma treatment. This leads to lower improvements in fiber-matrix adhesion, as well as higher dispersion due to the broad size distribution and different interactions between the polymer and different regions of the same fiber.

The second factor that can explain the poor behavior of the composites produced using technical fibers in relation to the ones with the micronized fibers can be the large size of the former, even after breaking, in comparison with the cross-section of the small ISO/DIN-527-2 tensile specimen. As the fibers are not fully oriented on the direction of load, any of them with orientation near to the transversal direction would become essentially a large defect, with little polymer left in this cross-section region. Due to the high stress concentration in this point, the sample suffers premature failure at different stress levels, according to the presence, size and orientation of large fibers, leading to high dispersion and poor ultimate tensile strength. A similar effect was reported by HO *et al*. (2012)

Since micronized fibers size is in the range of 450µm in length and 25µm wide, being comparatively small in relation to both the micro extruder channels and the tensile specimen cross-section, neither of the factors discussed above would be significant when testing their composites. Thus, the effect of the plasma treatment is easier to detect as a change in mechanical properties when the treated fibers are small, like in micronized flax.

Regarding the chemical composition changes from both kinds of fibers, some distinctions can be made, although a full model of the reaction of SF_6 plasma with natural fibers could not be developed, given the complexity of the fibers material, composed of at least 3 components, potentially more (waxes, pectin, etc.) with varying chemical composition and molecular structures.

Micronized flax fibers, with a surface composed mostly of cellulose, behaves differently from the technical flax, which has a high concentration of lignin on its surface. It is hypothesized that this difference in surface chemical composition is the responsible for the different responses to plasma modification, since different molecules have different preferential reaction sites, and the resulting product would also depend on the macromolecule where the reaction happens. From the results presented in section 5.1.2 and 5.2.1 it can be inferred that cellulose reacts with the SF_6 plasma by replacing hydroxyl groups and forming preferably covalent bonds between carbon and fluorine, as opposed to ionic bonds. Meanwhile, lignin has a tendency to make ionic character bonds between carbon and fluorine. When carbon forms covalent bonds to fluorine, it is more likely to make this bond with only one atom of fluorine, but it can also bond to two or three of them, though the likelihood is smaller, the more fluorines are bonded. This can be seen as higher percentages of C-F bonded carbon, followed by lower concentration of $C\text{-}F_2$ and even lower, when present, $C\text{-}F_3$ bonded carbon.

Furthermore, it is observed that plasma treatment of natural fibers always cause the increase in carbonyl (C=O) and carboxyl (O=C-OH) groups, even though no oxygen is present in the treatment gas. There is not enough evidence to confirm if this oxygen comes from atoms released from the fiber itself, from residual humidity adsorbed in the fibers or from reactions occurring after the treated samples are exposed to the atmosphere. The results from the wood sheet sample (table 4.3) show a decrease in carbonyl but an increase in carboxyl groups. Considering the much lower surface area in these samples, when compared to fiber samples, it can be hypothesized that lower residual humidity was present in the plasma for the wood sheet samples, and thus the decrease in carbonyl exclusively in these samples means that the C=O formation mechanism is dependent on oxygen from water in the plasma, while the carboxyl (O=C-OH) forms by the mechanism suggested by EBNESAJJAD (2000). Further research is needed to test this hypothesis.

5.3. *Effect of fiber size and fabrication method: Fiber breakage and loss of modification*

From the discussion presented in section 5.2, it can be concluded that the relation between fiber size and processing method is important to guarantee that plasma treatment will be effective in improving mechanical properties of extruded or injected composites. If treated fibers are extensively broken in the compounding process, not only will the mechanical properties on the resulting composite be below the expected, but also the energy and resources invested in the plasma treatment will be partially wasted. As such, as natural fibers gain industrial ground, it is important to evaluate the fabrication methods used and find adequate treatments to improve the properties of composites.

As cited in sections 2.2.1 and 2.3.2, composites with natural fibers fabricated by fiber lay-out, stacking of fiber mats (woven or non-woven) or single fiber embedded in the matrix display the most significant improvement in properties. All these methods have in common a very low or no damage to the fiber during processing, as no mixing is required. Thus, modified surfaces are not damaged (or suffer little damage) and the advantages of their modification process are maximized.

It is reasonable to assume that, as this class of materials gain industrial importance, these low-damage processing techniques will be the ones used to make higher performance composites, due to the better improvement from fiber modification as well as the longer fibers allowed. However, applications of short fibers are also industrially important and are in fact already an important part of the applications of natural fiber composites (GURUNATHAN *et al*., 2015, SOBCZAK *et al.*, 2012). To allow for improvements of properties in these materials, not only must an adequate modification of the fibers be developed, but also the compounding steps must be optimized considering fiber sizes, sheer stress and component dimensions.

5.4. Multiple fibers in PLA and differences in plasma reactor designs

The results for natural fibers incorporated into PLA matrix show very little sensitivity to the plasma treatment, as seen in section 4.3. This is thought to happen due to the already similar hydrophilic characteristics of the fibers and matrix, different from the polypropylene composites (sections 4.1 and 4.2) which have a very distinct characteristic and thus a very poor interaction with natural fibers. While the SF_6 treatment of the fibers improved the compatibility with the hydrophobic PP matrix (sections 4.1, 4.2, 5.1 and 5.2), it caused a decrease in tensile strength when the fibers were compounded with the hydrophilic PLA matrix. This drop, although below 10%, can be seen on figure 4.21.

The small changes in properties are a recurrent observation of the composites made in SLK-TUC (Germany). Even the statistically significant results have smaller percentage changes than the ones found for samples made at the SFF-UFRJ (Brazil). This is attributed to the different methodology used in each institute, based on the available equipment in each case. Besides the different compounding methods, of which the effects were discussed in section 5.3, the plasma treatment was very distinct in both institutes and the effects are measurable. Direct comparison between different kinds of fibers is not possible, since each have surface characteristics and chemistry that interact differently with the plasma. Still, the vast difference in treatment conditions between SLK-TUC and SFF-UFRJ points towards this hypothesis. For example, the XPS results showing the incorporation of the same 18at.% of fluorine in wood fibers (SFF-UFRJ) and technical flax fibers (SLK-TUC) were obtained with 30 minutes/50 W SF_6 plasma and 180 minutes/200 W plasma, respectively.

As mentioned earlier in section 2.3, comparison between parameters and results of different plasma reactors is complicated due to the complexity of the plasma physics involved combined with the many variables involved in the construction of the plasma chamber. This discrepancy between the results in the two institutes is a confirmation of such statement. It is however clear that the plasma reactor used at SFF-UFRJ is more effective at promoting modification of the fiber surface and incorporation of fluorine, given the clear difference in conditions used to reach an equivalent result. This is believed to be mainly due to differences in reactor design. At SFF-UFRJ, a radiofrequency source supplies power at a frequency of 13.56 MHz to a solenoid coil, inducing a magnetic field inside the plasma chamber, which in turn

induces an electric field that accelerates the free charges in the plasma. The high frequency means that a fast change in the magnetic field is created, which in turn induces a strong electric field in the chamber. This high intensity rotational electric field accelerates the electrons and ions to high speeds, colliding with the molecules in the chamber. This causes excitation and ionization of the molecules, as well as breakage of covalent bonds, creating monoatomic specimens, highly reactive. This is especially important to SF_6 plasma, since this molecule in its ground state is highly stable, and breaking it is necessary to cause the reaction of fluorine with the surfaces exposed to plasma. Furthermore, as shown in section 3.1.2, although the plasma is concentrated in the volume under the coil, this represents a large fraction of the sample holder, and the difference in brightness between plasma inside and outside the coil is not large.

The reactor at SLK-TUC used a 40 kHz power source, with a capacitive assembly and an electric field distribution as presented in figure 3.6, with concentration of the field lines in the region where anode and cathode are closest. This region is the neck of the bottle, which is the sample holder for the PICO plasma reactor. It is visible when the plasma is in operation (figure 3.5), that this region is the brightest, i.e. it has the most intense plasma. However, no fibers are present in this specific region. The simulation and calculation of the electric fields and ionization levels of the plasma inside the plasma chamber was beyond the scope of this work, but from the information available it is possible to hypothesize that, although 200 watts of power were applied, most of this power was used to ionize molecules in a region where no fibers could be found and thus, the system is not as effective in modifying fiber surfaces as the one used at SFF-UFRJ.

Given the differences observed, it can also be inferred that an optimized reactor design for treatment of natural fibers could achieve modifications in shorter times and maybe requiring lower operational powers. In case of industrial development of this technique, it is expected that great energy efficiency may be achieved. Combined with the other advantages of this process like very small consumption of gases and wastes to be treated (refer to section 2.3.2), this could make plasma modification of fibers a competitive industrial process.

5.5. *Coir fibers for incorporation in starch matrix*

The results of the plasma treatment of coir fiber, presented in section 3.5, show clearly that both air plasma and oxygen plasma are effective in modifying the surface of coconut based fibers, increasing the surface roughness and cellulose content. This is further confirmed by the improvement in mechanical properties of the composites made with such fibers and thermoplastic starch matrix. The strong modifications found for fibers treated in the plasma reactor at SFF-UFRJ further corroborate the arguments presented in the section 5.4.

5.5.1. *"Micro batch" and the effect of plasma on the fiber surface*

From the results presented in section 4.4.1, it can be seen that the main modification that happens on the fiber surfaces due to plasma treatment is morphological. Given the gasses used, it can be inferred that such a modification happens primarily due to etching of the surface by reaction with energetic oxygen specimens (YUAN *et al*., 2004). This amount of etching, i.e. the increase in surface roughness, is proportional to the treatment time, as would be expected, and increases considerably from the 'standard batch' (figure 4.23) to the micro batch (figure 4.22), since the later were plasma treated for nearly 60 minutes, while the normal batch had individual fibers exposed to the plasma only by about 12% of that time (section 3.1.2).

Considering the long exposure time of the fibers in the "micro batch", compared to both the 'standard batch' and other works in literature, the relatively small increase in power from 50 W to 80 W had a very large impact on surface morphology. This indicates that the power variable can be very sensitive in a certain range, and finding an optimal condition could increase efficiency and consume less energy, even if power had to be slightly increased, as the desired level of modification could be achieved in shorter times.

This is an expected effect, as the supplied RF power controls what the ionization and excitation state of the plasma are. Of the many distinct ions and excited specimens possible, one (or some) will react with higher intensity or rate with the surface molecules. Though the needed analysis could not be performed in this work, it is clear from the results of the micro batch that understanding the mechanism and finding the correct power level have the potential to increase treatment efficiency.

Furthermore, from FTIR data it can be concluded that the surface of treated fibers have a higher exposure of cellulose than untreated fibers (table 4.11). Combining this information with the SEM images, along with knowledge of the natural fiber basic structure (AZWA *et al.,* 2013), it can be inferred that the amorphous surface layer of coir fiber is rich in lignin. Meanwhile, the internal structure, which is partially visible in figure 4.22, is rich in cellulose, being formed by the typical elongated vegetable cell walls (BOS *et al.* 2006).

From figure 4.22, the fibers treated by condition [µ/O_2/60 min/80 W] are clearly the ones with most internal structure visible, while the fibers treated by condition [µ/Air/60 min/80 W] still retain a large amount of the amorphous layer, even though it is highly etched and some internal structure can be seen. This matches with the FTIR results, where oxygen is more effective than air in exposing the cellulose rich areas of the fibers, i.e. the cell walls bellow the amorphous lignin rich surface layer.

The internal structure can also be seen in the 50 W condition of the “micro batch”, but the effect is localized and not as intense as in the 80 W condition. Since FTIR analysis takes into account the signal from a large area compared to the fibers dimensions, and a depth of up to 2 µm, the averaged spectra are not sensitive enough to detect the difference caused by plasma treatment on the lower power level, as noted in section 4.4.1. The same is also valid for the “standard batch”, especially since very limited exposure of internal structure is observed under SEM for the “standard batch” conditions.

Combining both the SEM analysis and FTIR, it is possible to conclude that oxygen has a stronger etching effect when compared to air. The lower oxygen content in air is the most logical assumption, as the etching reaction occurs mainly due to reaction with oxygen, being the nitrogen less reactive, even in the plasma environment (BOZACI *et al*., 2013; YUAN *et al*., 2004). Thus, it was expected that oxygen plasma would be more effective in modifying the surface and would therefore yield better mechanical results than air plasma, since is effectively a diluted version of pure oxygen, with ≈21% O_2 and ≈78% N_2.

Figure 5.2 represents a proposed model of etching from the fiber outer layer. At first, the layer is thick and covers completely the internal structure (a). After treatment in a normal batch (short time), the outer layer is etched, becoming thinner and rougher, due to the variability of both the outer layer and of the plasma etching (b). As time is increased in the micro batch, the etching thins the outer layer further, and as this process is not homogeneous, holes start to form (c). Increasing the intensity of the

treatment further (achieved here by increasing power, but a longer time could have similar results), more of the outer layer is etched and only small portions of it remain, while the internal structure is mostly exposed (d).

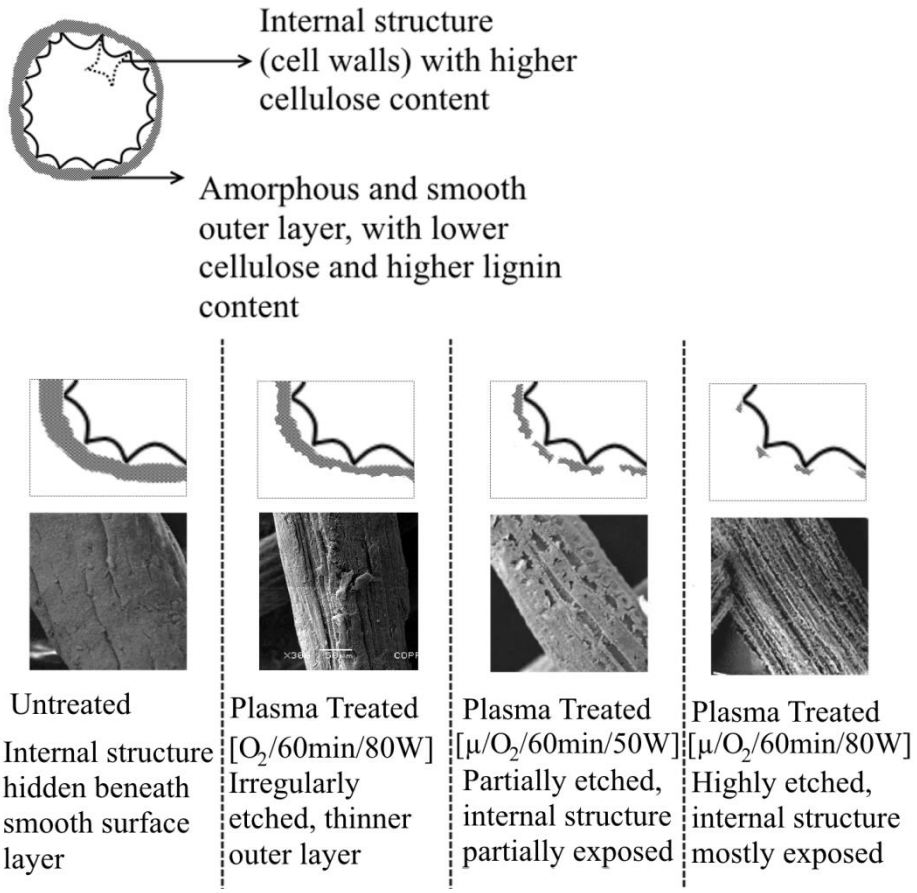

Figure 5.2 – Proposed mechanism of plasma etching of the coir fiber

5.5.2. "Normal batch" and the increase in mechanical properties

The elastic modulus of pure thermoplastic starch is typically low, in part due to the presence of the plasticizer, which can have a great effect on its properties. In the literature, elastic modulus for TPS varies typically from 12-125 MPa (AVÉROUS & BOQUILLON, 2004; GURUNATHAN *et al*., 2015) and at times even higher values when lower amounts of plasticizer are used (1691 MPa for 20% of plasticizer), as reported by LOPEZ-GIL *et al*. (2014). In this work, tensile tests were performed in specimens of the matrix material, 70% starch and 30% plasticizer. The Young's

modulus found in this case was 8.4 MPa and tensile strength was 0.5 MPa. Coir fiber is in the low end of natural fibers' mechanical properties spectrum, but still has a much higher elastic modulus (6 GPa) than the pure TPS (FARUK *at al*., 2012, GURUNATHAN *et al*., 2015). This means that, even though the 2022% increase in elastic modulus obtained in this work (section 4.4.2) may seem unrealistic at first glance, a composite of coir fibers and thermoplastic starch matrix with elastic modulus of 379.4 MPa is well within the expected values, if fiber/matrix interaction is sufficiently effective.

This can be calculated, as done previously by VILASECA *et al*. (2007) and LOPEZ-GIL *et al*. (2014), by the rules of mixture (equations 5.1 and 5.2), a simplified way to calculate lower and upper boundaries for expected properties in a composite, assuming ideal bonding and fibers longer than the critical size. E_C, E_F and E_M are the elastic modulus of the composite, fiber and matrix, respectively. f_F and f_M are the volume fractions of fiber and matrix, respectively, which were calculated using the densities found in literature for coir fiber (1.2 g/cm³, from GURUNATHAN *et al*., 2015) and starch with 30 wt% glycerol (1.34 g/cm³, from AVÉROUS & BOQUILLON, 2004).

$$E_C = f_F E_F + f_M E_M \qquad (5.1)$$

$$E_C = \left(\frac{f_F}{E_F} + \frac{f_M}{E_M}\right)^{-1} \qquad (5.2)$$

In the case of fibers aligned transversal to the applied load, i.e. the tensile test specimen length, the inverse rules of mixtures is used and the expected elastic modulus would be 10.7 MPa (equation 5.2). If all fibers were oriented in the direction of the applied load, the elastic modulus would be 1316.3 MPa, or 1.3 GPa (equation 5.1). The obtained experimental value of 379.4 MPa for composites made with fibers treated at the condition [O_2/60 min/80 W] lies close to 1/3 of the way from the lower to the upper boundary. Considering that orientation of the fibers occurs to some extent during compression molding and that tensile specimens are cut according to this partial orientation, the obtained value is well within reason, and the great difference between this plasma condition and the others is due to a great increase in load transfer, attributed to improved fiber/matrix interface adhesion.

Alternatively, the improvement in adhesion between fiber and matrix can be estimated by equation 5.3, as described by VILASECA *et al*. (2007), similar to the rule of mixtures (equation 5.1). The difference lies in another parameter, f_C, the "compatibility factor", which includes fiber length, aspect ratio, orientation and fiber-matrix adhesion at the interface. Since the first three factors should not change between the composites made with untreated and treated fibers, changes in f_C should be predominantly due to changes in the fiber-matrix adhesion. Using the obtained results of Young's modulus as E_C, it can be calculated that f_C increases from 0.0087 in composites of untreated coir to 0.2847 in composites made with fibers treated with [O_2/60 min/80 W].

$$E_C = f_C(f_F E_F) + f_M E_M \qquad (5.3)$$

With such small value for f_C in the composite of untreated fibers, it is clear that the interaction between fibers and matrix was very poor, leaving much room for improvement when using adequate plasma treatment. The same analysis can be done for ultimate tensile strength, following the equation 5.4 where σ_C, σ_F and σ_M represent the ultimate tensile strength of the composite, fiber and matrix, respectively. Taking the value of this property for the coir fiber as 175 MPa (FARUK *at al*., 2012; GURUNATHAN *et al*., 2015), the measured 0.5 MPa for the ultimate tensile strength of the starch matrix alone, 1.87 MPa for the composite made with untreated fibers and 7.51 MPa for the composite made with fibers treated with [O_2/60 min/80 W], the following results are found: $f_{C\text{-}Untreated}$ = 0.0388 and $f_{C\text{-}Plasma}$ = 0.1866. Although the values are not the same as for elastic modulus, the orders of magnitude of the results are the same and the trend is also of increase in f_C with plasma treatment.

$$\sigma_C = f_C(f_F \sigma_F) + f_M \sigma_M \qquad (5.4)$$

These calculations confirm the experimental results presented in section 4.4.2, indicating that oxygen plasma is indeed highly efficient in improving the interaction and load transfer between coir fibers and thermoplastic starch matrix.

6. Conclusions

The work developed for this thesis has led to conclusions for each of the materials and plasma treatments, with some important results that have not been reported in the literature.

Low pressure inductively coupled sulfur hexafluoride (SF_6) plasma treatment has caused the incorporation of fluorine covalently bonded to carbon in soft wood fibers and sheets. This has changed the behavior of wood surfaces from hydrophilic to highly hydrophobic (contact angle with water of up to 132°). Even more relevant to this work, this chemical modification of wood has increased the interaction between this kind of fiber and a polypropylene matrix. This was measured as an increase of 24% in the elastic modulus of composites made of polypropylene and 17wt% short wood fibers treated for 40 minutes at 60W power, when compared to composites made with untreated fibers. Since no detectable change in morphology has been observed, it can be concluded that this improvement was achieved only by the modification of the surface chemistry by the plasma treatment. A model for this reaction mechanism has been proposed based on XPS analysis. So far, no work in the literature reports on the use of SF_6 plasma for compatibilization of fiber and matrix. Future developments and studies in plasma conditions and reactor design may optimize this surface modification process, improving the mechanical properties even further.

A similar SF_6 plasma treatment, using low pressure glow discharge plasma, has similarly caused the incorporation of fluorine on the surface of two types of flax fibers: short or “technical” fibers and “micronized” fibers. When compounded with polypropylene matrix by micro-extrusion and micro-injection molding, both displayed improved mechanical properties after treatment, compared to composites made of untreated fibers. Micronized fibers had the best results, with an increase of ~10% in both ultimate tensile strength and elastic modulus, again only due to chemical modification of the fiber surface, with no change in mechanical interlocking. Works reported in the literature which improved the properties of the composites, due to chemical modification of the fiber surfaces, always have the increase in surface roughness also influencing the properties, not allowing to differentiate how important each of the two factors are. On the work presented in this thesis, however, improved mechanical properties were achieved solely due to chemical modification of the fiber surface, proving this is an important factor in the composites final properties. This

means that future developments of combined treatments that also increase surface roughness may improve mechanical properties even further. The same can be said for the composites made of technical flax fibers, although these displayed lower results when compared to micronized flax. The SF_6 plasma modification has caused an increase in elastic modulus of 5%. The difference in behavior between both kinds of fibers was investigated, and it was concluded that the surface chemical composition of micronized flax is different from technical flax, although both derive from the same plant species. This influences the way the SF_6 plasma reacts with the surface and thus the response measured in mechanical properties. Furthermore, the sizes of the fibers and the compounding process have a strong influence on the results obtained, since damage to the fibers occur, which reduce the effectiveness of the plasma treatment.

Work with coir fibers treated by air and oxygen plasma has led to the other extreme of modifications, leading to extremely rough surfaces due to strong etching effect. The results allowed creating a model of how the smooth, lignin rich surface layer of coir fibers is etched by oxygen-rich plasmas. It has also been observed that the power applied to the plasma, in a certain range, can have a very strong influence on the final surface morphology. Furthermore, these modifications have led to a considerable increase of mechanical properties of composites made with treated coir fibers and thermoplastic starch matrices. It was concluded that the combined effect of higher surface roughness and increased exposure of cellulose was responsible for increases of up to 375% in ultimate tensile strength and 2022% in elastic modulus, when comparing composites of untreated fibers to composites made with fibers treated for 60 min at 80 W of oxygen plasma.

In all cases, signs of improved fiber-matrix interface were observed by scanning electron microscopy of the fracture surfaces. All these results combined show that plasma treatment is a promising technique to modify the surfaces of natural fibers of many kinds, leading to composites of superior mechanical properties. This work was the first to use sulfur hexafluoride, an inert gas when not in a plasma environment, as a process gas to modify the surface of natural fibers and consequently improve their interaction with polymeric matrices. Furthermore, it has been shown that oxygen and, to a lesser extent, air plasma treatments are highly efficient in improving the mechanical properties of coir fiber and thermoplastic starch composites, a fully renewable and biodegradable material. With the results here presented and the models proposed, further developments can be made in order to reach higher efficiencies and better final mechanical properties, eventually making plasma modification a feasible and environmentally friendly alternative to improve the properties of composites

reinforced with natural fibers. This will hopefully lead to this class of materials to be applied in new markets, replacing components made with pure polymers and with glass fibers reinforced composites, which is a step in the right direction for a more sustainable material industry.

7. Suggestions for future work

Given the time constraints in a doctoral work as well as the broad field studied here, it is natural that many ideas for experiments and analysis had to be left for future works. In this section, a short list of suggestions is presented to continue the work presented and improve the knowledge of the mechanisms involved.

a) Optimization of the plasma treatment conditions for a specified material (i.e. micronized flax and PP composites, coir fibers and thermoplastic starch, etc.), investigating the response curve of power and time over a broader range of conditions.
b) Perform water vapor permeation and water diffusion tests in order to evaluate if the improvements in fiber-matrix interfaces have also made the composite materials less susceptible to wet environments
c) Perform and optimize two-steps plasma treatments, consisting of a first step designed to increase surface roughness of the fibers (e.g. oxygen or air plasma) and a second step designed to modify the surface chemical characteristics, according to the matrix material used (e.g. SF_6 plasma when using PP matrix).
d) Compare different compounding processes to evaluate the effect of fiber damage during the incorporation in the polymeric matrix.
e) Perform more detailed surface analysis, with complementary techniques, to further refine the reaction mechanisms involved in the plasma modification of lignocellulosic fibers by SF_6 plasma. Additionally perform an optical spectrometry analysis of the plasma environment during treatment, to determine the active ionic and excited specimens present.
f) Development of a continuous or semi-continuous low pressure plasma reactor, based on the RF inductively coupled reactor presented here, for treatment of larger amounts of fibers, aiming at industrial applications of the plasma surface modification process.
g) Perform biodegradability tests to evaluate if the plasma modification of fibers causes changes in the degradation time and if they influence the degradation products.

8. Bibliography

AGRAWALA, S. *et al*. Mechanics of media motion in tumbling mills with 3d discrete element method. **Minerals Engineering**, v. 10, n. 2, p. 215–227, 1997.

AGUILAR-RIOS, A. *et al*. Improving the bonding between henequen fibers and high density polyethylene using atmospheric pressure ethylene-plasma treatments. **Express Polymer Letters**, v. 8, n. 7, p. 491–504, 2014.

ANWER, M., BHUIYAN, A. H. Influence of Low Temperature Plasma Treatment on the surface , Optical and DC Electrical Properties of jute. **IOSR Journal of Applied Physics**, v. 1, n. 5, p. 16–22, 2012.

AVÉROUS, L., BOQUILLON, N. Biocomposites based on plasticized starch: thermal and mechanical behaviour. **Carbohydrate Polymers**, v. 56, n. 2, p. 111–122, 2004.

BLEDZKI, A. K., GASSAN, J. Composites reinforced with cellulose based fibres. **Progress in Polymer Science (Oxford)**, v. 24, n. 2, p. 221–274, 1999. (Bledzki & Gassan, 1999)

BOGDANOWICZ, R. Investigation of H2:CH4 Plasma Composition by Means of Spatially Resolved Optical Spectroscopy. **Acta Physica Polonica A**, v. 114, n. 6-A, p. 33–38, 2008.

BOS, H. L., MÜSSIG, J., VAN DEN OEVER, M. J. A. Mechanical properties of short-flax-fibre reinforced compounds. ***Composites Part A: Applied Science and Manufacturing***, v. 37, n. 10, p. 1591–1604, 2006.

BOZACI, E. *et al*. Effects of the atmospheric plasma treatments on surface and mechanical properties of flax fiber and adhesion between fiber–matrix for composite materials. **Composites: Part B**, v. 45, p. 565–572, 2013.

CORRADINI E., MOTTOSO L.H.C., MORAIS L.C., *et al*., "Mechanical and morphological characterization of the biodegradable composites". *World polymer congress and 41st international symposium on macromolecules,* 1520, Rio de Janeiro, RJ, Brazil, 16-21 July 2006.

COUSINS, W. J., 1978, "Young's modulus of hemicellulose as related to moisture content", ***Wood Science and Technology***, v. 12, n. 3, pp.161-167.

DÁNYÁDI, L. *et al*., 2007, "Wood flour filled PP composites: Compatibilization and adhesion" ***Composites Science and Technology***, v. 67, pp. 2838–2846.

DÁNYÁDI L, MÓCZÓ J, PUKÁNSZKY B., 2010, “Effect of various surface modifications of wood flour on the properties of PP/wood composites”, ***Composites part A,*** v.41, pp. 199–206.

DITTENBER, D. B., GANGARAO, H. V. S. Critical review of recent publications on use of natural composites in infrastructure. **Composites Part A: Applied Science and Manufacturing**, v. 43, n. 8, p. 1419–1429, 2012.

EBNESAJJAD, S. “Fluoroadditives”. In: Ebnesajjad, S. (ed), *Non-Melt Processible Fluoroplastics: the definitive user’s guide and databook*, 1 ed., chapter 11, Norwich, NY, USA , Plastics Design Library, 2000.

FARUK, O. *et al*. Biocomposites Reinforced with Natural Fibers: 2000-2010. ***Progress in Polymer Science***, v. 37, n. 11, p. 1552–1596, maio. 2012.

FELEKOGLU, B., TOSUN, K., BARADAN, B. A comparative study on the flexural performance of plasma treated polypropylene fiber reinforced cementitious composites. **Journal of Materials Processing Technology**, v. 209, n. 11, p. 5133–5144, 21 jun. 2009.

FERRARIA, A. M., LOPES DA SILVA, J. D., BOTELHO DO REGO, A. M. XPS studies of directly fluorinated HDPE: Problems and solutions. **Polymer**, v. 44, p. 7241–7249, 2003.

GIRONÈS, J. *et al*. Natural fiber-reinforced thermoplastic starch composites obtained by melt processing. **Composites Science and Technology**, v. 72, n. 7, p. 858–863, 2012.

GOLDSTON, R..J, RUTHERFORD, P. H., *Introduction to Plasma Physics,* 1 ed., Institute of Physics Publishing Bristol and Philadelphia, 1995.

GURUNATHAN, T., MOHANTY, S., NAYAK, S. K. A Review of the Recent Developments in Biocomposites Based on Natural Fibres and Their Application Perspectives. **Composites Part A: Applied Science and Manufacturing**, v. 77, p. 1–25, 2015.

GUPTA, B.S., REINIATI, I., LABORIE, M-P.G, “Surface properties and adhesion of wood fiber reinforced thermoplastic composites”, ***Colloids and Surfaces A: Physicochemical and Engineering Aspects***, v. 302, n. 1-3, pp. 388-395, 2007.

HAN, Y. *et al*. Cold plasma treatment on starch foam reinforced with wood fiber for its surface hydrophobicity. **Carbohydrate Polymers**, v. 86, n. 2, p. 1031–1037, 2011.

HERRERA-FRANCO, P. J.; VALADEZ-GONZÁLEZ, A. A study of the mechanical properties of short natural-fiber reinforced composite. **Composites Part B: Engineering**, v. 36, p. 597–608, 2005.

HO, M-P., WANG, H., LEE, J-H., *et al.*, 2012, “Critical factors on manufacturing processes of natural fibre composites”, ***Composites Part B: Engineering***, v. 43, n. 8 (dez), pp. 3549-3562.

HUANG, S*. et al.* Langmuir probe measurements in inductively coupled CF4 plasmas. **Surface and Coatings Technology**, v. 200, n. 12-13, p. 3963–3968, 31 mar. 2006.

JOHANSSON, L.-S. *et al*. Evaluation of surface lignin on cellulose fibers with XPS. **Applied Surface Science**, v. 144-145, p. 92–95, 1999.

JOHN, M.; THOMAS, S., “Biofibres and biocomposites”, ***Carbohydrate Polymers***, v. 71, n. 3, p. 343–364, 2008.

KIM, M., KIM, H. S., LIM, J. Y. A Study on the Effect of Plasma Treatment for Waste Wood Biocomposites. **Journal of Nanomaterials**, v. 2013, p. 1-6, 2013.

KARGER-KOCSIS, J., MAHMOOD, H., PEGORETTI, A. Recent advances in fiber/matrix interphase engineering for polymer composites. **Progress in Materials Science**, v. 73, p. 1–43, 2015.

KUSANO, Y., TEODORU, S., HANSEN, C. M. The physical and chemical properties of plasma treated ultra-high-molecular-weight polyethylene fibers. **Surface and Coatings Technology**, v. 205, p. 2793–2798, 2011.

LA MANTIA, F. P.; MORREALE, M. Green composites: A brief review. **Composites Part A: Applied Science and Manufacturing**, v. 42, n. 6, p. 579–588, 2011.

LI, R., YE, L., MAI, Y.-W. Application of plasma technologies in polymer composites : a review of recent developments. **Composites part A**, v. 28A, n. 28A, p. 73–86, 1997.

LI, S., JINJIN, D. Improvement of hydrophobic properties of silk and cotton by hexafluoropropene plasma treatment. **Applied Surface Science**, v. 253, n. 11, p. 5051–5055, 2007.

LI, Y., PICKERING, K. L. Hemp fibre reinforced composites using chelator and enzyme treatments. **Composites Science and Technology**, v. 68, n. 15-16, p. 3293–3298, dez. 2008.

LI, Y. *et al.* Helium plasma treatment of ethanol-pretreated ramie fabrics for improving the mechanical properties of ramie/polypropylene composites. **Industrial Crops and Products**, v. 51, p. 299–305, 2013.

LOPEZ-GIL, A. *et al*. Strategies to Improve the Mechanical Properties of Starch-based Materials : Plasticization and Natural Fibers Reinforcement. **Polímeros**, v. 24, p. 36–42, 2014.

MAHLBERG, R. *et al*. Application of AFM on the adhesion studies of oxygen-plasma-treated polypropylene and lignocellulosics. **Langmuir**, v. 15, n. 8, p. 2985–2992, 1999.

MALEKI-MOGHADDAM, M., YAHYAEI, M., BANISI, S. A method to predict shape and trajectory of charge in industrial mills. **Minerals Engineering**, v. 46-47, p. 157–166, 2013.

MARAIS, S. *et al*. Unsaturated polyester composites reinforced with flax fibers: Effect of cold plasma and autoclave treatments on mechanical and permeation properties. **Composites Part A: Applied Science and Manufacturing**, v. 36, n. 7, p. 975–986, 2005.

MARTIN, A. R. *et al*. **Plasma modification of sisal on high density polyethylene composites: effect on mechanical properties,** In Proceedings from the Third International Symposium on Natural Polymers and Composites-ISNaPol. **Anais**...2000Disponível em: <http://128.104.77.228/documnts/pdf2000/marti00a.pdf>

MARTINS, C. R., de JESUS JÚNIOR, L. A. **Evolução da produção de coco no Brasil e o comércio internacional : panorama 2010.** In: Documentos 164 / Embrapa Tabuleiros Costeiros ISSN 1517-1329. Embrapa, Aracaju, SE, 2011.

MOHANTY, A. K., MISRA, M., HINRICHSEN, G. Biofibres, biodegradable polymers and biocomposites: An overview. **Macromolecular Materials and Engineering**, v. 276-277, p. 1–24, 2000.

MOHANTY, A. K., MISRA, M., DRZAL L.T. Surface modifications of natural fibers and performance of the resulting biocomposites: an overview. **Composite Interfaces** v. 8, n. 5, p. 313-342, 2001.

MUKHOPADHYAY, S., FANGUEIRO, R. Physical Modification of Natural Fibers and Thermoplastic Films for Composites -- A Review. **Journal of Thermoplastic Composite Materials**, v. 22, n. 2, p. 135–162, 2009.

MUELLER, D.H., KROBJILOWSKI A. New discovery in the properties of composites reinforced with natural fibers. **Journal of Industrial Textiles**, v. 33, n. 2, p. 111-130, 2003.

MÜLLER, P. *et al*. Thermoplastic starch/wood composites: Interfacial interactions and functional properties. **Carbohydrate Polymers**, v. 102, n. 1, p. 821–829, 2014.

MUTNURI, B., AKTAS, C.J., MARRIOTT, J., *et al*. “Natural fiber reinforced pultruded composites” In: **Proceedings of COMPOSITES 2010**, Las Vegas, Nevada, USA, 9–11 February 2010.

NECHWATAL, A., MIECK, K-P., REUßMANN, T. Developments in the characterization of natural fibre properties and in the use of natural fibers for composites, ***Composites Science and Technology***, v. 63, n. 9, pp. 1273-1279, 2003.

OKUMURA, T. Inductively Coupled Plasma Sources and Applications. **Physics Research International**, v. 2010, n. 1, p. 1–14, 2010.

OLARU, N., OLARU, L., COBILIAC, G. Plasma-modified wood fibers as fillers in polymeric materials • . **Romanian Journal of Physics**, v. 50, n. July 2004, p. 1095–1101, 2005.

PANDEY, K. ., PITMAN, A. . FTIR studies of the changes in wood chemistry following decay by brown-rot and white-rot fungi. **International Biodeterioration & Biodegradation**, v. 52, n. 3, p. 151–160, 2003.

PATEL, M., NARAYAN, R., "How sustainable are biopolymers and biobased products? The hope, the doubt, and the reality". In: Mohanty A.K., Misra M., Drzal L.T. (eds), *Natural fibers, biopolymers, and biocomposites*, 1 ed., chapter 27, Boca Raton, USA, CRC Press, 2005.

PAPPAS, D. *et al*. Surface modification of polyamide fibers and films using atmospheric plasmas. **Surface and Coatings Technology**, v. 201, n. 7, p. 4384–4388, 20 dez. 2006.

PÉREZ, E., FAMÁ, L., PARDO, S.G., *et al*., 2012, "Tensile and fracture behavior of PP/wood flour composites", ***Composites Part B: Engineering,*** vol. 43, pp. 2795–2800.

QIN, C., SOYKEABKAEW, N., XIUYUAN, *et al.,* 2008, "The effect of fibre volume fraction and mercerization on the properties of all-cellulose composites", ***Carbohydrate Polymers***, v. 71, n. 3, pp. 458-467.

RAFFAELEADDAMO, A. *et al*. Cold plasma-induced modification of the dyeing properties of poly(ethylene terephthalate) fibers. **Applied Surface Science**, v. 252, n. 6, p. 2265–2275, 15 jan. 2006.

RAMÍREZ, M. G. L. *et al*. Study of the properties of biocomposites. Part I. Cassava starch-green coir fibers from Brazil. **Carbohydrate Polymers**, v. 86, n. 4, p. 1712–1722, 2011.

RAY, D., SARKAR, B.K., RANA A.K., *et al*., 2001, "The mechanical properties of vinylester resin matrix composits reinforced with alkali-treated jute fibres", ***Composites Part A: Science and Manufactruring***, v. 32, n. 1, pp. 119-127.

ROSA, M. F. *et al*. Effect of fiber treatments on tensile and thermal properties of starch/ethylene vinyl alcohol copolymers/coir biocomposites. **Bioresource Technology**, v. 100, n. 21, p. 5196–5202, 2009.

SANTOS, A. E. F. *et al*. Chemical analysis of a cornstarch film surface modified by SF6 plasma treatment. **Carbohydrate Polymers**, v. 87, n. 3, p. 2217–2222, 2012.

SANTOS, A. E. F. *et al*. Inducing Surface Hydrophobization on Cornstarch Film by SF6 and HMDSO Plasma Treatment. **Carbohydrate Polymers**, v. 91, n. 2, p. 675–681, ago. 2013.

SANTOS, P. A. *et al*. Polyamide-6/vegetal fiber composite prepared by extrusion and injection molding. **Composites Part A: Applied Science and Manufacturing**, v. 38, n. 12, p. 2404–2411, 2007.

SATYANARAYANA, K. G., ARIZAGA, G. G. C., WYPYCH, F. Biodegradable composites based on lignocellulosic fibers-An overview. **Progress in Polymer Science (Oxford)**, v. 34, n. 9, p. 982–1021, 2009.

SEKI, Y. *et al*. "The influence of oxygen plasma treatment of jute fibres on mechanical properties of jute fibre reinforced thermoplastic composites". *5th International Advanced Technologies Symposium*, Karabuk, Tukey, 13-15 May 2009.

SEKI, Y. *et al*. Effect of the low and radio frequency oxygen plasma treatment of jute fiber on mechanical properties of jute fiber/polyester composite. **Fibers and Polymers**, v. 11, n. 8, p. 1159–1164, 2010.

SINHA, E., PANIGRAHI, S. Effect of Plasma Treatment on Structure, Wettability of Jute Fiber and Flexural Strength of its Composite. **Journal of Composite Materials**, v. 43, n. 17, p. 1791–1802, 2009.

SOBCZAK, L., LANG, R. W., HAIDER, A. Polypropylene composites with natural fibers and wood – General mechanical property profiles. **Composites Science and Technology**, v. 72, n. 5, p. 550–557, mar. 2012.

SREEKUMAR, PA., THOMAS, S.P., SAITER, J.M., *et al*. Effect of fiber surface modification on the mechanical and water absorption characteristics of sisal/polyester composites fabricated by resin transfer molding. **Composites Part A: Applied Science and Manufacturing**, v. 40, n. 11, p. 1777–1784, nov. 2009.

STAMBOULIS, A. *et al*. Environmental durability of flax fibres and their composites based on polypropylene matrix. **Applied Composite Materials**, v. 7, n. 5-6, p. 273–294, 2000.

SUANPOOT, P. *et al*. Surface analysis of hydrophobicity of Thai silk treated by SF6 plasma. **Surface and Coatings Technology**, v. 202, n. 22-23, p. 5543–5549, ago. 2008.

SUMMERSCALES, J. *et al*. A review of bast fibres and their composites. Part 1 – Fibres as reinforcements. **Composites Part A: Applied Science and Manufacturing**, v. 41, n. 10, p. 1329–1335, 2010.

TEZANI, L. L. *et al*. Chemistry studies of SF6/CF4, SF6/O2 and CF4/O2 gas phase during hollow cathode reactive ion etching plasma. **Vacuum**, v. 106, p. 64–68, 2014.

TOMCZAK, F., SYDENSTRICKER, T. H. D., SATYANARAYANA, K. G. Studies on lignocellulosic fibers of Brazil. Part II. Structure and properties of Brazilian coconut fibers. **Composites. Part A, Applied Science and Manufacturing**, v. 38, p. 1710–1721, 2007.

TOUZIN, M. *et al*. Study on the stability of plasma-polymerized fluorocarbon ultra-thin coatings on stainless steel in water. **Surface and Coatings Technology**, v. 202, n. 19, p. 4884–4891, 2008.

VILASECA, F*. et al*. Composite materials derived from biodegradable starch polymer and jute strands. **Process Biochemistry**, v. 42, n. 3, p. 329–334, 2007.

WATTANAKORNSIRI, A.; TONGNUNUI, S. Sustainable green composites of thermoplastic starch and cellulose fibers. **Songklanakarin Journal of Science and Technology**, v. 36, n. 2, p. 149–161, 2014.

XIE, Y., HILL, C.A.S., XIAO, Z., *et al*. Silane coupling agents used for natural fiber/polymer composites: A Review. **Composites: Part A**, v. 41, n. 7, p. 806-819, 2010.

YU, L., DEAN, K., LI, L. Polymer blends and composites from renewable resources. **Progress in Polymer Science (Oxford)**, v. 31, n. 6, p. 576–602, 2006.

YUAN, X., JAYARAMAN, K., BHATTACHARYYA, D. Effects of plasma treatment in enhancing the performance of woodfibre-polypropylene composites. **Composites Part A: Applied Science and Manufacturing**, v. 35, n. 12, p. 1363–1374, dez. 2004.

YUAN, Y., LEE, T. R. “Contact Angle and Wetting Properties”. In Bracco, G., Holst, B. (eds), *Surface Science Techniques*, 1 ed., chapter 1, Berlin, Germany, Springer Berlin Heidelberg, 2013.

ZAMPALONI, M. *et al*. Kenaf natural fiber reinforced polypropylene composites: A discussion on manufacturing problems and solutions. **Composites Part A: Applied Science and Manufacturing**, v. 38, n. 6, p. 1569–1580, 2007.

ZHOU, Z. *et al*. Hydrophobic surface modification of ramie fibers with ethanol pretreatment and atmospheric pressure plasma treatment. **Surface and Coatings Technology**, v. 205, n. 17-18, p. 4205–4210, 2011.

ANNEX 1

Reference	Fibers	Matrix	Disposition	Treatment	Plasma Gas	Power	Time	Fiber fraction	Improvement	Due to..
AGUILAR-RIOS *et al*. (2014)	Henequen	HDPE	Unidirectional	Dielectric barrier discharge (1ATM)	Etylane	n/a	1-8 min	single-fiber	130% increase in IFSS	Increase in fiber surface roughness and presence of vinyl groups on fiber surface
BOZACI *et al.,* 2013	Flax	HDPE / Unsaturated polyester	Woven fabric	Atmospheric pressure glow discharge	Air and Ar	100-300W	2 min	n/a	40% increase in IFSS (PE) / 45% increase in IFSS (unsat. Polyester)	Increase in fiber surface roughness (PE) / increased O/C ratio (unsat. Polyester)
LI *et al.,* 2013	Ramie	PP	Woven fabric	Atmospheric pulse plasma	He (fiber pre-soaked in ethanol)	60W	15, 30, 45 sec	35 wt%	39% ILSS	Increased hydrophobicity and roughness of fiber surface
ZHOU *et al., 2011*	Ramie	PP	Single fiber	Atmospheric pressure plasma jet	He (alcool pre soaked)	40W	8, 16, 24 sec	single-fiber	20-46% IFSS	Increased hydrophobicity and roughness of fiber surface
SINHA & PANIGRAHI, 2009	Jute	Unsaturated Polyester	Unidirectional	Cylindrical DC cold plasma	Argon	20W	5, 10, 15 min	15 wt%	14% Flexural strength	Rough surface morphology and development of hydrophobicity on fiber
YUAN *et al.* 2004	Wood fibers	PP	Short fibers	RF cold plasma	Argon and air	60W	30 sec	20 wt%	20% Tensile strength and modulus	Higher fiber O/C ratio and roughness after treatment
SEKI et al., 2010	Jute	Polyester	Woven fabric	Low pressure LF/RF plasma	Oxygen	30, 60, 90W	15 min	27 vol%	Interlaminar sheer stress increases of 72% (LF) and 129%(RF). Slight decrease in tensile strengh	Increase in fiber surface roughness
SEKI *et al.* , 2009	Jute	HDPE	Woven fabric	Low pressure LF (40kHz) plasma	Oxygen	30, 60, 90W	15 min	n/a	45% in flexural strength	Increase in fiber surface roughness
KIM *et al.* 2013	Wood (waste)	PP	Short fibers/powder	Atmospheric pressure glow discharge	HMDSO	3kV	n/a	55 wt%	14.6% increase in tensile strenght	Cleaner surface and lower polarity of the fiber surface
ANWER& BHUIYAN, 2012	Jute	n/a	n/a	Low pressure cold plasma	Argon	50, 75, 100W	5, 10, 15, 20 min	n/a	n/a	Increase in fiber surface roughness
MAHLBERG *et al.* , 1999	wood	PP	Veneer (3mm thick slice)	Low pressure RF (50kHz) plasma	Oxygen	100W	15, 30, 45, 60, 75, 90 sec	n/a	45-95% increase in bonding strengh (from peeling test)	n/a
MARTIN *et al.* , 2000	Sisal	HDPE	Short fibers	Low pressure RF plasma	Dichlorosilane	N/A	n/a	30 wt%	10-15% tensile strength	Surface functionalization
OLARU *et al.* , 2004	Wood fibers	PE and Rubber	Short fibers	Low Pressure RF plasma	Methane	N/A	10 min	0-30 wt%.	53% E-Moduli (20% wt.), 50% tensile strengh (30% wt.)	increased hydrophobicity of fiber surface
SANTOS *et al.* , 2007	Curaua	PA-6	Short fibers	Low Pressure RF plasma	Nitrogen	30W	15min	20, 30, 40 wt%.	6% tensile stregth, 21% E-moduli	n/a
MARAIS *et al.* , 2005	Flax	Unsaturated Polyester	Nonwoven fabric	Low pressure microwave plasma	Helium	50W	5 min	n/a	35% increase in E-moduli, 25% Decrease in tensile strength	Cleaner surface

ANNEX 2

A-B Series

				30wt%	E_t		σ_M		ε_M	
Matrix	Fiber	Plasma Treatment	Treatnent number	Compsite Code	MPa	DesvPad	MPa	DesvPad	%	DesvPad
PP				**PP-A1**	1780	61	33,4	0,57	7,64	0,37
PP	*Wood*	No Treatment		**HW-A1**	3550	100	30,8	0,44	2,29	0,15
PP	*Wood*	No Treatment		**HW-A7**	3470	74	30,5	0,24	2,46	0,11
PP	*Wood*	30 min SF6 / 150W	**#011**	**HW-A2**	3580	71	30,2	0,40	2,15	0,10
PP	*Wood*	30 min SF6 / 200W	**#016**	**HW-A3**	3670	107	31,0	0,51	2,04	0,07
PP	*Wood*	45 min SF6 / 175W	**#017**	**HW-A4**	3580	68	30,2	0,91	2,10	0,10
PP	*Wood*	60 min SF6 / 150W	**#018**	**HW-A5**	3580	60	29,8	0,40	2,17	0,07
PP	*Wood*	60 min SF6 / 200W	**#019**	**HW-A6**	3570	61	30,3	0,53	2,11	0,08
PP	*Wood*	180 min SF6 / 200W	**#101**	**HW-B1**	3510	142	30,2	0,56	2,08	0,09
PP	*Flax*	No Treatment		**FL-A1**	3360	89	28,7	0,25	2,42	0,15
~~**PP**~~	~~*Flax*~~	~~30 min O2+30min SF6 / 150W~~	~~**#014**~~	~~**FL-A2**~~	~~3419~~	~~89~~	~~27,5~~	~~0,54~~	~~2,40~~	~~0,23~~
PP	*Flax*	30 min SF6 / 150W	**#015**	**FL-A3**	3306	57	27,5	0,49	2,40	0,11
PP	*Flax*	60 min SF6 / 200W	**#022**	**FL-A6**	3500	82	28,1	0,57	2,09	0,25
PP	*Flax*	180 min O2 / 200W	**#104**	**FL-B1**	3540	78	28,5	0,38	2,17	0,16
PP	*Flax*	180 min SF6 / 200W	**#105**	**FL-B2**	3500	96	27,6	0,52	2,07	0,20
PP	*Sisal*	No Treatment		**SI-A1**	2740	55	31,1	0,46	2,59	0,13
PP	*Sisal*	30 min O2+30min SF6 / 150W	**#012**	**SI-A2**	2780	105	30,5	0,30	2,54	0,06
PP	*Sisal*	30 min SF6 / 150W	**#013**	**SI-A3**	2780	61	30,7	0,37	2,54	0,12
PP	*Sisal*	60 min SF6 / 200W	**#024**	**SI-A4**	2780	61	31,4	0,45	2,47	0,08
PP	*Sisal*	180 min O2 / 200W	**#102**	**SI-B1**	2670	64	30,2	0,40	2,65	0,18
PP	*Sisal*	180 min SF6 / 200W	**#103**	**SI-B2**	2590	64	28,8	0,29	2,55	0,14
PP	*micro-Flax*	No Treatment		**mF-A1**	4480	98	31,7	0,89	2,58	0,34
PP	*micro-Flax*	60 min SF6 / 200W	**#028**	**mF-A2**	4820	98	32,4	0,35	1,88	0,06
PP	*micro-Flax*	180 min O2 / 200W	**#106**	**mF-B1**	4680	143	32,4	0,61	2,22	0,16
PP	*micro-Flax*	180 min SF6 / 200W	**#107**	**mF-B2**	4790	56	34,4	0,64	1,81	0,09

D Series

				10wt%	E_t		σ_M		ε_M	
Matrix	Fiber	Plasma Treatment	Treatnent number	Compsite Code	MPa	DesvPad	MPa	DesvPad	%	DesvPad
PP	*Holz*			HW-D1	2460	52,5	32,7	0,31	3,9	0,15
PP	*Holz*	30 min / 40% SF6	#016	HW-D2	2449	53,5	32,8	0,36	3,9	0,11
PP	*Holz*	60 min / 40% SF6	#019	HW-D3						
PP	*Holz*	180 min / 40% SF6	#101	HW-D4	2462	62,9	32,8	0,24	3,8	0,18
PP	*Sisal*			SI-D1						
PP	*Sisal*	30 min / 30% + O2	#012	SI-D2	2231	34,0	32,3	0,68	3,7	0,26
PP	*Sisal*	60 min / 40% SF6	#024	SI-D3	2230	60,1	32,4	0,58	3,8	0,22
PP	*Sisal*	120 min / 40% O2	#111	SI-D4	2208	35,4	31,9	0,62	3,9	0,48
PP	*Sisal*	120 min / 40% SF6	#112	SI-D5						
PP	*Sisal*	120 O2 + 60 SF6 / 40%	#113	SI-D6	2218	43,1	32,5	0,23	4,0	0,12

E Series

				20wt%	E_t		s_M		e_M	
Matrix	Fiber	Plasma Treatment	Treatnent number	Compsite Code	MPa	DesvPad	MPa	DesvPad	%	DesvPad
PP	*Holz*	-		HW-E0	3146	28,7	32,0	0,33	3,0	0,15
PP	*Holz*	30min/40% - SF6+Ar	#304	HW-E1	3225	127,0	32,8	0,46	2,6	0,14
PP	*Holz*	30min/20% - SF6+Ar	#305	HW-E2	3123	75,0	32,3	0,31	2,8	0,10
PP	*Holz*	180min/40% - SF6+Ar	#306	HW-E3	3194	69,3	33,2	0,52	2,6	0,10
PP	*micro-Flax*	-		mF-E0	3582	133,5	32,7	0,50	3,4	0,29
PP	*micro-Flax*	30min/20% - SF6+Ar	#303	mF-E1	3957	96,4	33,4	0,58	2,9	0,21
PP	*micro-Flax*	30min/40% - SF6+Ar	#302	mF-E2	3988	82,3	34,4	0,40	2,5	0,15
PP	*micro-Flax*	180min/40% - SF6+Ar	#301	mF-E3	4037	139,7	36,0	0,72	2,3	0,11
PP	*Kokos*	-		KO-E1	2473	52,6	29,9	0,57	2,7	0,26
PP	*Kokos*	SF6-30min/60W (BR)	BR	KO-E2	2564	87,3	30,7	0,95	2,5	0,21
PP	*Kokos*	30min/20% - SF6+Ar	#307	KO-E3	2364	59,2	28,8	0,60	2,8	0,24

L Series

				30wt%	E_t		σ_M		ε_M	
Matrix	Fiber	Plasma Treatment	Treatnent number	Compsite Code	MPa	DesvPad	MPa	DesvPad	%	DesvPad
PLA	*Wood*			HW-L1	5696	325	58,2	0,70	1,45	0,08
PLA	*Wood*	120 min / 200W O2	#108	HW-L2	5811	157	58,6	1,39	1,42	0,10
PLA	*Wood*	120 min / 200W SF6	#109	HW-L3	5693	153	58,5	0,39	1,47	0,05
PLA	*Wod*	120 O2 + 60 SF6 / 40%	#110	HW-L4	5820	128	59,5	1,46	1,47	0,10
PLA	*Sisal*			SI-L1	4767	104	58,3	0,63	1,66	0,06
PLA	*Sisal*	120 min / 40% O2	#111	SI-L2	4796	84	59,6	0,50	1,69	0,03
PLA	*Sisal*	120 min / 40% SF6	#112	SI-L3	4737	114	56,8	1,80	1,57	0,10
PLA	*Sisal*	120 O2 + 60 SF6 / 40%	#113	SI-L4	4753	89	59,1	1,36	1,65	0,10
PLA	*Flax*			FL-L1	5970	67	58,3	1,40	1,38	0,12
PLA	*Flax*	120 min / 40% O2	#114	FL-L2	6162	97	57,2	2,08	1,25	0,09
PLA	*Flax*	120 min / 40% SF6	#115	FL-L3	6142	72	53,6	4,21	1,17	0,16
PLA	*Flax*	120 O2 + 60 SF6 / 40%	#116	FL-L4	6039	121	56,3	1,27	1,27	0,07
PLA	*micro-Flax*			mF-L1	6545	69	65,4	0,70	1,71	0,14
PLA	*micro-Flax*	120 min / 40% O2	#117	mF-L2	6683	73	65,4	0,65	1,61	0,07
PLA	*micro-Flax*	120 min / 40% SF6	#118	mF-L3	6771	117	64,1	1,05	1,54	0,07
PLA	*micro-Flax*	120 O2 + 60 SF6 / 40%	#119	mF-L4	6758	160	64,3	1,16	1,48	0,11

M Series

				20wt%	E_t		s_M		e_M	
Matrix	Fiber	Plasma Treatment	Treatnent number	Compsite Code	MPa	DesvPad	MPa	DesvPad	%	DesvPad
PLA	*Holz*	*Ohne*	-	HW-M1	5442	97,08	59,96	0,39	1,58	0,029
PLA	*Holz*	15 min / 40% O2	#201	HW-M2	5560	192,55	60,56	0,95	1,55	0,031
PLA	*Holz*	30 min / 40% O2	#202	HW-M3	5603	86,19	61,78	0,22	1,56	0,038
PLA	*Holz*	60 min / 40% O2	#203	HW-M4	5591	104,09	60,99	0,56	1,56	0,050
PLA	*Holz*	120 min / 40% O2	#204	HW-M5	5570	75,84	61,29	0,37	1,56	0,035
PLA	*Holz*	15 min / 50% O2	#205	HW-M6	5503	136,56	60,71	0,70	1,52	0,066
PLA	*Holz*	15 min / 60% O2	#206	HW-M7	5593	156,00	59,85	0,59	1,50	0,092
PLA	*micro-Flax*	*Ohne*	-	mF-M1	6202	61,64	65,50	1,25	1,83	0,03
PLA	*micro-Flax*	15 min / 40% O2	#207	mF-M2	6381	69,96	61,59	0,54	1,70	0,01
PLA	*micro-Flax*	30 min / 40% O2	#208	mF-M3	6447	84,66	61,20	0,50	1,66	0,02
PLA	*micro-Flax*	60 min / 40% O2	#209	mF-M4	6427	57,67	62,07	0,65	1,63	0,02
PLA	*micro-Flax*	120 min / 40% O2	#210	mF-M5	6370	89,31	65,35	0,67	1,71	0,03
PLA	*micro-Flax*	15 min / 50% O2	#211	mF-M6	6401	67,63	61,19	0,78	1,67	0,02
PLA	*micro-Flax*	15 min / 60% O2	#212	mF-M7	6478	64,21	61,07	0,29	1,65	0,02

ANNEX 3

Typical stress strain curves for some composites formulations used in this thesis.

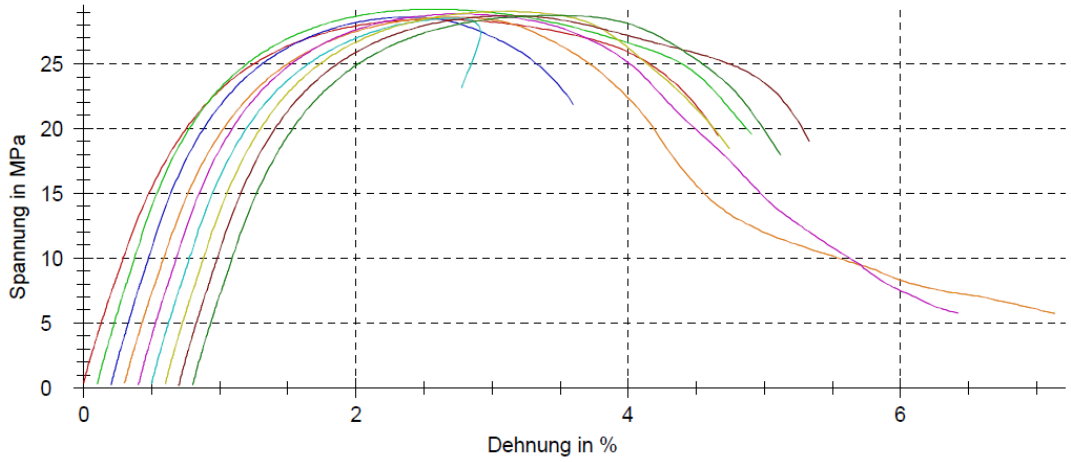

Figure A.1. Flax-PP composite with untreated technical flax fibers.

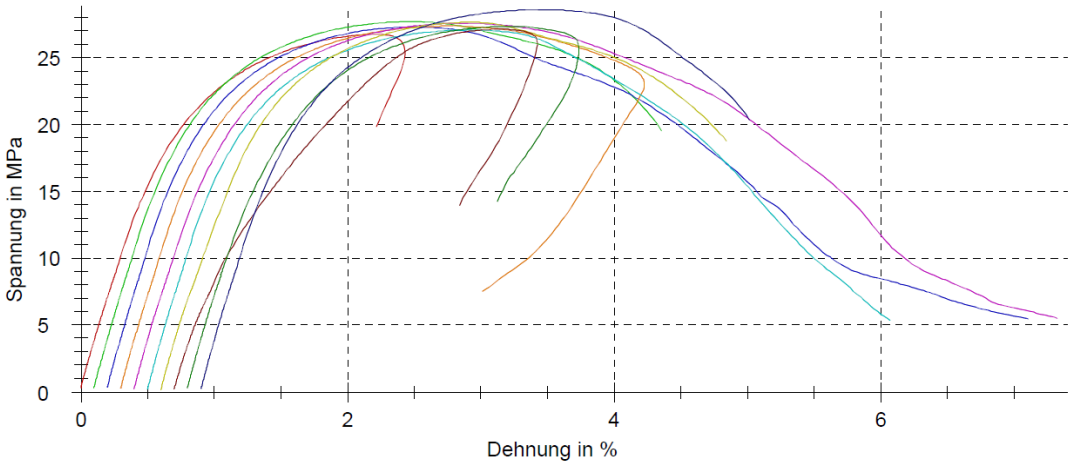

Figure A.2. Flax-PP composite with technical flax fibers treated in SF_6 plasma for 30 minutes at 150W power.

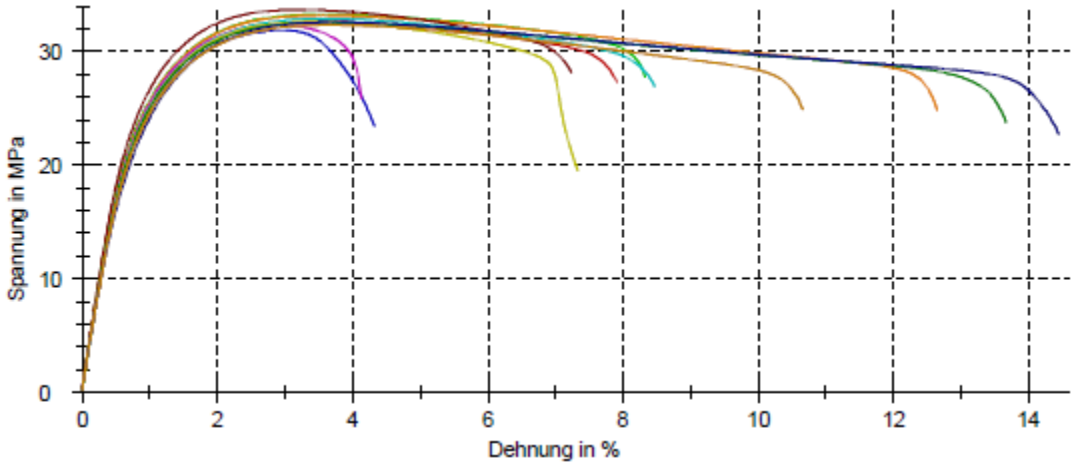

Figure A.3. Flax-PP composite with untreated micronized flax fibers.

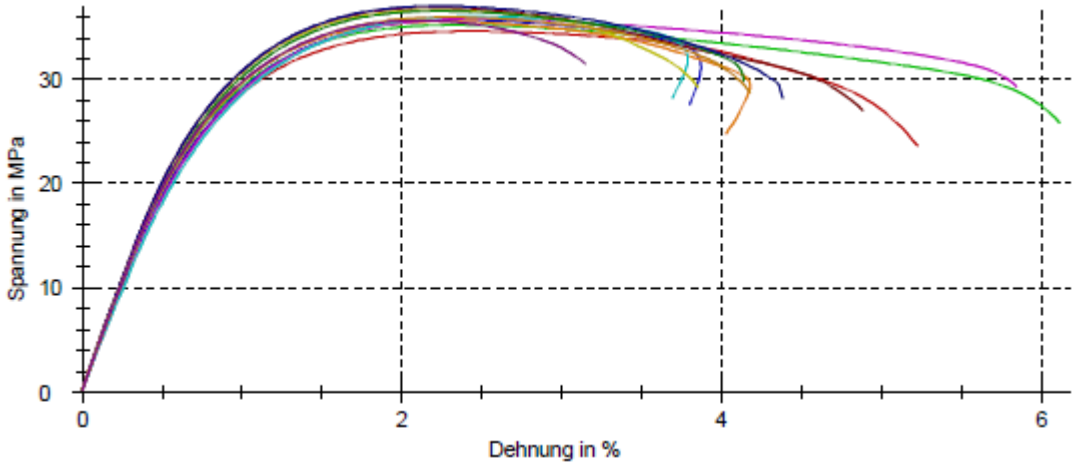

Figure A.4. Flax-PP composite with micronized flax fibers treated in SF_6 plasma for 180 minutes at 200W power.

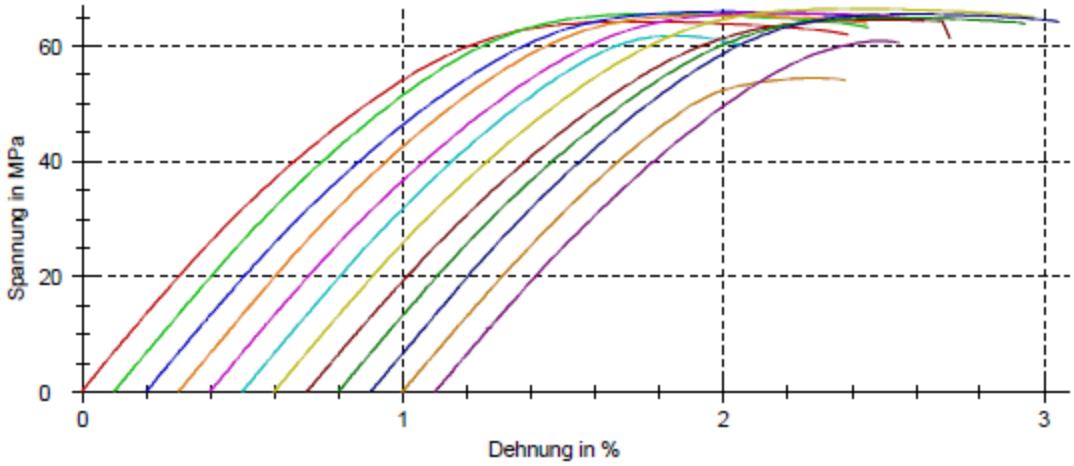

Figure A.5. Flax-PLA composite with untreated micronized flax fibers.

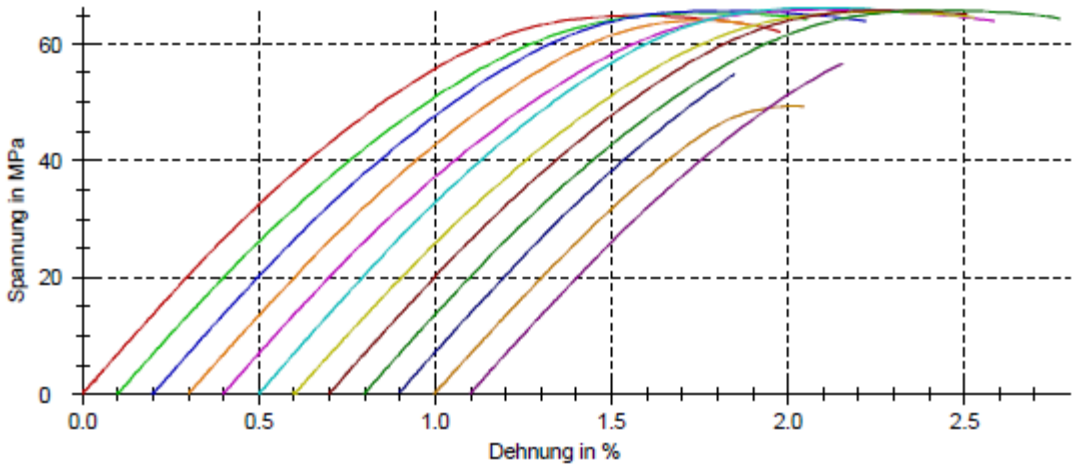

Figure A.6. Flax-PLA composite with micronized flax fibers treated in SF_6 plasma for 120 minutes at 200W power.

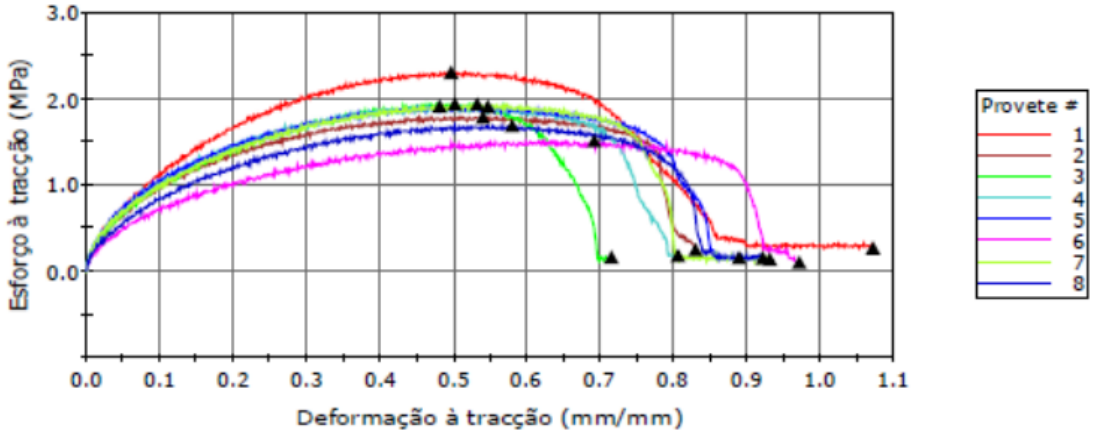

Figure A.7. Coir-Thermoplastic Starch composite with untreated coir fibers.

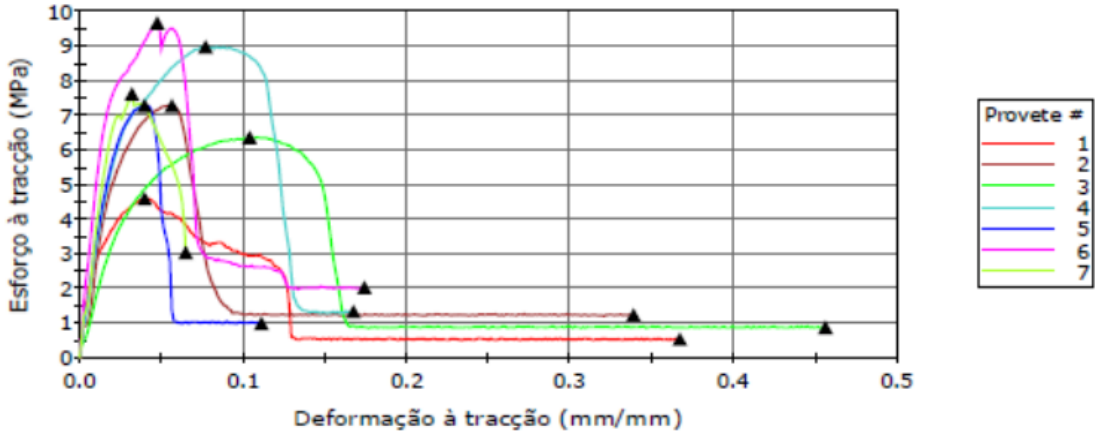

Figure A.8. Coir-Thermoplastic Starch composite with coir fibers treated by oxygen (O_2) plasma for 60 minutes at 80W power.